THE HONG KONG POLYTECHNIC UNIVERSITY

Department of Applied Biology and Chemical Technology

A Sol-gel Encapsulated Biomass Process for the Removal of Copper(II) Ions from Water and Wastewater

Cheung Oi Yee

A thesis submitted in partial fulfillment of the requirements for the Degree of Master of Philosophy

September, 2007

Certificate of Originality

I hereby declare that this thesis is my own work and that, to the best of my knowledge and belief, it reproduces no material previously published or written, nor material that has been accepted for the award of any other degree or diploma, except where due acknowledgement has been made in the text.

Cheung Oi Yee

Abstract

Industrial effluents laden with heavy metals must be pretreated before they are discharged into the aquatic environment. The chemical precipitation treatment method produces a large amount of hazardous sludge for disposal. Other conventional treatment methods such as electrochemical treatment and ion exchange are expensive and incapable of removing trace levels of copper(II) ions. Alternatively, biological materials can be applied for the removal and recovery of heavy metals due to their good performance and low cost. *Micrococcus* sp., which is a Gram-positive bacterium isolated from a local activated sludge process, was proved to be an effective biosorbent for copper(II) removal. However, the use of freely-suspended biomass for biosorption is impractical. This study therefore aimed to develop a novel immobilized cell process for copper(II) removal and recovery from industrial wastewater. The *Micrococcus* sp. suspended cells were first immobilized in sol-gel/PVA matrix and the immobilized cells were then applied in the biosorption and desorption processes for the removal and recovery of copper(II) ions.

The novel sol-gel immobilization technique was used to entrap *Micrococcus* sp. cells in a sol-gel derived material of silica and polyvinyl alcohol, which has been shown to provide a biocompatible microenvironment for microorganisms.

Immobilized biosorbents with both spherical and cylindrical shapes were prepared and their biosorption performances were compared. The optimum conditions for the preparation of immobilized biosorbents were determined. The results indicate that the copper(II) uptake capacity of the spherical biosorbent was higher than that of the cylindrical biosorbent. The biosorption of copper(II) ions was affected by the composition of the sol-gel/PVA matrix as well as the concentration of biomass in the biosorbent. The optimum drying time of the spherical and cylindrical biosorbents was two days and three days, respectively. The effects of pH, biomass dosage, metal concentration, contact time and agitation speed on copper(II) biosorption by the biosorbents were studied in a batch system. Copper(II) biosorption was highly dependent on the solution pH and a maximum biosorption capacity was generally reached at pH 5.0.

The Langmuir and Freundlich isotherm models were applied to simulate mathematically the equilibrium data. The Langmuir model could better simulate the experimental data with $r^2 \geq 0.99$. The pseudo-second order kinetic model could simulate the kinetic data very well with $r^2 \geq 0.96$. The rate of copper(II) uptake increased significantly with an increase in the agitation speed from 30 rpm to 100 rpm, and a slight enhancement was observed with a further increase in the

agitation speed. The surface morphology of the immobilized biosorbents before and after the copper(II) uptake was examined by a scanning electron microscopy and the surface morphology of the biosorbent changed after the copper(II) uptake.

Desorption studies were then conducted to determine the metal recovery efficiency of the metal-laden biosorbent using nine different desorbing agents. The most effective desorbing agent for copper(II) recovery was 0.1 M NTA. The optimum desorption time for both the spherical and cylindrical biosorbents was 6 h. Spherical biosorbent was preferred to cylindrical biosorbent due to its faster copper(II) biosorption and desorption rates. The reusability of the suspended biomass and immobilized biosorbent was compared by performing repeated biosorption/desorption cycles. In contrast to suspended cells, immobilized biosorbent can solve the problem of cell loss in multiple biosorption/desorption cycle operations. Finally, a four-stage semi-continuous immobilized cell batch reactor system was applied for removing and recovering copper(II) from both synthetic and industrial wastewater. This process was capable of producing the effluent at low copper(II) concentration for both synthetic and industrial wastewater. The results indicate that the immobilized cell process can be further developed into practical reactor systems for advanced wastewater treatment.

Acknowledgements

I wish to express my sincere gratitude to my supervisor Dr. Wai-Hung Lo, Thomas, and co-supervisor Dr. Yun Chung Leung for allowing me to pursue my academic interests. I would like to thank them for their encouragement, support and advice.

I am also grateful to Dr. K.H. Lam, Dr. L.M. Ng, Mr. C.C. Li, and Ms. P.S. Leung for their valuable comments, suggestions and help.

I would like to thank my family and my friends for their continuous encouragement and support during my M.phil. study.

Table of Contents

List of Abbreviations

AAS	Atomic absorption spectrophotometer
b	Affinity constant (L/mg)
CA	Citric acid
C_e	Equilibrium metal concentration (mg/L)
C_i	Initial metal concentration (mg/L)
DDI water	Distilled and deionized water
K	Freundlich constant
k_1	Pseudo-first order kinetic constant (min^{-1})
k_2	Pseudo-second order kinetic constant (g/mg·min)
MTMS	Methyltrimethoxysilane
n	Freundlich constant
PVA	Polyvinyl alcohol
q	Biosorption capacity or metal adsorbed (mg/g-biomass)
q_{max}	Maximum biosorption capacity (mg/g-biomass)
r^2	Correlation coefficient
SEM	Scanning electron microscopy
TEOS	Tetraethoxysilane
TMOS	Tetramethoxysilane

List of Figures

List of Tables

Chapter 1. Introduction

1.1 Motivations

Copper(II) contaminants are commonly found in the aqueous effluents of many industries, such as mining operations, metal finishing, plating and chemical manufacturing industries. Their release into the environment poses serious risks to human health and the environment. Copper(II) is persistent in the environment and it can be accumulated in living organisms. Thus, industrial effluents laden with copper(II) ions must be pretreated before they can be discharged into the aquatic environment.

Heavy metal removal can be achieved by several conventional treatment processes including chemical precipitation, coagulation, flotation, electrochemical techniques, membrane filtration and solvent extraction (Kurniawan *et al.*, 2006; Martinez *et al.*, 2006). However, some of these technologies only provide partially effective treatment and they are costly to use. They may also generate hazardous sludge and create additional treatment and disposal problems. For example, the chemical precipitation treatment method produces a large amount of hazardous sludge for disposal. Other conventional treatment methods such as electrochemical treatment and ion exchange are expensive and incapable of removing trace levels of copper(II) ions.

The use of biosorption process for heavy metal removal has gained considerable attention due to its low cost and high efficiency even in decontaminating very dilute effluents. The major advantages of the biosorption process include its effectiveness of removing the contaminants in the wastewater and its use of inexpensive biological materials. The reusability of the biosorbents also provides an economical and effective alternative to remove and recover heavy metals. Biosorption is a method utilizing inactive and dead biological materials, such as bacteria, agricultural waste and fermentation waste, to accumulate and remove toxic heavy metals by different mechanisms including adsorption, ion exchange, complexation, and surface microprecipitation (Yang and Volesky, 1999; Aksu and İşoğlu, 2005; Vijayaraghavan *et al.*, 2006). It has been shown that the presence of functional groups in the biomass cell wall, such as carboxylate, hydroxyl, sulfate, phosphate and amino groups, can help remove metal ions (Göksungur *et al*., 2005).

The use of freely-suspended biomass provides better contact with heavy metal ions in the biosorption process. However, the use of suspended biomass for biosorption is impractical because it is difficult to separate the cells from the solution and the amounts of cells will lose continuously during the biosorption

and desorption processes. Furthermore, low mechanical strength and low rigidity of the suspended cells are unsuitable for column application. In order to enhance the mechanical strength of the biomass, different immobilization techniques have been introduced. Immobilization of biomass in a compact, accessible and recoverable form, such as pellets, granules or beads, can overcome the disadvantages in the use of suspended cells (Wase and Forster, 1997). Unlike suspended cells, the immobilized biosorbents can be easily separated from the solution in the biosorption and desorption processes. Thus, the adsorbed metal ions can be recovered easily and the immobilized biosorbents can be used repeatedly without any loss of the biomass.

Many research studies have been conducted to examine the removal of heavy metals using the immobilized biosorbent. Biomass immobilized in calcium alginate, polyacrylamide, polysulfone, polyethylenimine, polyisoprene and polyvinylalcohol have been tested for their abilities to remove heavy metals (Bai and Abraham, 2003; Beolchini *et al*., 2003; Deng and Ting, 2005; Pan *et al*., 2005). However, little empirical research has been conducted for metal removal using the sol-gel immobilized adsorbent. Sol-gel matrix offer several advantages for biomass immobilization. First, the sol-gel matrix is non-toxic and the cells

are covalently bonded to the silicate material easily. Second, the sol-gel matrix can produce an immobilized biosorbent with high mechanical strength which can withstand pressure during the column applications. Third, the biosorption capacity, reactivity and chemical functionality of the biomass can be retained after immobilizing the biomass in the sol-gel matrix. Many studies have been conducted to prepare the ceramics, electrode materials, optical devices, chemical sensors, biosensors, proton-conductive membranes and nanoparticles using the sol-gel process (Chen *et al*., 2008; Kato *et al*., 2007; Kwok *et al*., 2005; Lavela *et al*., 2007; Livage, 1997; Maduraiveeran and Ramaraj, 2007). However, only a very limited number of studies have been carried out to investigate the encapsulation of biological materials in sol-gel matrix to remove heavy metals (Chen and Lin, 2007; Marseaut *et al*., 2004).

PVA has been used as an immobilization material due to its economical large-scale production, non-toxicity to biomaterials, and good chemical and mechanical stabilities (Chu and Hashim, 2007). Nakane *et al*. (1999) reported that the PVA and silica could associate well with interactions such as hydrogen bond. No study has been reported on the removal of heavy metals using bacterial cells encapsulated in the sol-gel matrix containing PVA. The

sol-gel/PVA composite material could be an excellent matrix for immobilizing bacterial cells for metal removal. This motivate us to study the applicability of the sol-gel/PVA matrix for immobilizing *Micrococcus* sp. cells for the removal and recovery of copper(II) ions from wastewater.

1.2 Objectives

The objectives of this study are listed as follows:

1. To develop a novel and cost-effective immobilized cell process for removing and recovering copper(II) using *Micrococcus* sp.
2. To immobilize *Micrococcus* sp. in sol-gel/PVA matrix for improving biomass rigidity and facilitating biomass separation from metal-laden wastewater.
3. To examine the optimum conditions for preparing the sol-gel immobilized biosorbents with both spherical and cylindrical shapes, including the composition of sol-gel/PVA matrix, concentration of biomass encapsulated in the sol-gel/PVA matrix and the drying time of the immobilized biosorbents.
4. To investigate and compare the biosorption performances of the spherical and cylindrical biosorbents in a batch study, including the effects of solution pH, copper(II) concentration, contact time, and agitation speed.
5. To investigate the changes in surface morphology of immobilized

biosorbents before and after copper(II) uptake using SEM.

6. To study and compare the desorption performances of the spherical and cylindrical biosorbents in a batch study.

7. To compare the reusability of the suspended biomass and the immobilized biosorbent by performing the repeated biosorption/desorption cycles.

8. To apply a four-stage semi-continuous immobilized cell batch reactor system for removing and recovering copper(II) from both synthetic and industrial wastewater.

1.3 Organization of thesis

There are a total of six chapters in this dissertation. The chapters of the dissertation are organised as follows:

Chapter 1 Introduction: the current chapter.

Chapter 2 Literature Review: this presents the literature related to the biosorption process and reviews the work in earlier research.

Chapter 3 Materials and Methods: this describes the materials and instruments used in the experiment and states the experimental procedures used for data collection.

Chapter 4 Results and Discussion: this presents, discusses and interprets the

findings obtained in this study.

Chapter 5 Conclusions: this summarizes the major findings of this research.

Chapter 6 Further Studies: this lists the limitations of this research and gives recommendations for future studies.

Chapter 2. Literature Review

2.1 Introduction to the chapter

This chapter begins with a review of the literature on heavy metal contamination in the environment, which presents the major toxicity problems that exist in the presence of heavy metals, including copper, cadmium, chromium, lead, nickel and zinc. The limitations of the conventional treatment methods for heavy metal removal will then be addressed, followed by an introduction of an alternative method which is known as biosorption. Biosorption process can involve several mechanisms, including ion exchange, physical adsorption, complexation and precipitation. The literature of these mechanisms on the biosorption process will be reviewed. The factors affecting the biosorption process will then be reviewed. Desorption of heavy metal and regeneration of biosorbent is necessary after the biosorption process, therefore a review of the literature on biomass regeneration will then be addressed. Immobilized biomass gives a better performance than freely-suspended biomass in the biosorption/desorption cycles. Therefore, different types of immobilization methods will be reported and discussed at length. Finally, different types of reactor systems for biosorption will be discussed.

2.2 Heavy metal contamination in water

The intensification of industrial activities in recent years contributes greatly to the increase of heavy metals in the environment, especially in the aquatic system. Heavy metals are a group of pollutants which is almost indefinitely persistent in the environment.

According to the report of the Hong Kong Marine Water Quality in 2004 provided by the Environmental Protection Department (EPD), the heavy metal contents of sediment, especially copper and silver in the Victoria Harbour, Junk Bay and Tsuen Wan Bay, were high and exceeded the upper chemical exceedance levels (UCELs). This was mainly caused by the discharges of the metal-bearing sewage from printed circuit board and electroplating industries (EPD, 2004). Cheung *et al*. (1997) investigated the concentrations of arsenic, cadmium, chromium, copper, mercury, lead and zinc in the sediments collected from different Hong Kong coastal wasters. Results indicate that the sediments collected from Kowloon Bay and Tsing Yi gave higher copper, chromium, zinc and mercury concentrations than that collected from Chek Lap Kok and Double Haven. Wong *et al*. (2000) found that the concentrations of cadmium, chromium, copper, nickel, lead and zinc in Green-lipped mussels, *Perna viridis*, did not

exceed the maximum permissible levels that were developed by the Hong Kong Government.

The presence of heavy metals in the environment is a major threat to plants, animals and humans due to their toxicity, persistence in nature and tendency to accumulate in the food chain (Malik, 2004). Unlike organic toxicants, which can be degraded, inorganic metal species are immutable and they persist indefinitely in the environment. Therefore, legislation is needed to control the amount of heavy metals discharged into the aqueous system. In the following sections, 2.2.1 to 2.2.6, the toxicity and pollution sources of selected heavy metals are discussed.

2.2.1 Copper

Copper occurs naturally in its elemental form and as a component of many minerals. Because of its high electrical conductivity, thermal conductivity and malleability, it is used to manufacture electrical equipment. There are two oxidation states in copper salts, which are Cu(I) (cuprous) and Cu(II) (cupric). The biological availability and toxicity of copper are most likely associated with the divalent state (ATSDR, 1990).

Copper is an essential trace element for animal and plant tissues. It is important for both physical and mental health. It is also critical for energy production in the cells. Copper is closely related to estrogen metabolism, and is required for women's fertility to maintain pregnancy. The maximum contaminant level of copper in drinking water established by the United States Environmental Protection Agency (USEPA) is 1.3 mg/L (USEPA, 2002). In humans, the excessive uptake of copper is deposited in brain, skin, liver, pancreas and myocardium. It may cause headaches, heart disease, hyperactivity, nausea, diarrhoea, hemolysis, hematuria, hypotension, tachycardia, convulsions, Wilson's disease, genetic disorder and other adverse effects (Volesky, 1990).

Anthropogenic sources of copper to the environment mainly come from mining operations, printed circuit board and electroplating industries. In Hong Kong, the maximum copper concentration allowed to be discharged into foul sewers leading to the government sewage treatment plants is 4 mg/L, for a flow rate less than 200 m^3/day. After the sewage treatment, the maximum copper concentration allowed to be discharged into different Water Control Zones is 0.1 mg/L, for a flow rate between 4000 and 6000 m^3/day (EPD, 2000).

2.2.2 Cadmium

Cadmium is a very toxic heavy metal commonly found in batteries, paint pigments, coatings, plating and plastics. Cadmium may occur naturally in grain and leafy vegetables. It may also be found as a contaminant in sewage sludge, fertilizers, groundwater and mining effluent. Cadmium can accumulate in human kidney and liver by ingestion and inhalation. Exposure to cadmium causes kidney damage, lung damage, Itai-itai disease, proteinuria, dyspnoea, cyanosis, fever, tachycardia, gastrointestinal irritation, nausea, diarrhea and osteomalacia. Cadmium is also carcinogenic, which can cause lung cancer and prostate cancer (Volesky, 1990).

2.2.3 Chromium

Chromium(III) and chromium(VI) are the most common oxidation states of chromium. Chromium(VI) is generally known to be more toxic than chromium(III) because of its carcinogenic and mutagenic effects. Chromium is extensively used in electroplating, tanning, stainless steel and welding industries, which results in discharge of chromium-containing effluent to the environment. Long term exposure to chromium(VI) may cause nasal irritation, kidney damage, and lung cancer (Volesky, 1990).

2.2.4 Lead

Lead is commonly found in the earth's crust and it can enter the food chain easily. It is harmful to human and it persists in the environment for a long period of time. Therefore, it is banned for the use in gasoline and house paints. However, lead is still used in batteries and insecticides, and also found in cigarette smoke. Accumulation of lead in human body, such as kidney and brain, causes improper function of these organs. Exposure to lead may impair gastrointestinal tract, central nervous system and blood cells of humans. Other symptoms included memory loss, insomnia, convulsions, coma, progressive mental deterioration and behavioral disorders (Volesky, 1990).

2.2.5 Nickel

Nickel can be found in soil, plants and animals. Human activities, such as burning fossil fuels, mining operations and incineration of municipal waste, can release nickel into the atmosphere. It is also found in the effluent of textile and electroplating industries. Ingestion of nickel will damage gastrointestinal tract. It is irritant to people with skin allergy and some forms of nickel compounds are carcinogenic (Volesky, 1990).

2.2.6 Zinc

Zinc is one of the least toxic heavy metals and it is an essential element in human growth. However, it may affect human health and cause environmental problems if the concentration is high enough (Volesky, 1990). It is commonly found in the effluent from textile facilities and in sewage sludge.

2.3 Conventional methods for heavy metal removal

Conventional methods for removing heavy metals from metal-laden wastewater includes filtration, chemical precipitation, chemical oxidation or reduction, electrochemical techniques, flocculation, coagulation and solvent extraction (Kurniawan *et al*., 2006; Zhang and Banks, 2005). Application of these methods is sometimes restricted because of technical or economical constraints. The major disadvantages are incomplete metal removal, high operating cost and generation of toxic sludge or other waste products (Aksu *et al*., 2005). These disadvantages of conventional methods together with the need for more economical and effective methods for metal removal have led the researchers to develop new technologies.

2.4 Biosorption

To remove heavy metals from the metal-laden wastewater, it is necessary to develop an inexpensive technology to meet the demands and reduce the operating cost for small companies and developing countries (Iqbal and Edyvean, 2005). Biosorption is defined as the passive binding of heavy metals to inactive, non-living and dead biomass from an aqueous solution. The term "passive" implies that the removal mechanism is not metabolically controlled (Davis *et al*., 2003). Biosorption is a low operating cost process, which can minimize the volume of chemical and/or biological sludge to be disposed and is highly efficient in detoxifying very dilute effluent (Marques *et al*., 2000). In recent years, the application of biosorption to remove heavy metals has been extensively studied (Amuda *et al*., 2007; Leung *et al*., 2001; Melgar *et al*., 2007; Naja and Volesky, 2006; Papageorgiou *et al*., 2006; Pavasant *et al*., 2006; Wong *et al*., 2001). Biosorption of heavy metals involves several mechanisms that differ qualitatively and quantitatively according to the species and origin of the biomass as well as the processing steps (Volesky and Holan, 1995). The mechanisms of this process can include physical and/or chemical adsorption, ion exchange, coordination, complexation, chelation and microprecipitation.

Biomass, which is abundant in nature or collected as a by-product and waste material produced from various industries, can be developed into biosorbent for heavy metal removal (Martinez *et al.*, 2006). Dead biological cells such as bacteria, fungi, yeast and algae are common types of biomass employed in the biosorption process since they offer several advantages over the corresponding living cells. In particular, they can be reused after the desorption process (Kiran *et al.*, 2005).

The efficiency of the biosorption process depends on factors varying from the types of biomass and metal ions being studied. In order to enhance the biosorption efficiency, the biomass should be cheap, reusable and widely available with suitable particle sizes, shapes and mechanical properties. In addition, the metal removal and recovery by the biomass should be efficient and economically feasible (Volesky, 1987).

Micrococcus sp. is a Gram-positive aerobic bacterium, which belongs to the *Micrococcaceae* family. This family can be found in freshwater environment, soil and human skin. Although this bacterium is a common human skin contaminant, they are generally harmless to human. *Micrococcus* sp. can be

observed under the microscope as spherical cells with pairs or clusters.

Micrococcus sp. used in this study was first isolated from the activated sludge process of a local sewage treatment plant. This bacterium was found to be capable of removing copper(II) effectively from aqueous solution. Wong *et al*. (2001) studied the copper(II) biosorption behaviors of freely-suspended *Micrococcus* sp. It was found that *Micrococcus* sp. could be applied to the development of potentially cost-effective biosorbents for the removal and recovery of copper(II) because of its high copper(II) biosorption capacity. However, the use of freely-suspended biomass for biosorption is impractical because of its small particle size, low density, poor mechanical strength, low rigidity and difficulty in separation from the liquid stream. These problems can be solved by immobilizing the freely-suspended cells (Sekhar *et al*., 2004). Therefore, this study was conducted to develop a novel immobilized cell process for improving the copper(II) biosorption and desorption processes.

2.5 Biosorption mechanisms

To better understand the physico-chemical aspects of the biosorption process, a large effort has been spent in recent years to study the mechanisms of biosorption. However, it is difficult to determine the mechanism involved in the biosorption process, since the biomass comprises a highly complex structure with different binding sites and one binding site can participate in different binding mechanisms. Vegliò and Beolchini (1997) reported that there are several mechanisms which can be involved in the metal biosorption process and they are summarized below.

2.5.1 Ion exchange

There are a lot of polysaccharides containing in the cell wall of microorganisms. The cations of the polysaccharides can be exchanged with the metal ions during the biosorption process (Tsezos and Volesky, 1981). Apiratikul and Pavasant (2008) reported that the Ca^{2+}, Mg^{2+} and Mn^{2+} ions on the surface of *Caulerpa lentillifera* were released and exchanged with the Pb^{2+}, Cu^{2+} and Cd^{2+} ions. Raize *et al*. (2004) reported that the nickel(II) binding mechanism was probably ion exchange because the binding process caused a significant increase in Ca^{2+} and Mg^{2+} concentrations.

2.5.2 Physical adsorption

Physical adsorption involves van der Waals' force and electrostatic interaction between metal ions in solution and negative ions in cell wall. Li *et al*. (2006) reported that the chromium(III) ion was physically adsorbed on the unoccupied sites of *Spirulina platensis* algal cell walls by electrostatic attraction. Electrostatic interaction was also responsible for copper(II) (Zhou and Kiff, 1991), nickel(II), zinc(II), cadmium(II) and lead(II) removal (Fourest and Roux, 1992) by *Rhizopus arrhizus*.

2.5.3 Complexation

Metal removal can be caused by the complex formation between metal ions and the active groups on the cell surface. Li *et al*. (2006) showed that the chromium(III) ions could form complex with biologic ligands such as proteins, polysaccharides and lipids in *Spirulina platensis* by displacing Fe^{3+}, Mn^{2+}, Ca^{2+}, Mg^{2+}, Zn^{2+}, Na^{+}, K^{+}, and H^{+} ions. Ion exchange mechanism may be the main strategy for complexation of chromium(III) in *Spirulina platensis*. Pagnanelli *et al*. (2003) verified that the carboxylic and phenolic groups of olive pomace were mainly responsible for the removal of lead(II), copper(II) and cadmium(II) by surface complexation mechanism.

2.5.4 Precipitation

Precipitation may be metabolic dependent or metabolic independent. In the case of metabolic dependency, microorganism reacts with metal ions and causes precipitation. In the case of metabolic independency, chemical interaction between metal ions and the cell surface will occur. For example, Zhou *et al*. (2005) reported that the complexation of lead(II) with nitrogen atoms in chitin followed by the hydrolysis of the lead-chitin complex caused the micro-precipitation of lead(II) in the cellulose/chitin beads.

2.6 Factors affecting biosorption

Heavy metal removal by microorganism is affected by several factors including the specific surface properties of the biomass, the methods of pretreatment, the presence of other cations or anions as well as the physicochemical parameters of the solution such as pH, temperature, initial metal ion concentration and biomass concentration (Sağ and Kutsal, 1996).

2.6.1 Effect of temperature

In general, temperature in the range of 20-35℃ seems not to affect the biosorption significantly (Aksu *et al*., 1992). Vilar *et al*. (2006) reported that the temperature range of 10-35℃ had no significant effect on lead(II) removal by algal waste and *Gelidium*. However, the biosorption capacity of lead(II) ions increased slightly with the further increase of the temperature, which indicated the endothermic nature of the process. Aksu and İşoğlu (2005) showed that copper(II) ion uptake by dried sugar beet pulp was affected by temperature. This material showed a drop in biosorption with an increase of temperature up to 45℃, which indicated that this process was exothermic. In most cases, high temperature is unsuitable for biosorption since the surface of the biomass may be damaged.

2.6.2 Effect of contact time

Contact time is one of the most important parameters affecting the amount of metal ions adsorbed on the biomass. Metal removal is relatively rapid in the initial stage of the biosorption process and the uptake of heavy metals slow down in the later stage because a large number of available sites are occupied by the metal ions.

2.6.3 Effect of pH

Solution pH is one of the most important parameters in the biosorption process. pH affects the solution chemistry of the metals, the activity of the functional groups on the biomass and the competition of metallic ions. At pH values below the isoelectric point of the biomass, the biomass surface will be surrounded by hydronium ions, which compete with the metal cations for the binding sites on the biomass. In contrast, at pH values above the isoelectric point, more ligands, such as amino and carboxyl groups, will be exposed and thus the biomass surface will carry a negative charge, which increases the attractive force between the biomass and metal ions, and hence increases the biosorption capacity (Kiran *et al*., 2005). Metal hydroxide will form as the solution pH further increases, which causes decrease in metal uptake. Thus, the metal uptake capacities would decrease significantly at very low or high pH values. The optimum pH value of the biosorption process depends on the nature of the biomass and metal ions. In most reported cases, the optimum pH value is between 4.0 and 8.0.

2.6.4 Effect of metal ion concentration

Abu Al-Rub *et al*. (2004) suggested that an increase in equilibrium metal

concentration could increase the driving force and decrease the mass transfer resistance of ions between the biomass and bulk fluid phases. Increase in the equilibrium metal concentration could also increase the number of collisions between metal ions and biomass. As a result, the metal biosorption capacity increased with the equilibrium metal concentration. Two common models are used for estimating the surface properties and affinities of the biosorbents. They are Langmuir and Freundlich isotherm models (Han *et al.*, 2005).

2.6.4.1 Langmuir isotherm model

Langmuir model is probably the most popular isotherm model for the description of biosorption equilibrium due to its simplicity and good agreement with experimental data. Langmuir model assumes that the biosorption occurs uniformly on the active sites of the biosorbent and no further sorption can take place on the sites which are already occupied by adsorbates (Volesky, 2003). The Langmuir isotherm model is represented as:

$$q = \frac{q_{\max} b C_e}{1 + b C_e} \qquad (1)$$

The linear form of the Eq. (1) is expressed as:

$$\frac{C_e}{q} = \frac{C_e}{q_{\max}} + \frac{1}{b q_{\max}} \qquad (2)$$

where C_e is the equilibrium metal concentration (mg/L); q is the amount of metal

ion adsorbed (mg/g-biomass); q_{max} is the maximum amount of metal adsorbed when the biosorbent surface is fully occupied by the metal ions (mg/g-biomass); and, *b* is the affinity between the biosorbate and biosorbent (L/mg).

2.6.4.2 Freundlich isotherm model

Freundlich model is based on the biosorption of metal ions onto heterogeneous surface and is represented as:

$$q = KC_e^{1/n} \qquad (3)$$

The linear form of the Eq. (3) is expressed as:

$$\ln q = \ln K + (\frac{1}{n}) \ln C_e \qquad (4)$$

where *K* and *n* are Freundlich constants.

2.6.5 Effect of biomass concentration

A decrease in the biomass concentration in solution will increase the metal biosorption capacity and reduce the metal biosorption percentage. Gong *et al*. (2005) reported that an increase in the biomass concentration of a bacterium, *Spirulina maxima*, would cause a decrease in lead(II) biosorption but the total percentage of lead(II) removal would increase accordingly. The decrease in the biosorption capacity may be due to an increase of the interferences between the

neighboring binding sites and the electrostatic interactions between biomass as well as an increase of the difficulty for well mixing in a condition of high biomass concentration (Fourest and Roux, 1992). However, the increase in total percentage removal with an increase of biomass concentration is mainly due to the total increase in binding sites on the biomass.

2.6.6 Effect of biomass pretreatment

Different pretreatment methods can be applied to enhance the amount of metal removal, including alkaline treatment, acid treatment, organic treatment, detergent treatment and heat treatment. The effect of pretreatment on biosorption mainly depends on the types of biomass studied. Kiran *et al*. (2005) studied the biosorption of lead(II) and copper(II) by pretreated *Neurospora crassa*. Various pretreatment methods with various chemicals including sodium hydroxide, acetic acid, dimethyl sulfoxide and detergent were reported. All treatment methods could improve the lead(II) and copper(II) uptake. Similar results were reported by Akar and Tunali (2005) using *Botrytis cinerea* as the biosorbent. However, Wang (2002) reported that the methanol-treated and formaldehyde-treated *Saccharomyces cerevisiae* could decrease the copper(II) biosorption capacity by 35% and 65%, respectively.

2.6.7 Effect of competitive cations

Various types of cations such as alkali metals, alkaline earth metals and heavy metals are present in industrial wastewater. The presence of these cations will increase the competition of binding sites and decrease the metal biosorption capacity. Wong *et al*. (2001) demonstrated that the copper(II) uptake of *Micrococcus* sp. was affected in the presence of lead(II), zinc(II) and nickel(II) ions.

2.6.8 Effect of counter anions

Anions such as chloride, nitrate, sulfate and acetate are common components in wastewater effluent. The presence of these anions could reduce the biosorption capacity of metal ions because stable complexes could be formed between metal ions and anions. As a result, fewer amounts of metals could be removed. Hashim and Chu (2004) found that a 10% loss in cadmium(II) uptake by *Sargassum baccularia* was observed in the presence of 3.24 mmol/L acetate, which caused the formation of $Cd(acetate)^{+}$ complex and decreased the cadmium(II) uptake by the biomass.

2.7 Regeneration of biosorbent

Desorption efficiency of the metal-laden biosorbent is an important parameter for the development of a continuous flow effluent treatment system (Saeed *et al*., 2005). In commercial application, biomass regeneration can help to reduce the operating cost, recover the adsorbed metal ions and regenerate the biosorbent for biosorption in the following cycles (Iqbal and Edyvean, 2003). A good desorption process should be able to elute the adsorbed metals (i.e., high desorption efficiency), and to maintain the stability of the biosorbent without any physico-chemical damage but with a reasonable metal uptake capacity in the following cycles (Volesky, 2001).

In general, desorbing agents can be divided into three main types: (1) mineral acids (e.g., nitric acid, hydrochloric acid and sulphuric acid); (2) aqueous mineral salt solution (e.g., sodium chloride and calcium chloride) and (3) complexing agents (e.g., citric acid, oxalic acid, tartaric acid and EDTA). Mineral acids act as proton exchangers, which compete with the metal ions for the binding sites. Sodium and calcium salts can provide competitive ions (Na^+ and Ca^+) to elute the adsorbed cations. Complexing agents can form stable complexes with metal ions and thus release them from the binding sites.

Vijayaraghavan *et al*. (2005) investigated the desorption efficiency of cobalt(II) and nickel(II) from *Sargassum wightii* by nitric acid, hydrochloric acid, sulphuric acid and calcium chloride. Mineral acids were reported to be better in comparison to calcium chloride due to their high elution efficiency. However, the biomass which has been exposed to the mineral acids would get more fragile with a weight loss of over 30% and appear to be unsuitable for the following cycles. The strong acidity of mineral acids would result in physico-chemical damage to the biosorbent. However, positive effect can be observed using mineral acids as the desorbing agent. Tunali and Akar (2006) found that hydrochloric acid could elute over 97% of zinc(II) ions from *Botrytis cinerea* without any detectable loss in biosorption capacity in the following cycles.

2.8 Immobilization of biomass

The use of microbial biomass in its native form for large-scale process is impracticable because of its small particle size, low density, poor mechanical strength, low rigidity and difficulty in separation from the liquid stream. Immobilization of biomass can solve these problems. Moreover, immobilized biomass performs better than freely-suspended biomass in batch reactor, packed bed reactor and fluidized bed reactor with benefits such as ease in separation from

the liquid stream, better capabilities of regeneration, reuse and recovery without destruction of the biosorbent (Sekhar *et al*., 2004). Immobilization may also enhance the metal biosorption capacity (Abu Al-Rub *et al*., 2004).

2.8.1 Immobilization methods

Various methods have been introduced to immobilize the biomass for a wide variety of applications. The immobilization process can be classified into four categories, which are based on the nature of the process and the material used. They are (1) adsorption on inert supports; (2) entrapment in polymeric matrix; (3) covalent bond formation between cells and vector compounds; and (4) cross-linking (Vegliò and Beolchini, 1997). These processes will be discussed in the following paragraphs.

(1) Adsorption on inert supports

Adsorption on inert supports is a physical immobilization method. Bai and Abraham (2003) studied chromium(VI) adsorption using *Rhizopus nigricans* immobilized on polyurethane foam cubes and coconut coir fibres. The inert supporting materials were sterilized and inoculated with starter culture. Then, the cells were incubated in the continuous culture for a period of time. They also

reported that this method was not as effective as the chemical entrapment methods. This could be due to poor linkage between the biomass and the supporting material, which caused detachment of the biomass during the biosorption process.

(2) Entrapment in polymeric matrix

Entrapment in polymer matrix is a chemical immobilization method. The biomass can be immobilized by entrapment in different matrices, including calcium alginate (Pan *et al*., 2005), polyacrylamide (Chang *et al*., 1998), polysulfone (Beolchini *et al*., 2003), polyethylenimine (Deng and Ting, 2005), polyisoprene (Bai and Abraham, 2003), and polyvinyl alcohol (PVA) (Stoll and Duncan, 1997). Selection of immobilization matrix is an important factor because it determines the mechanical strength and chemical resistance of the immobilized biosorbent. Ting and Sun (2000) compared the performances of PVA and calcium alginate for immobilizing the yeast biomass. A higher degree of mechanical and chemical strength was achieved using PVA only as the immobilization matrix. The PVA-immobilized biosorbent gave a lower mass transfer resistance than the Ca-alginate-immobilized biosorbent.

(3) Covalent bond formation between cells and vector compounds

Silica gel is the most common vector compound, which forms covalent bond

with cells. This technique is mainly used for algal immobilization. Rangsayatorn *et al*. (2004) used this technique to immobilize *Spirulina platensis* on silica gel for cadmium(II) biosorption.

(4) Cross-linking

In this method, biomass is immobilized by the formation of cross-linkage with cross-linking agents such as formaldehyde, glutaric dialdehyde, divinylsulfone, calcium alginate and formaldehyde-urea (Holan *et al.*, 1993). The cross-linking agent can form stable cellular aggregates with biosorbent. Lin and Lin (2005) reported that the epichlorohydrin could be used as cross-linking agent to increase the mechanical strength of the immobilized biosorbent.

2.8.2 Sol-gel matrix

Sol-gel matrix is a novel material for enzyme and biomass immobilization. Sol-gel process generally involves the transition of a colloidal suspension "sol" into a solid "gel" phase. Encapsulation of biomass in sol-gel matrix typically involves the use of metal alkoxide precursors $M(OR)_n$ where M is metal (e.g., Al, Si, Ti) and R is alkyl group (e.g., Me, Et) (Dunn *et al*., 1998). The most common precursors used are tetramethoxysilane (TMOS) or tetraethoxysilane

(TEOS). Hydrolysis and condensation reactions of these precursors cause the formation of gel network as follows (Livage, 1997):

$$(RO)_3SiOR + H_2O \longrightarrow (RO)_3SiOH + ROH \qquad \textbf{(Hydrolysis)}$$

$$(RO)_3SiOH + ROSi(OR)_3 \longrightarrow (RO)_3Si\text{-}O\text{-}Si(OR)_3 + ROH \qquad \textbf{(Condensation)}$$

As the condensation reaction continues, the degree of cross-linking between particles increases with an increase of viscosity. Alcohol and water produced in the hydrolysis and condensation reactions will be evaporated, which results in the shrinkage of the matrix. After gel shrinkage, the pore size and pore wall strength will change. Finally, the viscous material solidifies and leads to the formation of a porous gel. The physical characteristics of the gel network depend on the size of the particles and the extent of cross-linking before gelation (Hench, 1998).

The sol-gel process offers several advantages:

1. Compared with organic cross-linking agents, such as epichlorohydrin, inorganic silica is non-toxic (Kursawe *et al.*, 1998) and it gives a more chemically and mechanically stable matrix (Ahn *et al.*, 1998);
2. Highly porous materials and nanocrystalline materials can be produced;
3. Possibility to attach the organic and biological species to porous silicate material via covalent bonding;

4. The pore size and mechanical strength of the sol-gel matrix are easily controlled by changing the drying conditions.

The sol-gel matrix is porous enough to allow small molecules to diffuse through. Moreover, the matrix is hard enough to withstand pressure during column applications (Marseaut *et al*., 2004). The sol-gel process has been used in many studies to immobilize enzymes and cells for a wide variety of applications, such as production of biosensors and biocatalysts (Avnir *et al*., 2006; Kwok *et al*., 2005; Livage, 1997). These studies showed that the enzymes and cells could retain their biological activity, reactivity, and chemical functionality after they were encapsulated in the sol-gel matrix. Braun *et al*. (1990) reported that alkaline phosphatase encapsulated in the sol-gel matrix could retain its biocatalytical activity. The application of sol-gel process for removal of pollutants has gained considerable attention. Szilva *et al*. (1998) and Marseaut *et al*. (2004) found that the yeast cell wall (*Saccharomyces cerevisiae*) could be immobilized in the sol-gel matrix and it could give large copper(II) and cadmium(II) biosorption capacities in column experiment. Bányik *et al*. (2000) reported that a mixed microbial culture (*Stenotrophomonas maltophilia*, *Ochrobactrum anthropi* and *Moraxella* sp.) encapsulated in the sol-gel matrix

could be used for the degradation of phenol. The sol-gel matrix has been demonstrated to be an excellent material for enzyme and cell immobilization. However, only a limited number of studies have investigated the applicability of the sol-gel matrix for immobilizing bacterial cells for heavy metal removal.

2.8.3 Polyvinyl alcohol

Polyvinyl alcohol (PVA) is a water-soluble polymer which can be synthesized by the hydrolysis of polyvinyl acetate. Its physical properties depend on the degree of polymerization and the percentage of hydrolysis. PVA can resist oils, greases and hydrocarbon solvents. Recently, PVA has been used as an alternative immobilization matrix due to its economical large-scale production, non-toxicity to biomaterials, as well as chemical and mechanical stabilities during applications (Chu and Hashim, 2007; Ting and Sun, 2000). PVA has been added to the sol-gel mixture for increasing the stability of the entrapped *Bacillus licheniformis, Dietzia maris and Marinobacter marinus* (Lin *et al*., 2006). Nakane *et al*. (1999) reported that the PVA and silica could associate well with interactions such as hydrogen bond. However, no study has been reported on the removal of heavy metals using bacterial cells encapsulated in the sol-gel matrix containing PVA.

2.9 Reactors for biosorption processes

There are several types of reactors employed in ion exchange and adsorption processes, which are generally classified as batch, semicontinuous-flow and continuous-flow systems (Volesky, 1990). Batch stirred tank reactor, continuous stirred tank reactor, fluidized bed reactor and packed bed reactor are commonly applied in these processes. These choices of reactor system arrangements can be used in biosorption process. Each type of reactor has its own advantages and drawbacks, and this will be discussed in the following sections.

2.9.1 Batch stirred tank reactor

The biomass is dispersed throughout a stirred tank reactor. Therefore, the stirring rate should be controlled appropriately to prevent any damage of the biosorbent by the impeller. To separate the metal-laden biosorbent from wastewater, a solid/liquid separation technique is required. The most common techniques are sedimentation, centrifugation, filtration and magnetic separation (Lovley, 2000). However, the main disadvantage of this reactor is the loss of biosorbent during the separation process. The collected metal-laden biosorbent can then be regenerated and reused afterwards (Volesky, 1990).

2.9.2 Continuous stirred tank reactor

The contact vessel of this reactor is similar to the batch stirred tank reactor. However, this reactor is operated under a continuous feed of the metal-laden solution until the biosorbent becomes saturated with metal. The biosorbent used in this reactor is in a powder or granular form. After the biosorption process, a solid/liquid separation process is required to separate the metal-laden biosorbent from the wastewater. The main disadvantage of this reactor is the low concentration gradient between the metal solution and the biosorbent (Volesky and Naja, 2005). The concentration of the metal in the reactor is the same as that in the effluent. In order to improve the biosorption process and assure the effluent standards, a series of reactors are often utilized to treat the wastewater. Counter-current flow between the metal-laden wastewater and the biosorbent is more efficient than the co-current flow. In a counter-current scheme, the fresh biosorbent is always fed to the reactor containing the lowest adsorbate concentration and it leaves the process after contacting with the most adsorbate-rich wastewater. Therefore, the biosorbent leaving the process is saturated with the highest metal concentration.

The performance of the packed-bed reactor can be approached in a series of

counter-current stirred tank reactors as the number of reactors approaches infinity (Volesky and Naja, 2005).

2.9.3 Fluidized bed reactor

In this type of reactor, the metal-laden solution is continuously flowing upward through the biomass particles in a column. The flow rate should be high enough and balanced with the size and density of the biomass to maintain the biosorbent in a low-dense bed without any elution of the biosorbent (Olguin *et al*., 2000). This reactor can avoid the clogging problem. However, the biosorbent occupies a large volume in the column. Therefore, its space efficiency is not as good as that in the packed bed reactor. Moreover, the conditions in this reactor may not be easily controlled and the biosorbent may easily be lost from the reactor (Volesky, 1990; Lovley, 2000). One major disadvantage of this reactor system is the low concentration gradient between the metal solution and the biosorbent (Volesky and Naja, 2005).

2.9.4 Packed bed reactor

The packed bed reactor is the most convenient process in a continuous-flow system. This type of reactor is usually packed with the immobilized cells (Chang *et al*., 1998). The metal-laden solution usually passes through the column in a downflow arrangement. Granules of the biosorbent should be large enough (1 mm to 3 mm) to prevent excessive pressure drop across the column. The diameter and height of the column are typically not more than 1.5 m and 5 m, respectively. The solution flows to the end of the reactor is contacting with a relatively fresh biosorbent. The packed bed reactor has several advantages. First, it provides a simple process and high yield operation, which can be easily scaled up in laboratory. Second, the stages in the separation protocol can be automated and a high degree of purification can often be achieved in a single-step process (Aksu and Kutsal, 1998). The main disadvantage is that the column could be clogged if the wastewater contains a significantly high concentration of suspended solids (Lovley, 2000). Deposition of the solid in the column causes a high pressure drop and the process cannot be continued (Volesky, 1990).

2.10 Conclusion to the chapter

This chapter provides an understanding of the previous research in this area. Current technologies for heavy metal removal provide only partially effective treatment. The use of biosorption process for heavy metal removal has gained considerable attention. However, the use of freely-suspended biomass for biosorption is impractical. Therefore, different immobilization techniques have been developed to improve the biosorption process. Little empirical research has been conducted to immobilize the bacterial cells using the sol-gel process for heavy metal removal. Thus, this research mainly aimed to develop a novel and cost-effective process, which employed sol-gel/PVA matrix for immobilizing bacterial cells, for removing and recovering copper(II) ions from wastewater. The materials and methods will be discussed in the next chapter.

Chapter 3. Materials and Methods

3.1 Introduction to the chapter

This chapter describes the research materials and methods used in this study. It firstly describes the instruments and chemicals used in the experiment. The procedures used for the data collection will then be presented. Biomass immobilization is one of the most important steps in this study. Therefore, the procedures for the preparation and immobilization of *Micrococcus* sp. will be described. The preparation procedures of sol-gel encapsulated *Micrococcus* sp. with spherical and cylindrical shapes will be presented. The procedures and experimental conditions of the biosorption studies (effects of contact time, agitation speed, pH, copper(II) concentration and sodium concentration) and the desorption studies (screening of desorbing agent and desorption kinetics) will be reported. The procedures of the biosorption/desorption cycles will then be presented. The procedures used for investigating the surface morphology of the immobilized biosorbents will be described. Finally, the operation of a four-stage semi-continuous immobilized cell batch reactor system for the removal and recovery of copper(II) ions will be reported and discussed.

3.2 Instrumentation

Growth media and other equipments were sterilized in an autoclave machine operating at 121℃ for 20 min (Tokyo Hirayama HA-300MIV). The cells of *Micrococcus* sp. were inoculated in an agar plate and incubated at 37℃ in an LEEC incubator. Single colonies on the plate were cultivated on 2XTY medium containing glucose on an orbital shaker (Unitwist 400) operating at 37℃. The culture was further incubated in a 15-L fermentor (B. Braun model BIOSTAT® C). Optical density of the culture was measured by a Spectronic GENESYS™ VIS spectrophotometer. The cells were harvested and centrifuged by Beckman J2-M1 and J2-21 centrifuge machines and then dried in a Heto FD8 freeze dryer. Biosorption and desorption experiments were conducted at 25℃ on an orbital shaker (Unitwist 400). The solution pH of all samples was measured by an Orion 920 pH meter. The metal concentration of the samples was analyzed by a Perkin Elmer AAnalyst 100 atomic absorption spectrophotometer (AAS). The organic carbon of the samples was analyzed by a Shimadzu TOC-5000A analyzer. The surface of the biosorbents was observed by a Leica Stereoscan 440 scanning electron microscope (SEM).

3.3 Chemicals

Standards, chemicals and samples were prepared and diluted in distilled and deionized (DDI) water. Copper(II) stock solution was prepared by dissolving a desired quantity of copper sulfate (A.R. grade) in DDI water. For the calibration of the atomic absorption spectrophotometer, spectroscopic grade copper(II) standard solution was used and diluted to corresponding concentrations.

3.4 Preparation of *Micrococcus* sp.

Micrococcus sp. was first inoculated in a nutrient agar plate (Oxoid). Colonies of the cells were inoculated and then incubated in two sterilized 1-L Erlenmeyer flasks containing 500 mL of 2XTY medium for 19 h at 37℃ and 250 rpm shaking rate. The 2XTY medium was composed of 16 g/L tryptone, 10 g/L yeast extract, 5 g/L NaCl and 10 g/L glucose. The cultivated cells in the Erlenmeyer flasks were then transferred and grown in a fermentor containing 9 L of sterilized 2XTY medium at pH 7.0 and 37℃. The growth conditions in fermentor were controlled with pO_2 of 20%, stirring speed from 200 rpm to 1000 rpm and flow rate from 2 L/min to 26 L/min. Optical density of the culture was monitored periodically by a VIS spectrophotometer at 600 nm. The cells were harvested, centrifuged and then washed twice with DDI water. The washed cells

were then freeze-dried for two days to remove any remaining water. Finally, the cells were grounded by a mortar and pestle and then stored at 4℃.

3.5 Preparation of immobilized biomass biosorbent

3.5.1 Encapsulation of cells in sol-gel/PVA matrix

A sol-gel stock solution containing tetraethyloxysilane (TEOS), methyltrimethoxysilane (MTMS) and 0.01 M HCl in the volume ratio of 2.10:1.00:1.40 was mixed with 8% w/w polyvinyl alcohol (PVA, molecular weight 146000-186000) in the volume ratio of 1:2 (v/v). The silica sol/polymer mixture was then mixed with 200 g/L *Micrococcus* sp. cell suspension in a ratio of 3:1 (v/v). The sol-gel control was prepared using DDI water instead of cell suspension to mix with the silica sol/polymer mixture. Biosorbents with two different shapes (spherical and cylindrical) were prepared in this study for investigating their copper(II) removal ability.

Spherical shape

Biosorbent with a spherical shape was prepared by dropping the silica sol/polymer/cell mixture into liquid nitrogen. The biosorbent was then shaped at -18℃ for one day followed by drying at 4℃ in the refrigerator for two days.

Cylindrical shape

Biosorbent with a cylindrical shape was prepared in a small cylindrical mold and allowed to dry at 4℃ in the refrigerator for three days. The diameter, thickness and volume of the cylindrical mold were 8 mm, 5 mm and 0.27 mL, respectively.

3.5.2 Immobilization of *Micrococcus* sp.

The copper(II) biosorption capacities of the sol-gel/PVA matrix with and without encapsulated *Micrococcus* sp. were investigated. The biosorption experiment was performed by mixing the same amount of sol-gel control or sol-gel/PVA encapsulated biosorbent, which was prepared by either TMOS or TEOS precursor with both cylindrical and spherical shapes. The biosorption experiments were conducted according to the procedures described in Section 3.6.1.

3.5.3 Optimization of immobilization agent

Different metal alkoxide precursors in sol-gel stock solution

The biosorbents with both spherical and cylindrical shapes were prepared using two different metal alkoxide precursors (TMOS or TEOS). The

biosorption experiments were then conducted according to the procedures described in Section 3.6.1.

Ratio of composition in sol-gel stock solution

The biosorbents were prepared by changing the ratio of the sol-gel composition. The composition of the sol-gel stock solution is listed in Table 3.1. The biosorption experiments were then carried out according to the procedures described in Section 3.6.1.

Table 3.1. Composition of sol-gel stock solution.

Biosorbent	TEOS (mL)	MTMS (mL)	HCl (mL)
A	4.20	1.00	1.40
B	1.05	1.00	1.40
C	2.10	0.51	1.40
D	2.10	2.10	1.40
E	2.10	1.00	0.51
F	2.10	1.00	2.10
G	2.10	1.00	1.40

Ratio of sol-gel stock solution to PVA

The ratio of the sol-gel stock solution to PVA was also studied and the detailed information is listed in Table 3.2. The biosorption experiments were then conducted according to the procedures described in Section 3.6.1.

Table 3.2. Volume ratio of sol-gel stock solution to PVA for the preparation of biosorbents.

Biosorbent	Sol-gel stock solution (mL)	PVA (mL)
H	1	1
I	1	2
J	1	3

3.5.4 Optimization of drying time on immobilized biosorbent

The procedures for the preparation of biosorbents with different drying time were similar to those described in Section 3.5.1. The cylindrical biosorbents were prepared and allowed to dry at 4℃ for two days, three days, four days, five days and six days. The spherical biosorbents were prepared and allowed to dry at 4℃ for one day, two days, three days, four days and five days. The biosorption experiments were then carried out according to the procedures described in Section 3.6.1.

3.5.5 Optimization of biomass concentration in immobilized biosorbent

The effect of biomass concentration in biosorbent on copper(II) removal was studied by preparing 40 g/L, 100 g/L and 200 g/L cell suspensions. The immobilized biosorbents were then prepared according to the procedures described in Section 3.5.1. The resulting biomass concentration in the

sol-gel/PVA matrix was 10 g/L, 25 g/L and 40 g/L. In order to obtain a 1.5 g/L biomass concentration in the biosorption reactor, different amounts of immobilized biosorbent were added to the reactor. The biosorption experiments were then carried out according to the procedures described in Section 3.6.1.

3.6 Biosorption studies

3.6.1 Basic experimental procedures

Batch experiments were conducted to investigate the copper(II) biosorption by the sol-gel encapsulated *Micrococcus* sp. One hundred mg/L copper(II) solution was prepared and adjusted to pH 5.0 using diluted HNO_3 or NaOH. A suitable amount of immobilized biosorbent was mixed with 100 mg/L copper(II) solution in a 50-mL polypropylene tube to obtain a final biomass concentration of 1.5 g/L. For control, only copper(II) solution was added to the polypropylene tube without addition of the biosorbent. The solution pH was re-adjusted to 5.0. The polypropylene tubes containing the mixture were agitated on an orbital shaker operating at 25℃ and 250 rpm for 24 h. The solution pH was adjusted to 5.0 after 3 h and 21 h. Samples were collected after 3 h and 24 h and were acidified by adding concentrated nitric acid. The copper(II) concentration of these samples was then determined by AAS (Perkin Elmer AAnalyst 100) at a

wavelength of 324.8 nm. The copper(II) biosorption capacity of the biomass was calculated using the following equation:

$$q = \frac{V(C_i - C_e)}{W} \qquad (5)$$

where q is the metal biosorption capacity (mg/g-biomass); V is the volume of metal solution (L); W is the amount of biomass (g); and, C_i and C_e are the initial and equilibrium metal concentrations (mg/L), respectively.

3.6.2 Effect of contact time

Effect of contact time on copper(II) biosorption by spherical and cylindrical biosorbents were studied in 500-mL Nalgene polypropylene bottles containing 150 mL of 100 mg/L copper(II) solution. A suitable amount of biosorbents was added to the bottle in order to obtain a final biomass concentration of 1.5 g/L. The solution pH was then adjusted to 5.0. Samples were then taken at predetermined time intervals ranging from 1 min to 1620 min and retained for copper(II) analysis. The pseudo-first order and pseudo-second order kinetic models were used for the modelling of the experimental kinetic data with both linear and non-linear regression analyses. For non-linear regression analysis, computer software (GraphPad Prism 3.0) was used to analyse the experimental data.

3.6.3 Effect of agitation speed on kinetic profiles

The effect of agitation speed on the kinetic profiles was investigated to determine the biosorption rate under different agitation speeds. The experimental procedures were similar to those described in Section 3.6.2. The agitation speed ranging from 0 rpm to 300 rpm was examined.

3.6.4 Effect of pH

The effect of pH on copper(II) removal was studied in 100 mg/L copper(II) solution with an initial pH from 2.0 to 6.0. The biosorption experiments were then carried out according to the procedures described in Section 3.6.1.

3.6.5 Effect of biomass dosage

The copper(II) biosorption efficiency and biosorption capacity with biomass dosage in the range of 0.5 g/L to 3 g/L were investigated. The biosorption experiments were then conducted according to the procedures described in Section 3.6.1.

3.6.6 Biosorption isotherms

Equilibrium biosorption isotherm was determined with an initial copper(II)

concentration in the range of 10 mg/L to 200 mg/L and a biomass concentration of 1.5 g/L at pH 5.0. The biosorption experiments were then conducted according to the procedures described in Section 3.6.1. The Langmuir and Freundlich isotherm models were used for the modelling of the experimental biosorption equilibrium data with both linear and non-linear regression analyses.

3.6.7 Effect of sodium ions

Sodium sulphate was used for the preparation of sodium solution. The effect of sodium ions on copper(II) uptake was investigated by mixing 50 mg/L copper(II) solution with sodium sulphate solution ranging from 0 mg/L to 500 mg/L. The solution pH was then adjusted to 5.0. A suitable amount of spherical biosorbents was added to the mixture in order to obtain a final biomass concentration of 1.5 g/L. The mixture was agitated on an orbital shaker operating at 25℃ and 250 rpm for 24 h.

3.7 Desorption studies

3.7.1 Screening of desorbing agents

Copper(II)-laden biosorbents were eluted using nine different desorbing agents, including mineral acids (0.1 M HCl, 0.1 M HNO_3 and 0.05 M H_2SO_4),

complexing agents [0.1 M citric acid (CA), 0.1 M ethylenediaminetetra-acetic acid disodium salt dehydrate (EDTA) and 0.1 M nitrilotriacetic acid disodium salt (NTA)], salts (0.1 M $Na_5P_5O_{10}$ and 0.1 M $CaCl_2$) and DDI water. After the biosorption process was carried out as described in Section 3.6.1, biosorbents were washed using DDI water and mixed with 10 mL desorbing agent to obtain a final biomass concentration of 4.5 g/L. The suspension was then agitated at 250 rpm and 25℃ for 6 h. Samples were then collected and analyzed to determine the concentration of eluted copper(II) by AAS.

3.7.2 Desorption kinetics

Desorption kinetic studies were performed to determine the minimal equilibrium time required for eluting the copper(II) ions using two selected desorbing agents (0.1 M HNO_3 and 0.1 M NTA). After the biosorption process was carried out as described in Section 3.6.2, biosorbents were washed using DDI water and mixed with 50 mL desorbing agent to obtain a final biomass concentration of 4.5 g/L. The suspension was then agitated at 250 rpm and 25℃ for 7 h. Samples were collected at predetermined time intervals ranging from 1 min to 420 min for copper(II) analysis by AAS.

3.8 Biosorption/desorption cycles

3.8.1 Basic experimental procedures

After the biosorption process was carried out as described in Section 3.6.1, the copper(II)-laden biosorbents were washed with DDI water. The biosorbents were then mixed with 10 mL desorbing agent to obtain a final biomass concentration of 4.5 g/L. The mixture was agitated at 250 rpm and 25℃ for a required period of time. The regenerated biosorbents were separated from the desorbing agent and then washed with DDI water in order to remove the residual desorbing agent. The biosorbents were again mixed with 100 mg/L copper(II) solution for the next biosorption run. The biosorption/desorption process was repeated at least three times.

3.8.2 Effect of desorption time

Two selected desorbing agents, 0.1 M HNO_3 and 0.1 M NTA, were used to elute copper(II) ions from the cylindrical and spherical biosorbents, respectively. Different desorption time was used to elute the copper(II) ions. The biosorbents were desorbed by contacting with 0.1 M HNO_3 for 3 h and 6 h. On the other hand, the biosorbents were eluted by contacting with 0.1 M NTA for 4 h and 6 h. The copper(II) biosorption/desorption cycles were then carried out according to

the procedures described in Section 3.8.1.

3.8.3 Effect of NTA pretreatment

Effect of NTA pretreatment on the spherical biosorbent was conducted to compare the copper(II) biosorption and desorption ability between the NTA-treated and non-treated biosorbents. In order to evaluate the potential of NTA for increasing or decreasing the copper(II) biosorption capacity of the biosorbent in the biosorption/desorption cycles, spherical biosorbent was first treated by 10 ml of 0.1 M NTA for 6 h. After the pretreatment process, the biosorbent was washed with DDI water to remove the NTA solution. The copper(II) biosorption/desorption cycles were then carried out according to the procedures described in Section 3.8.1. The copper(II)-laden biosorbents were desorbed by 0.1 M NTA for 6 h.

3.8.4 Effect of NTA concentration

In order to find out the optimum concentration of NTA for copper(II) desorption, copper(II)-laden biosorbent was recovered by different concentrations of NTA. Copper(II) ions were eluted from the spherical biosorbent for 6 h using 0.010 M, 0.050 M, 0.075 M, 0.100 M and 0.200 M NTA . The copper(II)

biosorption/desorption cycles were then carried out according to the procedures described in Section 3.8.1.

3.8.5 Comparison of performances of suspended cells and immobilized cells

Copper(II) biosorption/desorption cycles of the suspended cells were also conducted to compare their biosorption performances with the immobilized cells. The experimental conditions of the biosorption and desorption processes used for the suspended cells were similar to those used for the immobilized cells. A suitable amount of suspended cells or spherical biosorbent was mixed with 100 mg/L copper(II) solution to obtain a final biomass concentration of 1.5 g/L. After the biosorption process was carried out, the copper(II)-laden biomass was then mixed with 10 mL of 0.1 M NTA for copper(II) desorption. The suspension was agitated at 250 rpm and 25℃ for 6 h. The biosorption/desorption process was repeated for six times.

3.9 Composition of industrial wastewater

Industrial wastewater was collected from a local electroplating plant. The composition in wastewater was measured using different analytical methods. The concentrations of copper(II), chromium(III), lead(II), nickel(II), zinc(II),

cadmium(II) and sodium were determined by AAS. The total carbon, inorganic carbon and total organic carbon content were analysed by a TOC analyzer (Shimadzu TOC-5000A).

3.10 Semi-continuous batch reactor system

A series of four-stage semi-continuous immobilized cell batch reactor system was applied to determine the copper(II) removal as well as the recovery efficiencies of the spherical and cylindrical biosorbents for treating the synthetic and industrial wastewater. In the first stage, a suitable amount of spherical biosorbent was added into a 500-mL polypropylene bottle containing 200 mL of 50 mg/L copper(II) solution at pH 5.0. The final biomass concentration in the first reactor was 1.5 g/L. The reactor was agitated continuously at 250 rpm and 25℃ for 24 h. Wastewater was fed counter-currently to the biosorbent. The fresh copper(II)-laden wastewater was always fed into reactor 1 and the treated effluent was always discharged from reactor 4 as shown in Figs. 3.1(a) to 3.1(d). A calibrated peristaltic pump was used to transfer the copper(II) solution from one reactor to the next reactor and a 5% remaining solution was used for copper(II) analysis. In the first cycle, the copper(II)-laden biosorbent (B1) was removed from reactor 1 after the biosorption process (Figs. 3.1(a)). The biosorbent (B1)

was then regenerated by mixing with 50 mL of 0.1 M NTA for 6 h. The regenerated biosorbent (B1) was then fed into reactor 4 in the second cycle and reused for biosorption (Fig. 3.1(b)). The copper(II)-laden biosorbent removed from reactor 1 was always regenerated and it was then transferred to reactor 4 for the next biosorption run. Copper(II)-laden biosorbent (B2) was removed from reactor 2 after the biosorption process in the first cycle and then transferred to reactor 1 for biosorption in the second cycle. Similarly, the copper(II)-laden biosorbent (B3) was removed from reactor 3 after the biosorption process in cycle 1 and then transferred to reactor 2 in cycle 2 followed by transferring to reactor 1 in cycle 3 for biosorption. The biosorption and desorption processes were repeated for eight cycles. From cycles 1 to 4, all immobilized biosorbents (B1, B2, B3 and B4) were regenerated and one circulation was completed. The second circulation was continued in cycles 5 to 8, the flow of the biosorbents was the same as that of cycles 1 to 4 in the first circulation.

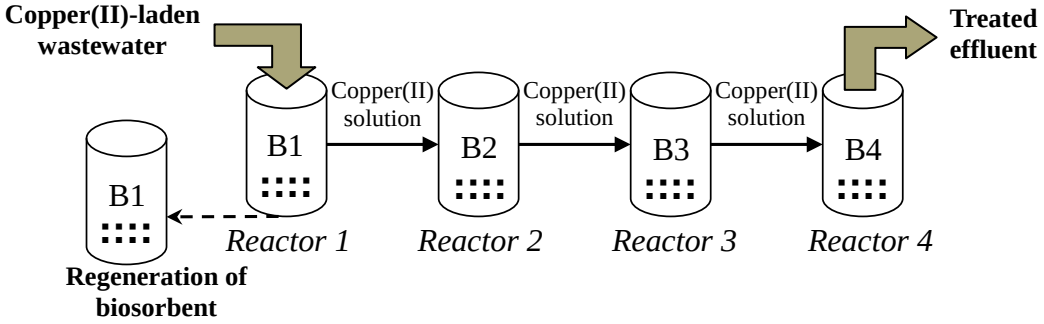

Figure 3.1(a). Scheme of the first cycle in a four-stage semi-continuous batch reactor system.

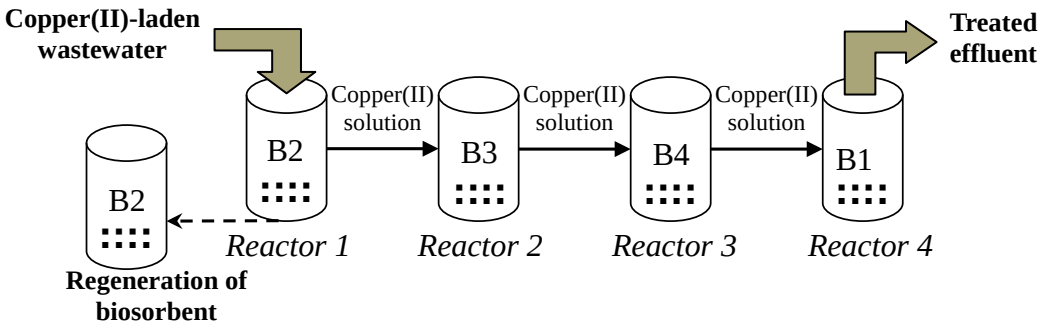

Figure 3.1(b). Scheme of the second cycle in a four-stage semi-continuous batch reactor system.

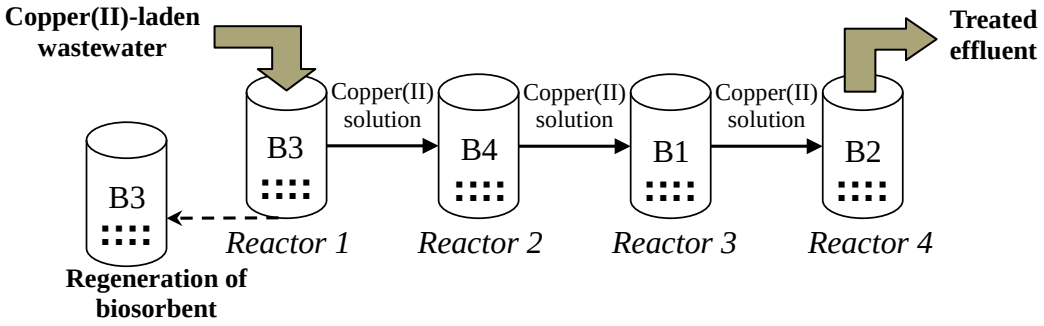

Figure 3.1(c). Scheme of the third cycle in a four-stage semi-continuous batch reactor system.

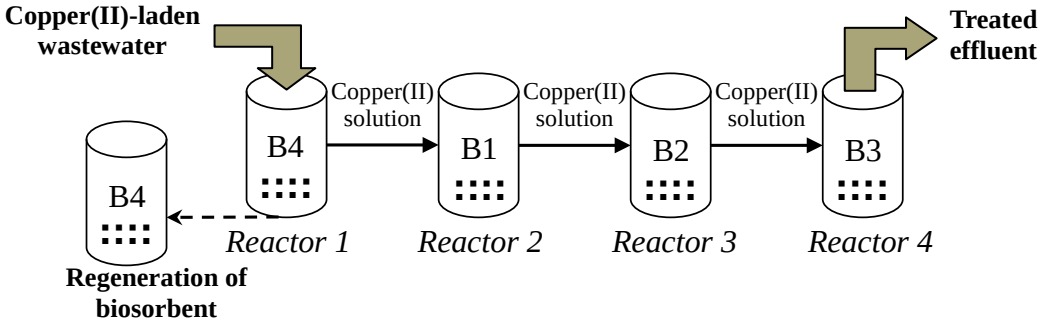

Figure 3.1(d). Scheme of the fourth cycle in a four-stage semi-continuous batch reactor system.

3.11 Scanning electron microscopy

The surface morphology of the immobilized biosorbents before and after copper(II) biosorption was examined using a scanning electron microscope (Stereoscan 440, Leica). The biosorbents were initially dried in an oven at 50℃ for three days followed by coating with a thin layer of gold by Polaron SC502 Sputter Coater. The biosorbents were analyzed by SEM with an acceleration voltage of 20 kV afterwards.

3.12 Statistical analysis

To ensure the accuracy, reliability, and reproducibility of the collected data, all the experiments were carried out in duplicate. The mean value and standard deviation of the data were presented. Statistical analysis was performed using a Student's *t*-test to compare the numerical difference between two sets of data. The analysis of variance (ANOVA) was employed to compare the significant difference between three or more categorical data. After performing ANOVA test, Tukey's HSD test was employed to compare the means of two categorical data. At a significance level of 0.05, all the calculated p values ≤ 0.05 were considered as statistically significance.

Chapter 4. Results and Discussion

4.1 Preparation of immobilized biomass biosorbent

Biological material in its freely-suspended form is impractical for biosorption of heavy metals. The use of suspended cells in the biosorption process presents serious problems, including difficulty in biomass separation, low mechanical strength and low rigidity. Suspended cells are also unsuitable for column application since they tend to clump together and increase pressure drop across the column. As a result, excessive hydrostatic pressure is required to attain a suitable flow rate.

In order to enhance the mechanical strength of the biomass, different immobilization techniques have been introduced. Immobilization of biomass in a compact, accessible and recoverable form, such as pellets, granules or beads, can overcome the disadvantages in the use of suspended cells (Wase and Forster, 1997). Immobilization can improve the biomass rigidity and facilitate the biomass separation from the metal-laden wastewater (Zouboulis *et al*., 2003) while it allows the solutes to diffuse to and from the biomass (Olguin *et al*., 2000). The loss of biomass from the immobilized biosorbent is less than that from the suspended cells, therefore the maintenance cost can be reduced (Ashley and Roach, 1989). Immobilization allows high biomass loading with minimal

clogging in a continuous flow system. There are several disadvantages exist in using the immobilized cells, which included high cost, blockage of some functional groups, and low mass transfer rate. The biosorption efficiency of the immobilized cells may thus be reduced.

In this study, a combination of sol-gel technique with entrapment in PVA was applied to immobilize the cells of *Micrococcus* sp. Sol-gel process is a versatile technique for the formation of various amorphous materials. The colloidal suspensions (sol) are first converted to viscous gels. Solid materials with three-dimensional network are then formed by linking the colloidal particles and condensed silica. The structure, texture and property of the immobilized biosorbent are affected by several parameters, such as composition of the starting materials, method of immobilization, drying temperature and drying time.

Cells of *Micrococcus* sp. were immobilized in sol-gel/PVA matrix with two different shapes, spherical and cylindrical, in this research. The spherical immobilized biosorbent was prepared by dropping the silica sol/polymer/cell mixture into liquid nitrogen. The immobilized biosorbent could not maintain its spherical shape once it was withdrawn from liquid nitrogen, unless it was kept at

-18℃ for one more day. The spherical biosorbent was further dried at 4℃ for two days. After drying, the surface area of the spherical biosorbent was reduced from 29.56 ± 2.89 mm^2 (diameter of biosorbent: 3.06 ± 0.15 mm) to 3.14 ± 0.22 mm^2 (diameter of biosorbent: 1.00 ± 0.10 mm). The mechanical strength of the spherical biosorbent increased with drying time until all water and volatile components were evaporated.

The sol-gel solution can also be easily cased in a mould of cylindrical shape (surface area: 226 mm^2) to obtain a cylindrical biosorbent. The selection of a suitable mould is important in order to prevent the adhesion of gel or the nucleation of bubbles at the mould-gel interface. The cylindrical mould used for the preparation of the cylindrical biosorbent is made of polypropylene material. Polypropylene is a good moulding material since the dried biosorbent can be separated from the mould easily without adhesion of gel in the mould. Similar to the spherical biosorbent, the mechanical strength of the cylindrical biosorbent increased with drying time. After drying at 4℃ for three days, the surface area of the cylindrical biosorbent shrunk significantly from 226.19 mm^2 (diameter: 8.00 mm; thickness: 5.00 mm) to 72.10 ± 5.67 mm^2 (diameter: 5.40 ± 0.42 mm; thickness: 1.55 ± 0.21 mm).

4.1.1 Immobilization of *Micrococcus* sp.

In order to investigate the copper(II) biosorption by the immobilized *Micrococcus* sp., the copper(II) uptake of the sol-gel/PVA matrix with and without biomass were examined and compared. Figs. 4.1(a) and 4.1(b) illustrate the amount of copper(II) uptake by the TMOS-encapsulated and TEOS-encapsulated biosorbents, respectively. The sol-gel/PVA material consisting TMOS or TEOS were also incapable of removing copper(II) ions. However, the copper(II) uptake increased significantly after the *Micrococcus* sp. was encapsulated in the sol-gel/PVA matrix (*t*-test, $p < 0.05$). The amount of copper(II) uptake by the sol-gel/PVA encapsulated biosorbents ($\geq$ 0.7 mg) was larger than that by the sol-gel/PVA matrix without biomass ($\leq$ 0.05 mg).

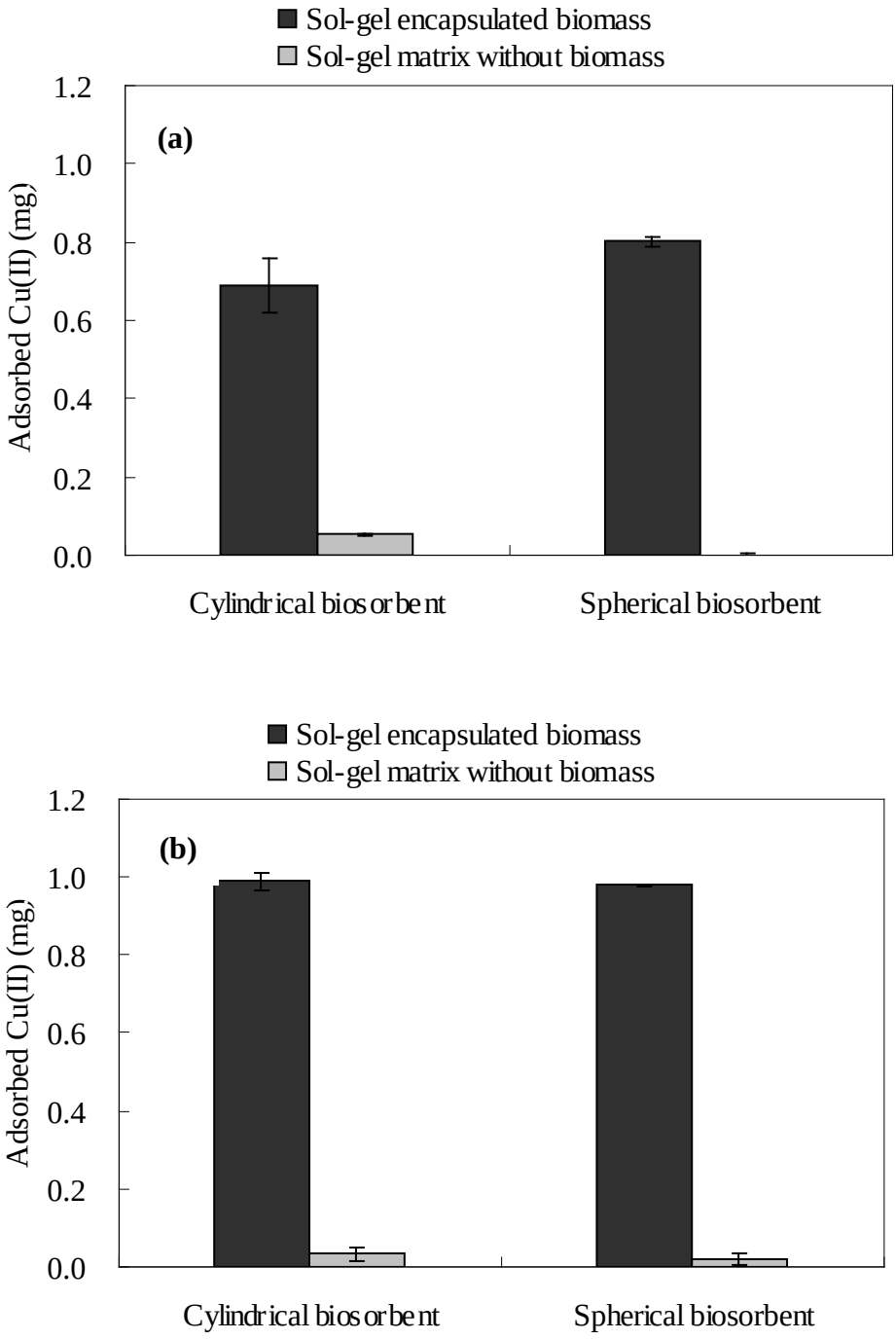

Figure 4.1. Amount of copper(II) adsorbed by (a) TMOS matrix and (b) TEOS matrix with and without the encapsulated biomass.

[Experimental conditions: initial copper(II) concentration = 100 mg/L; contact time = 24 h; agitation speed = 250 rpm; pH = 5]

4.1.2 Optimization of the composition of immobilization agent

The major chemicals used in the sol-gel process to immobilize the *Micrococcus* sp. include TMOS or TEOS, MTMS, HCl and PVA. The ratio of these chemicals used to immobilize the *Micrococcus* sp. was optimized and studied for the removal of copper(II) ions.

Either TMOS or TEOS can be used as a metal alkoxide precursor, which is the basic starting chemical in preparing sol-gel matrix. Both TMOS and TEOS can easily hydrolyze in the presence of water and induce the formation of porous gel with an oxide network. However, the larger ethoxy groups in TEOS may provide a stronger steric hindrance and cause overcrowding of the transition state during hydrolysis (Fig. 4.2), resulting in slower reaction rates (Wright and Sommerdijk, 2001).

Immobilized biosorbents were prepared using TMOS or TEOS as precursor. For the immobilization process, the composition ratio of TMOS(or TEOS):MTMS:HCl was 2.10:1.00:1.40 and the ratio of sol-gel stock solution to PVA was 1:2. The concentration of biomass encapsulated in the sol-gel/PVA matrix was 40 g/L. Table 4.1 lists the surface areas of the cylindrical

biosorbent prepared by the two different precursors. The surface area of the cylindrical biosorbent prepared by TMOS was significantly smaller than that prepared by TEOS (*t*-test, $p < 0.05$). The surface area obtained was smaller because of the faster drying rate of the sol-gel/PVA matrix containing TMOS. Table 4.1 also shows that the copper(II) biosorption capacities of the biosorbents prepared by different precursors were different, with that of the TEOS-encapsulated cylindrical biosorbent significantly higher than the TMOS-encapsulated cylindrical biosorbent (*t*-test, $p < 0.05$).

Table 4.1 also shows that the surface area of the spherical biosorbent was much smaller than that of the cylindrical biosorbent. Therefore, the number of the spherical biosorbent required in the reactor would be much larger than that of the cylindrical biosorbent in order to attain the same amount of biomass per reactor. Further, the surface area of spherical biosorbent was significantly affected by the types of metal alkoxide precursors (*t*-test, $p < 0.05$). Unlike the cylindrical biosorbent, the faster drying rate of the sol-gel/PVA matrix consisting of TMOS gave a larger surface area of the spherical biosorbent. Since the sol-gel/PVA matrix containing TMOS is more viscous than that containing TEOS, a more viscous mixture extruded a larger droplet from an autopipette into liquid

nitrogen and a larger bead of TMOS-encapsulated biosorbent was then formed. Table 4.1 further shows that TEOS-encapsulated spherical biosorbent gave a higher copper(II) biosorption capacity than the TMOS-encapsulated spherical biosorbent (*t*-test, $p < 0.05$).

In this part of study, both the spherical and cylindrical biosorbents prepared by TEOS showed a higher copper(II) biosorption capacities. As a result, only TEOS-encapsulated biosorbent of both spherical and cylindrical shapes was further studied.

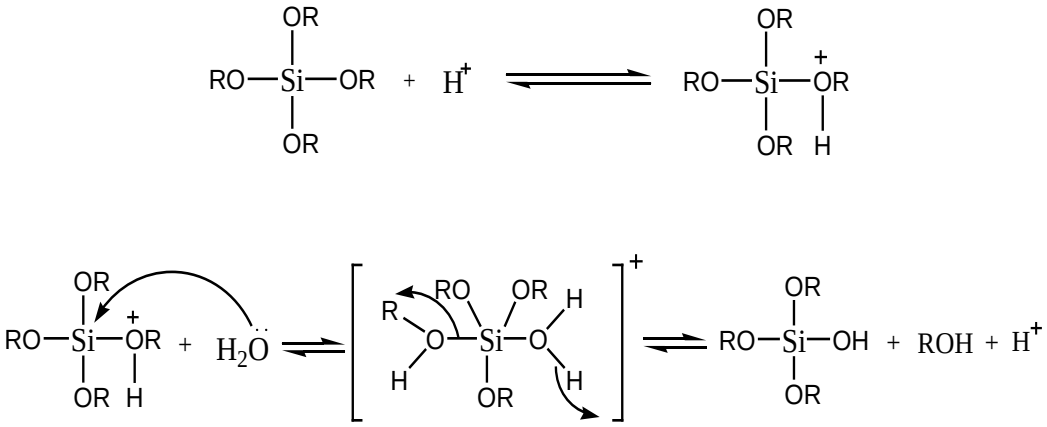

Figure 4.2. Mechanisms of acid-catalyzed hydrolysis in sol-gel process (Wright and Sommerdijk, 2001).

Table 4.1. Copper(II) biosorption capacities of immobilized *Micrococcus* sp. prepared by different metal alkoxide precursors.

Metal alkoxide precursor	Spherical biosorbent		Cylindrical biosorbent	
	Surface area per biosorbent (mm^2)	*q* (mg/g-biomass)	Surface area per biosorbent (mm^2)	*q* (mg/g-biomass)
TMOS	9.08 ± 1.24	21.23 ± 0.28	61.50 ± 6.31	15.72 ± 1.55
TEOS	3.14 ± 0.22	25.96 ± 0.05	68.09 ± 3.59	22.57 ± 0.48

[Experimental conditions: initial copper(II) concentration = 100 mg/L; biomass concentration = 1.5 g/L; contact time = 24 h; agitation speed = 250 rpm; pH = 5]

Spherical and cylindrical biosorbents prepared from sol-gel solution with different compositions were then investigated for their copper(II) uptake abilities. Table 4.2 presents the values of the copper(II) biosorption capacities of immobilized *Micrococcus* sp. prepared by seven different sol-gel stock solutions (A-G). The sol-gel stock solutions were mixed with PVA in a volume ratio of 1:2 and the concentration of biomass encapsulated in the sol-gel/PVA matrix was 40 g/L.

The amount of TEOS used for biomass immobilization was first optimized. The biosorption capacities of the immobilized biosorbents were significantly affected by the amount of TEOS in the sol-gel stock solution (biosorbents A, B and G in Table 4.2) (spherical biosorbent: *t*-test, $p < 0.05$; cylindrical biosorbent: one-way ANOVA, $F = 187.12$, $p = 0.001$). The biosorbent A had the smallest amount of TEOS, which was insufficient for the formation of gel network. As a result, an irregular shape of cylindrical biosorbent A was produced. The biosorbent B had the largest amount of TEOS, which produced a smallest cylindrical biosorbent with surface area of 58.06 mm^2. The drying rate of biosorbent B with the largest amount of TEOS was more rapid. As discussed before, a faster drying rate of the sol-gel/PVA matrix gave a smaller surface area

of the cylindrical biosorbent. However, a rapid drying rate of the sol-gel material is unsuitable for the preparation of the biosorbents because a rough surface of the cylindrical biosorbent was prepared. On the other hand, the spherical biosorbent B could not be prepared because the viscous solution of the sol-gel/PVA matrix containing the largest amount of TEOS clogged the autopipette and prevented the extrusion of beads. Thus, the TEOS compositions used to make biosorbents A and B were not suitable for the preparation of biosorbents while that used to make biosorbent G was selected as the optimal amount of TEOS to prepare the sol-gel stock solution.

In order to prevent the leaching of materials into liquid phase during the biosorption and desorption processes, MTMS was added to modify the sol-gel matrix by enhancing the polymer network (Wright and Sommerdijk, 2001). During the sol-gel process, TEOS first hydrolyzes and condenses to silica. The condensation reaction of MTMS is slower than that of TEOS. The silica network formed from TEOS is finally cross-linked with MTMS network. Immobilized biosorbents were prepared using different amounts of MTMS. The biosorption capacities of the immobilized biosorbents were significantly affected by changing the amount of MTMS (biosorbents C, D and G in Table 4.2)

(spherical biosorbent: one-way ANOVA, F = 22.31, p = 0.016; cylindrical biosorbent: one-way ANOVA, F = 759.08, p < 0.001). Table 4.2 indicates that the surface areas of both the spherical and cylindrical biosorbents were increased with an increase in the proportion of MTMS. The biosorbent C had the smallest amount of MTMS, which was insufficient for the formation of gel network. As a result, the shape of the cylindrical biosorbent C was irregular. The biosorbent D had the largest amount of MTMS. Its surface area was significantly larger than that of biosorbents C and G (Tukey's HSD test, p < 0.05). Karout *et al.* (2007) reported that the gel formed was not completely dried and shrunk when the content of MTMS was very high because of the poor hydrolysis and condensation reactions. In addition, increasing the content of MTMS will also increase the hydrophobicity and finally decrease the diffusion coefficient of the hydrophilic substrates (i.e., metal ions in this study) inside the gel. As a result, it is unnecessary to use excessive MTMS in the sol-gel process. Thus, the biosorbent D is not a good choice for further studies. Among the biosorbents C, D and G, biosorbent G had the optimum amount of MTMS and reasonable copper(II) biosorption capacity.

Hydrochloric acid is the catalyst used to promote the hydrolysis reaction of

the alkoxide groups. Under acidic conditions, the alkoxide group is protonated first, making it more susceptible to be attacked by water. The mechanisms of acid-catalyzed hydrolysis are shown in Fig. 4.2. Immobilized biosorbents were prepared using different amounts of HCl. The biosorption capacities of the immobilized biosorbents were significantly affected by changing the amount of HCl (biosorbents E, F and G in Table 4.2) (spherical biosorbent: one-way ANOVA, $F = 115.28$, $p = 0.001$; cylindrical biosorbent: one-way ANOVA, $F = 100.73$, $p = 0.002$). The surface areas of spherical biosorbents prepared by different amounts of HCl were not significantly affected (one-way ANOVA, $F = 2.64$, $p = 0.099$). However, a significant difference in the surface areas of cylindrical biosorbents prepared by different amounts of HCl was observed (one-way ANOVA, $F = 16.89$, $p < 0.001$). Among the biosorbents E, F and G, only biosorbent G had a uniform and regular shape.

Among the different sol-gel compositions studied, the optimum ratio of TEOS:MTMS:HCl selected to prepare biosorbents for further studies was 2.10:1.00:1.40 since it could produce spherical and cylindrical biosorbents G with the most regular and uniform shape, and reasonable copper(II) biosorption capacity.

Table 4.2. Copper(II) biosorption capacities of *Micrococcus* sp. encapsulated in different sol-gel compositions.

Biosorbent	Composition in sol-gel stock solution (v/v) (TEOS:MTMS:HCl)	Spherical biosorbent		Cylindrical biosorbent	
		Surface area per biosorbent (mm^2)	q (mg/g-biomass)	Surface area per biosorbent (mm^2)	q (mg/g-biomass)
A	1.05:1.00:1.40	3.14 ± 0.22	25.00 ± 0.14	78.78 ± 7.32	30.25 ± 0.20
B	4.20:1.00:1.40	--	--	58.06 ± 5.46	25.35 ± 0.45
C	2.10:0.51:1.40	3.14 ± 0.22	24.70 ± 0.56	54.10 ± 3.13	22.11 ± 0.35
D	2.10:2.10:1.40	5.31 ± 1.77	22.62 ± 0.33	81.81 ± 3.54	30.25 ± 0.10
E	2.10:1.00:0.51	3.80 ± 0.79	21.46 ± 0.19	88.47 ± 3.36	30.35 ± 0.65
F	2.10:1.00:2.10	3.80 ± 0.76	25.50 ± 0.28	83.75 ± 3.45	25.74 ± 0.10
G	2.10:1.00:1.40	3.14 ± 0.22	21.92 ± 0.37	76.11 ± 5.68	25.67 ± 0.00

[Experimental conditions: initial copper(II) concentration = 100 mg/L; biomass concentration = 1.5 g/L; contact time = 24 h; agitation speed = 250 rpm; pH = 5]

PVA was used to prevent the cracking of immobilized biosorbent by enhancing the mechanical strength and the chemical stability (Nguyen-Ngoc and Tran-Minh, 2006). Jin and Brennan (2002) reported that the shrinkage of the biosorbent could be reduced in the presence of polymer additive, such as PVA, which helped prevent the pore to collapse. A preliminary study indicated that the immobilized biosorbent prepared by sol-gel matrix without PVA was cracked. Therefore, PVA is an important material in the immobilization process. The amount of PVA used for biomass immobilization was optimized. The composition ratio of TEOS:MTMS:HCl used to prepare the biosorbents was 2.10:1.00:1.40 and the concentration of biomass encapsulated in the sol-gel/PVA matrix was 40 g/L. The copper(II) biosorption capacities of both the spherical and cylindrical biosorbents encapsulated in sol-gel stock solutions with different amounts of PVA are presented in Table 4.3. The results indicate that the copper(II) uptake by the cylindrical biosorbents increased significantly with an increase in the proportion of PVA (one-way ANOVA, $F = 2527$, $p < 0.001$). A significant difference in the surface areas of cylindrical biosorbents prepared by different amounts of PVA was observed (one-way ANOVA, $F = 7.92$, $p = 0.003$). However, the biosorption capacities of the spherical biosorbents with different amounts of PVA were similar (t-test, $p > 0.05$). The biosorbent H did not have a

spherical shape in liquid nitrogen. This was because the amount of PVA used was not enough for the formation of spherical beads. Since the appearance and biosorption capacity of biosorbent I were only slightly different from those of biosorbent J, the biosorbent I prepared with a smaller amount of PVA is preferred. Thus, the optimum ratio of the sol-gel stock solution to PVA was chosen as 1:2.

Table 4.3. Copper(II) biosorption capacities of *Micrococcus* sp. encapsulated in different ratios of sol-gel stock solution to PVA.

Biosorbent	Sol-gel stock solution:PVA (v/v)	Spherical biosorbent		Cylindrical biosorbent	
		Surface area per biosorbent (mm^2)	q (mg/g-biomass)	Surface area per biosorbent (mm^2)	q (mg/g-biomass)
H	1:1	--	--	80.91 ± 2.92	22.82 ± 0.00
I	1:2	3.14 ± 0.22	24.83 ± 0.98	76.11 ± 5.68	24.72 ± 0.00
J	1:3	3.14 ± 0.22	27.48 ± 0.14	73.21 ± 0.98	26.90 ± 0.10

[Experimental conditions: initial copper(II) concentration = 100 mg/L; biomass concentration = 1.5 g/L; contact time = 24 h; agitation speed = 250 rpm; pH = 5]

4.1.3. Effect of drying time on immobilized biosorbent

During the drying period, the sol-gel/PVA matrix shrinks as water and other volatile liquid evaporates from the matrix. The shrinkage of the gel is associated with the increases in the cross-linking and stiffness of the pellets. At the critical point, the gel becomes sufficiently rigid to resist further shrinkage. The volatile liquid evaporates continuously and the gel begins to recede into a porous structure (Wright and Sommerdijk, 2001).

The effect of drying time on copper(II) biosorption was examined by drying the spherical and cylindrical biosorbents for one to six days. The composition ratio of TEOS:MTMS:HCl used to prepare the biosorbents was 2.10:1.00:1.40 and the sol-gel stock solutions were mixed with PVA in a volume ratio of 1:2. The concentration of biomass encapsulated in the sol-gel/PVA matrix was 40 g/L. Fig. 4.3 presents the copper(II) uptake and the surface area of immobilized biosorbents prepared with different drying time. Since the surface area of the spherical biosorbent is smaller than that of the cylindrical biosorbent, the drying rate of the spherical biosorbent should be faster than that of the cylindrical biosorbent. Fig. 4.3 indicates that the spherical biosorbent shrunk to a constant size after drying for one day and their copper(II) biosorption capacity was

unaffected by the drying time (one-way ANOVA, $F = 0.95$, $p = 0.506$). In contrast, the cylindrical biosorbent was still very soft if only drying for one day and it was still incompletely dried after drying for two days. Further drying from two to four days reduced the surface areas of the cylindrical biosorbent. The biosorption capacity of the cylindrical biosorbent kept steady after the biosorbent was dried for three days. In order to prevent leaching of the biomass, hydrolysis and condensation reactions in the sol-gel process must be completed and thus the drying time should be sufficiently long. The optimum drying time of the spherical biosorbent and the cylindrical biosorbent was chosen as two days and three days, respectively.

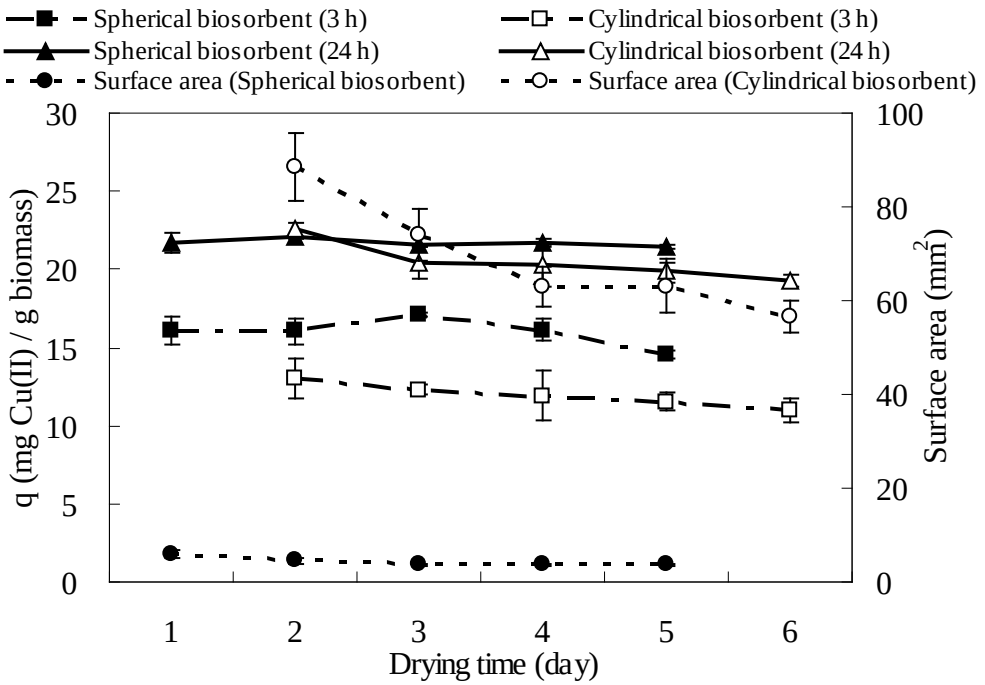

Figure 4.3. Effect of drying time of the immobilized biosorbents on copper(II) uptake.

[Experimental conditions: initial copper(II) concentration = 100 mg/L; biomass concentration = 1.5 g/L; agitation speed = 250 rpm; pH = 5]

4.1.4. Effect of biomass concentration in immobilized biosorbent

The effect of biomass concentration in the sol-gel/PVA matrix on copper(II) removal by the immobilized biosorbents was studied. The composition ratio of TEOS:MTMS:HCl used to prepare the biosorbents was 2.10:1.00:1.40 and the sol-gel stock solutions were mixed with PVA in a volume ratio of 1:2. Tables 4.4 and 4.5 present the surface areas and biosorption capacities of the spherical and cylindrical biosorbents encapsulated with different concentrations of biomass. In the biosorption process, the amounts of biomass in the reactor for biosorbents L, M and N were the same. Thus, the final biomass concentration in the reactor was always 1.5 g/L. As biosorbent L contained smaller amount of biomass in the sol-gel/PVA matrix, a larger number of biosorbent L was added to the reactor compared with that of biosorbents M and N, increasing the total surface area of biosorbent per reactor. A significant difference of copper(II) biosorption capacity between biosorbents L, M and N was observed (spherical biosorbent: one-way ANOVA, F = 145.18, p = 0.001; cylindrical biosorbent: one-way ANOVA, F = 13.86, p = 0.031). The biosorption capacities of both spherical and cylindrical biosorbents N were significantly higher than that of biosorbents L and M (Tukey's HSD test, $p < 0.05$).

The surface areas and biosorption capacities of the spherical biosorbents were compared with that of the cylindrical biosorbents. Tables 4.4 and 4.5 also show the difference of the surface areas and biosorption capacities between the spherical and cylindrical biosorbents. The surface area of a single spherical biosorbent bead was much smaller than that of a single cylindrical biosorbent bead. A smaller surface area of the spherical biosorbents consequently increased the surface areas per mL of biosorbents when comparing with that of cylindrical biosorbents (*t*-test, $p < 0.05$). Therefore, the total surface areas of the spherical biosorbents in the reactor were always larger than that of the cylindrical biosorbents. The biosorption capacities of spherical biosorbents were significantly higher than that of cylindrical biosorbents (*t*-test, $p < 0.05$).

In order to select an optimum concentration of biomass in the sol-gel/PVA matrix, it is important to consider the copper(II) removal ability by the immobilized biosorbents as well as the consumption of sol-gel/PVA materials in the immobilization process. Among the biosorbents L, M and N, biosorbent N had the highest copper(II) biosorption capacity. It also consumes smaller amount of sol-gel/PVA matrix in the immobilization process since an increase in biomass concentration in the sol-gel/PVA materials could reduce the number of

immobilized biosorbent required in the reactor. Less number of biosorbent consumes smaller amount of sol-gel/PVA materials. Therefore, the optimum biomass concentration in the sol-gel/PVA matrix was 40 g/L.

Table 4.4. Effect of biomass concentration in sol-gel/PVA matrix on copper(II) removal by spherical biosorbent (Reactor volume = 30 mL).

Spherical biosorbent	Biomass concentration in cell suspension (g/L)	Biomass concentration in sol-gel/PVA matrix (g/L)	No. of biosorbent per reactor	Surface area per biosorbent (mm^2)	Surface area per mL biosorbent (mm^2/mL)	Total surface area of biosorbent per reactor (mm^2)	q (mg/g-biomass)
L	40	10	381	3.80 ± 0.59	2104 ± 6	1447	25.60 ± 0.05
M	100	25	160	3.14 ± 0.29	1710 ± 21	502	25.17 ± 0.00
N	200	40	91	4.52 ± 0.80	2127 ± 22	411	27.78 ± 0.28

[Experimental conditions: initial copper(II) concentration = 100 mg/L; biomass concentration = 1.5 g/L; contact time = 24 h; agitation speed = 250 rpm; pH = 5]

Table 4.5. Effect of biomass concentration in sol-gel/PVA matrix on copper(II) removal by cylindrical biosorbent (Reactor volume = 30 mL).

Cylindrical biosorbent	Biomass concentration in cell suspension (g/L)	Biomass concentration in sol-gel/PVA matrix (g/L)	No. of biosorbent per reactor	Surface area per biosorbent (mm^2)	Surface area per mL biosorbent (mm^2/mL)	Total surface area of biosorbent per reactor (mm^2)	q (mg/g-biomass)
L	40	10	17	62.08 ± 3.49	1675 ± 24	1055	22.23 ± 0.10
M	100	25	7	63.71 ± 3.63	1480 ± 9	445	22.45 ± 0.35
N	200	40	4	69.98 ± 6.15	1407 ± 27	280	23.30 ± 0.10

[Experimental conditions: initial copper(II) concentration = 100 mg/L; biomass concentration = 1.5 g/L; contact time = 24 h; agitation speed = 250 rpm; pH = 5]

4.2 Biosorption of copper(II) ions

4.2.1 Effect of contact time

The time required for copper(II) uptake to reach equilibrium by the spherical and cylindrical biosorbents was studied. Fig. 4.4 compares the copper(II) biosorption capacity of the spherical and cylindrical biosorbents as a function of contact time. The kinetic profiles for copper(II) removal by the two immobilized biosorbents showed a similar trend. The copper(II) uptake rate of both the spherical and cylindrical biosorbents at the first 100 min was relatively rapid. Then, the copper(II) uptake rate was reduced gradually after 100 min and reached equilibrium at 1400 min. At the first 100 min, the biosorption rate of the spherical biosorbent was faster than that of the cylindrical biosorbent. The spherical biosorbent reached 90% of equilibrium biosorption capacity at 720 min, whereas the cylindrical biosorbent used a longer time (1100 min) to reach 90% of equilibrium biosorption capacity.

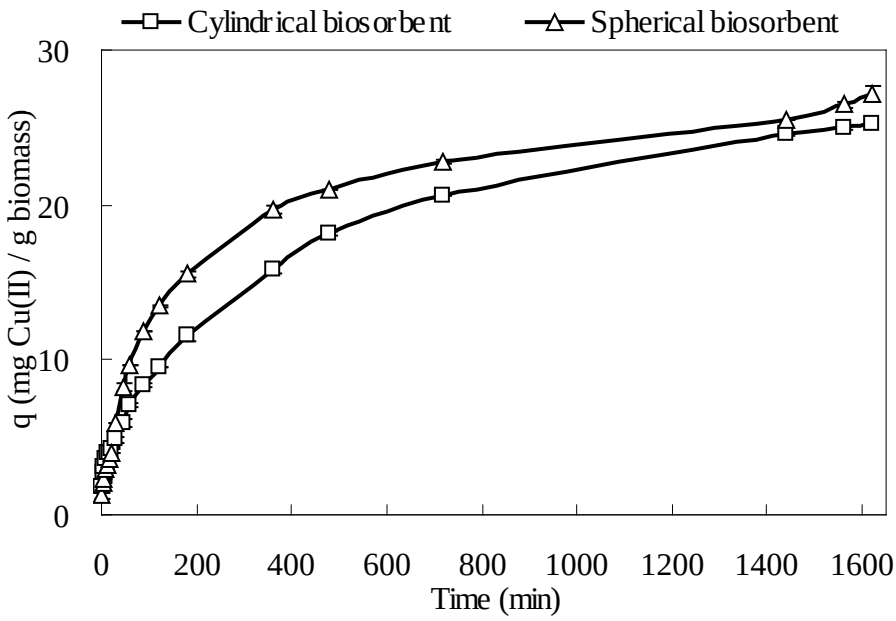

Figure 4.4. Effect of contact time on copper(II) biosorption by spherical and cylindrical biosorbents.

[Experimental conditions: initial copper(II) concentration = 100 mg/L; biomass concentration = 1.5 g/L; agitation speed = 250 rpm; pH = 5]

4.2.2 Biosorption kinetics

The pseudo-first order and pseudo-second order kinetic models are usually applied to determine the controlling mechanism of the biosorption process. Both linear and non-linear regression analyses were used to describe the experimental kinetic data. The pseudo-first order kinetic model is described as:

$$q = q_e(1 - \exp(-k_1 t)) \qquad (6)$$

The linear form of Eq. (6) is expressed as:

$$\ln(q_e - q_t) = -k_1 t + \ln q_e \qquad (7)$$

The pseudo-second order kinetic model is described as:

$$q = \frac{t}{\frac{1}{k_2 q_e^{\,2}} + \frac{t}{q_e}} \qquad (8)$$

The linear form of Eq. (8) is expressed as:

$$\frac{t}{q_t} = \frac{1}{k_2 q_e^{\,2}} + \frac{t}{q_e} \qquad (9)$$

where q_e and q_t are the amount of copper(II) adsorbed per unit weight of biomass (mg/g-biomass) at equilibrium and at time (t), respectively; k_1 is the rate constant of the pseudo-first order kinetic model (min^{-1}); and, k_2 is the rate constant of the pseudo-second order kinetic model (g/mg·min).

The linear plots of ln ($q_e - q_t$) versus t for the pseudo-first order model and t/q_t versus t for the pseudo-second order model are illustrated in Figs. 4.5 and 4.6,

respectively. A non-linear regression analysis was also applied to fit the experimental data using Eqs. (6) and (8). Fig. 4.7 shows plots of the non-linearized pseudo-first order and pseudo-second order kinetic models for copper(II) biosorption. The parameters and correlation coefficients (r^2) estimated from the pseudo-first order and pseudo-second order kinetic models for copper(II) biosorption by the spherical and cylindrical biosorbents are calculated and summarized in Tables 4.6 and 4.7, respectively. Table 4.6 clearly shows that the pseudo-second order kinetic model could better simulate the experimental data of spherical biosorbent when compared with the pseudo-first order kinetic model. The first reason is the higher values of r^2 obtained from the pseudo-second order model (r^2 = 0.99 for both linear and non-linear regression analyses). Second, the values of q_e (27.82 mg/g-biomass or 27.59 mg/g-biomass) obtained from the pseudo-second order model were in close agreement with the q_e determined experimentally (27.17 mg/g-biomass). Non-linear regression analysis in Fig. 4.7 and the simulation results of the copper(II) biosorption kinetics by linearized kinetic models in Fig. 4.8(a) further indicate that the biosorption of copper(II) followed the pseudo-second order model. A similar q_e (*t*-test, $p > 0.05$) and r^2 (*t*-test, $p > 0.05$) were calculated from the linearized and non-linearized pseudo-second order model, which indicated that the data treatment using linear

and non-linear regression analyses was similar.

Similarly, Table 4.7 also indicates that the pseudo-second order kinetic model could better simulate the experimental data of cylindrical biosorbent when compared with the pseudo-first order kinetic model. The r^2 estimated from the pseudo-second order model ($r^2 \geq 0.96$) were higher than that determined from the pseudo-first order model ($r^2 \geq 0.94$). The values of q_e (26.42 mg/g-biomass or 27.23 mg/g-biomass) obtained from the pseudo-second order model were in close agreement with the q_e determined experimentally (25.26 mg/g-biomass). Non-linear regression analysis in Fig. 4.7 and the simulation results of the copper(II) biosorption kinetics by linearized kinetic models in Fig. 4.8(b) further indicate that the biosorption of copper(II) followed the pseudo-second order model. The values of q_e and r^2 calculated from the linearized and non-linearized pseudo-second order model were similar.

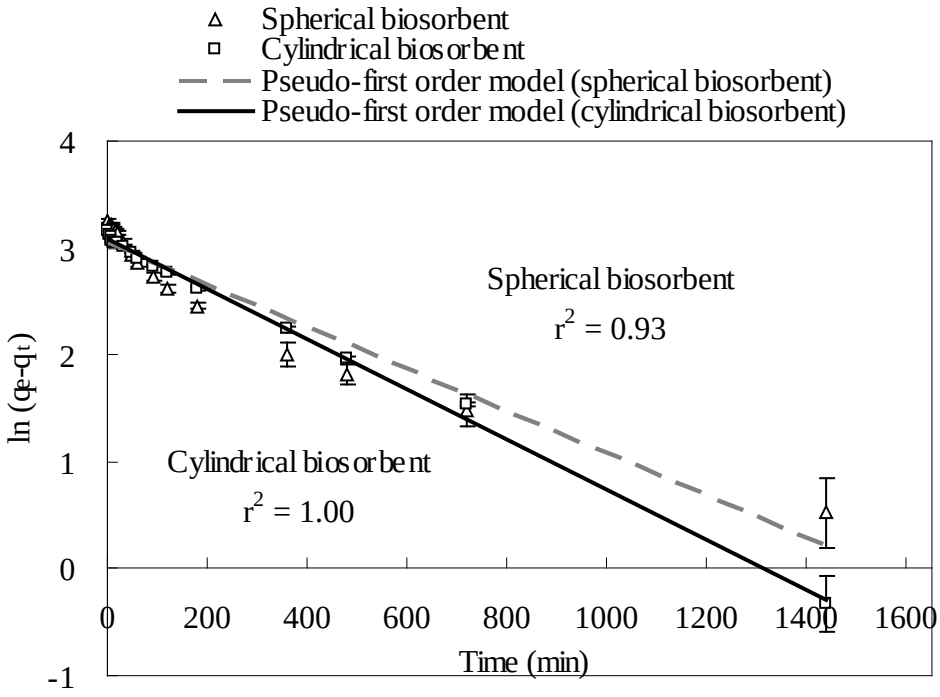

Figure 4.5. Pseudo-first order kinetic model of copper(II) biosorption by spherical and cylindrical biosorbents.

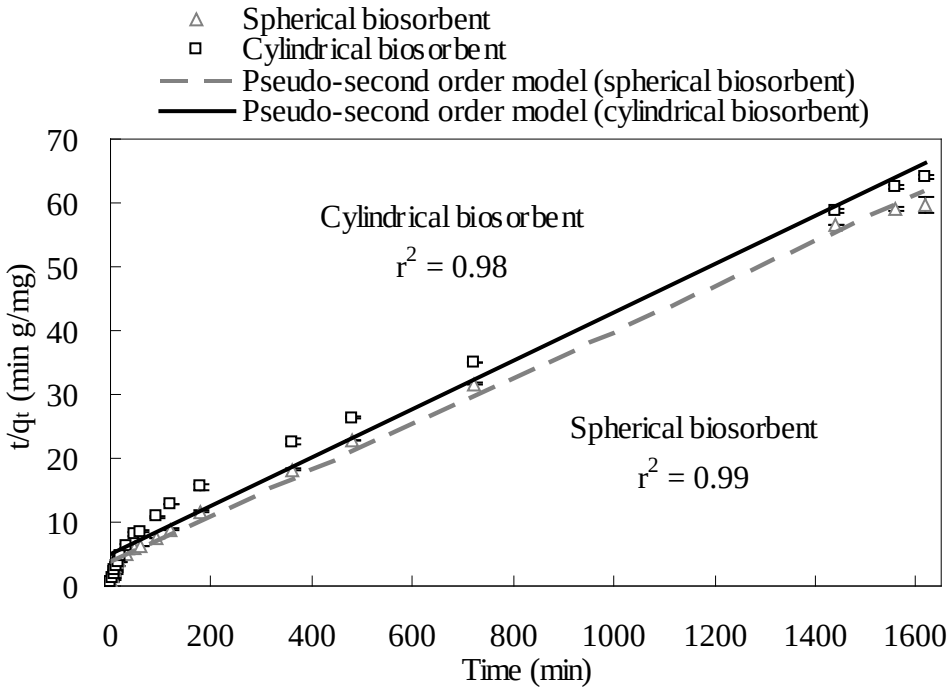

Figure 4.6. Pseudo-second order kinetic model of copper(II) biosorption by spherical and cylindrical biosorbents.

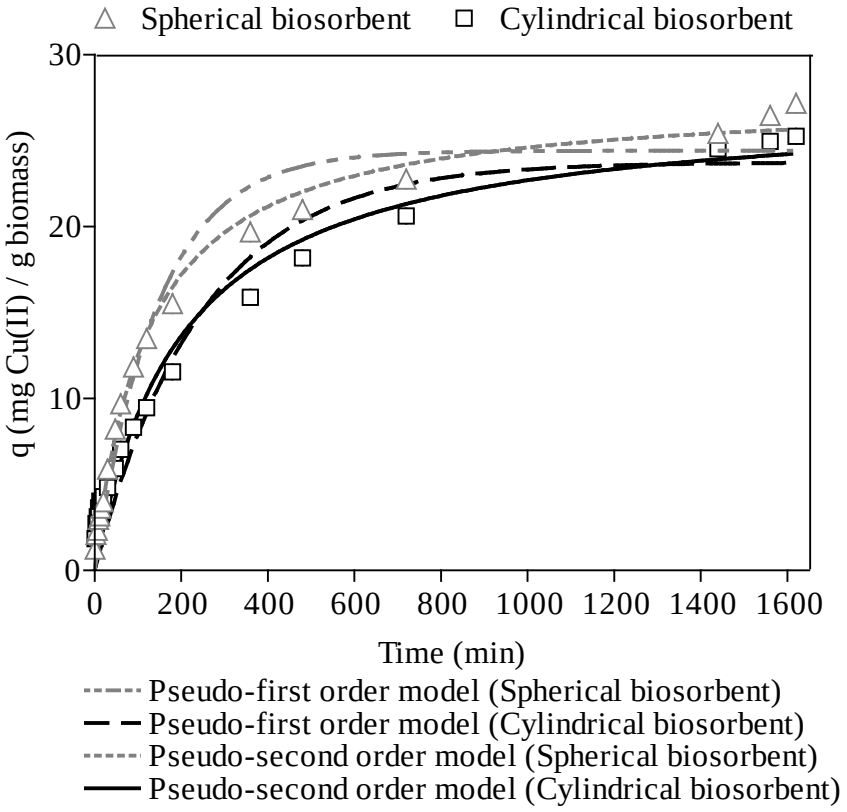

Figure 4.7. Non-linearized pseudo-first order and pseudo-second order kinetic models of copper(II) biosorption by spherical and cylindrical biosorbents.

Table 4.6. Parameters of pseudo-first order and pseudo-second order kinetic models for copper(II) biosorption by spherical biosorbent.

	Pseudo-first order			Pseudo-second order		
	k_1 (min^{-1})	q_e (mg/g-biomass)	r^2	k_2 (g/mg·min)	q_e (mg/g-biomass)	r^2
Linearized	0.0020 ± 0.0002	21.22 ± 0.33	0.93 ± 0.02	$3.49x10^{-4} \pm 0.09 x10^{-4}$	27.82 ± 0.02	0.99 ± 0.01
Non-linearized	0.0069 ± 0.0000	24.42 ± 0.10	0.97 ± 0.00	$2.99x10^{-4} \pm 0.03x10^{-4}$	27.59 ± 0.10	0.99 ± 0.04

Table 4.7. Parameters of pseudo-first order and pseudo-second order kinetic models for copper(II) biosorption by cylindrical biosorbent.

	Pseudo-first order			Pseudo-second order		
	k_1 (min^{-1})	q_e (mg/g-biomass)	r^2	k_2 (g/mg·min)	q_e (mg/g-biomass)	r^2
Linearized	0.0023 ± 0.0001	21.94 ± 0.22	1.00 ± 0.00	$2.95x10^{-4} \pm 0.01x10^{-4}$	26.42 ± 0.05	0.98 ± 0.00
Non-linearized	0.0041 ± 0.0001	23.74 ± 0.01	0.94 ± 0.00	$1.84x10^{-4} \pm 0.03x10^{-4}$	27.23 ± 0.02	0.96 ± 0.00

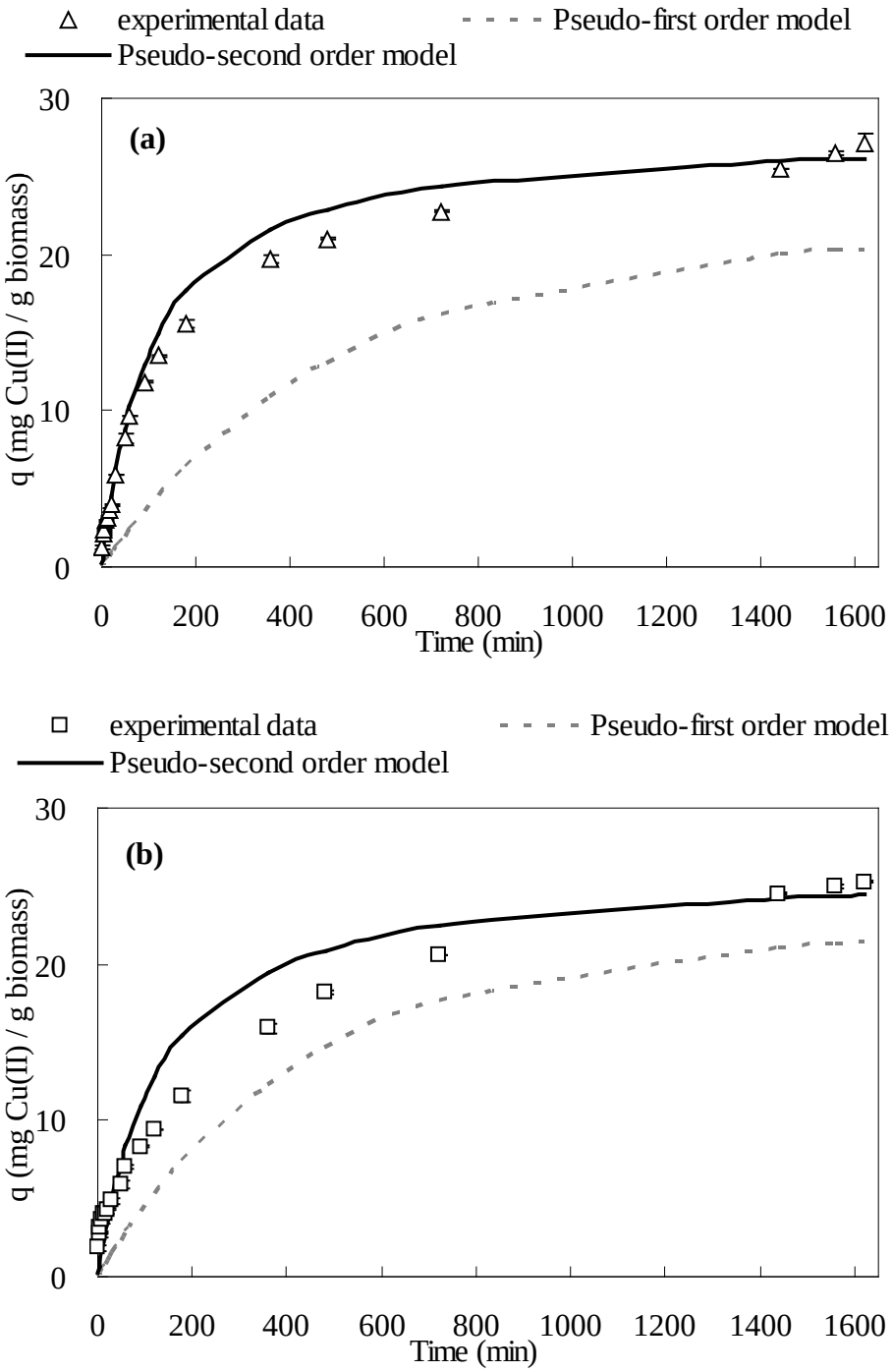

Figure 4.8. Simulation of copper(II) biosorption kinetics of (a) spherical biosorbent and (b) cylindrical biosorbent by linearized pseudo-first order and pseudo-second order kinetic models.

4.2.3 Effect of agitation speed on kinetic profiles

In general, the transfer of a heavy metal ion from the bulk liquid phase onto a biomass surface may be described as occurring in three stages: (i) external mass transfer of metal ions from the bulk liquid to biosorbent surface; (ii) intraparticle diffusion within the pores of the biosorbent; and, (iii) biosorption reaction on the biomass surface at an internal site of the sol-gel/PVA matrix.

The external mass transfer of copper(II) ions is significantly affected by agitation speed. Fig. 4.9 shows the effect of agitation speed on the kinetic profiles of copper(II) biosorption. The agitation speed was varied from 0 rpm to 300 rpm. The copper(II) uptake increased significantly when the agitation speed was increased from 30 rpm to 100 rpm (*t*-test, $p < 0.05$). A further increase in the agitation speed from 100 rpm to 200 rpm only gave little enhancement in the rate of copper(II) uptake but the equilibrium biosorption capacity was unaffected. Both the copper(II) uptake rate and the equilibrium biosorption capacity were not increased with an increase in the agitation speed from 200 rpm to 300 rpm.

The linear plots of ln ($q_e - q_t$) versus t for the pseudo-first order model and t/q_t versus t for the pseudo-second order model under different agitation speeds

are illustrated in Figs. 4.10 and 4.11, respectively. Figs. 4.12 and 4.13 show plots of the non-linearized pseudo-first order and pseudo-second order kinetic models under different agitation speeds for copper(II) biosorption by spherical and cylindrical biosorbents, respectively. Tables 4.8 and 4.9 list the kinetic parameters estimated from the pseudo-first order and pseudo-second order kinetic models with both linear and non-linear regression analyses. The higher values of r^2 ($\geq$ 0.98) and the close agreement of estimated q_e with the experimental q_e obtained at 100 rpm, 200 rpm and 300 rpm in the pseudo-second order kinetic model indicate that this model could better simulate the experimental data. The experimental data obtained at 0 rpm and 30 rpm were well described by the pseudo-first order kinetic model with $r^2 \geq 0.97$. The rate constants of both the spherical and cylindrical biosorbents significantly increased with an increase of agitation speed from 0 rpm to 200 rpm (one-way ANOVA, $p < 0.001$), which indicated that the biosorption rate was affected by the agitation speed. However, only small changes of the rate constants were observed with a further increase in the agitation speed from 200 rpm to 300 rpm. It was found that agitation is an important parameter in the biosorption process and the rate of copper(II) biosorption can significantly increase in the system with agitation.

External mass transfer is used to describe the mass transfer resistance at the solid-liquid interface. The external mass transfer resistance is proportional to the film thickness surrounding the particle (Vilar *et al*., 2005). Increase in the agitation speed will decrease the film thickness and hence increase the external diffusion rate. The bulk diffusion rate and external mass transfer rate were slow in the biosorption system without agitation. In this case, the experimental data show that external mass transfer would control the biosorption process at an agitation speed of 0 rpm and 30 rpm. Similarly, Zogorski *et al*. (1975) demonstrated that the external mass transfer was a rate-limiting step in a system of poor mixing. The external mass transfer rate increased significantly when the agitation speed was increased to 100 rpm and little enhancement was observed with a further increase in the agitation speed. Thus, intraparticle diffusion may become the dominant mechanism controlling the biosorption process when the agitation speed is increased to 100 rpm and beyond.

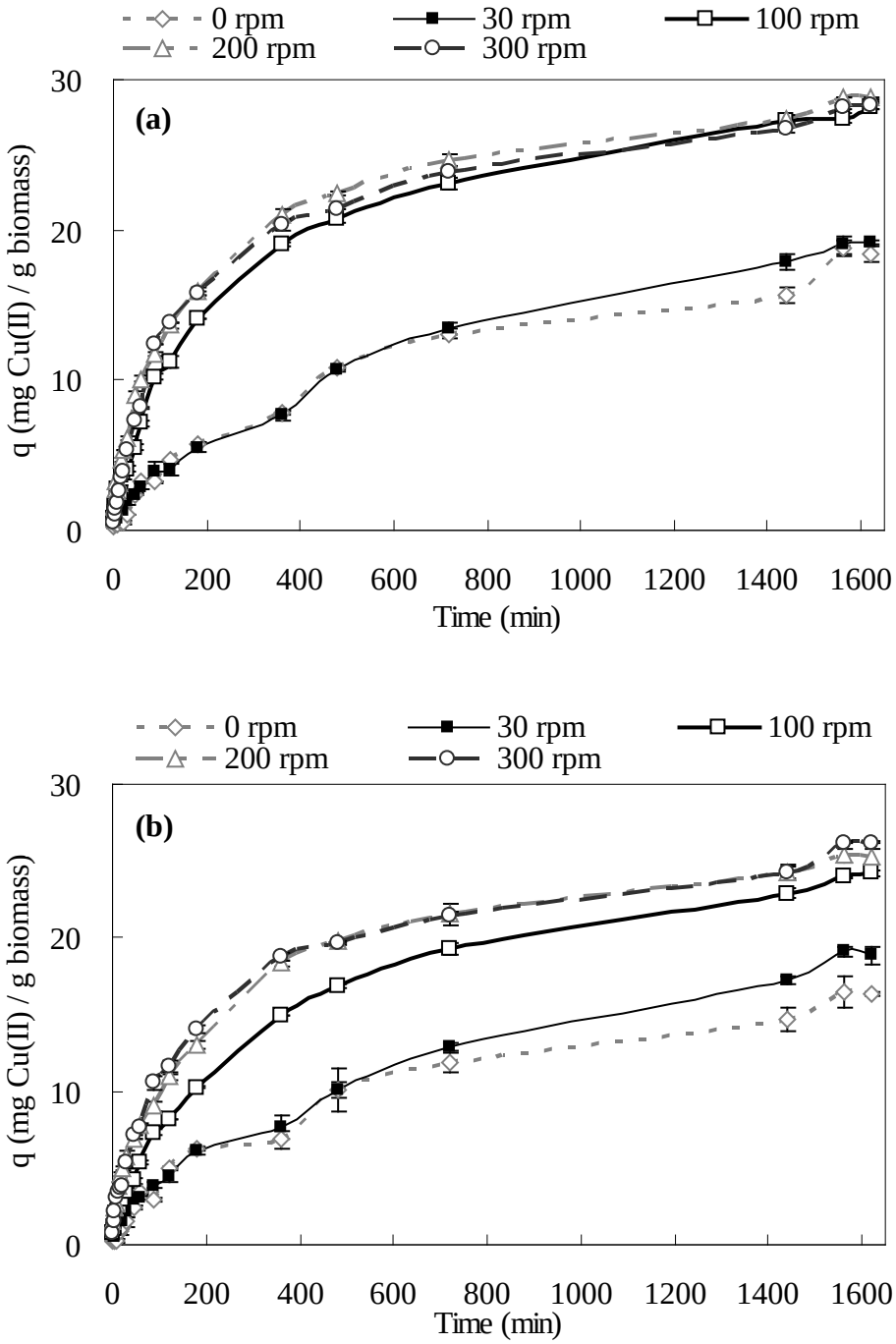

Figure 4.9. Effect of agitation speed on copper(II) biosorption kinetics by (a) spherical biosorbent and (b) cylindrical biosorbent.

[Experimental conditions: initial copper(II) concentration = 100 mg/L; biomass concentration = 1.5 g/L; pH = 5]

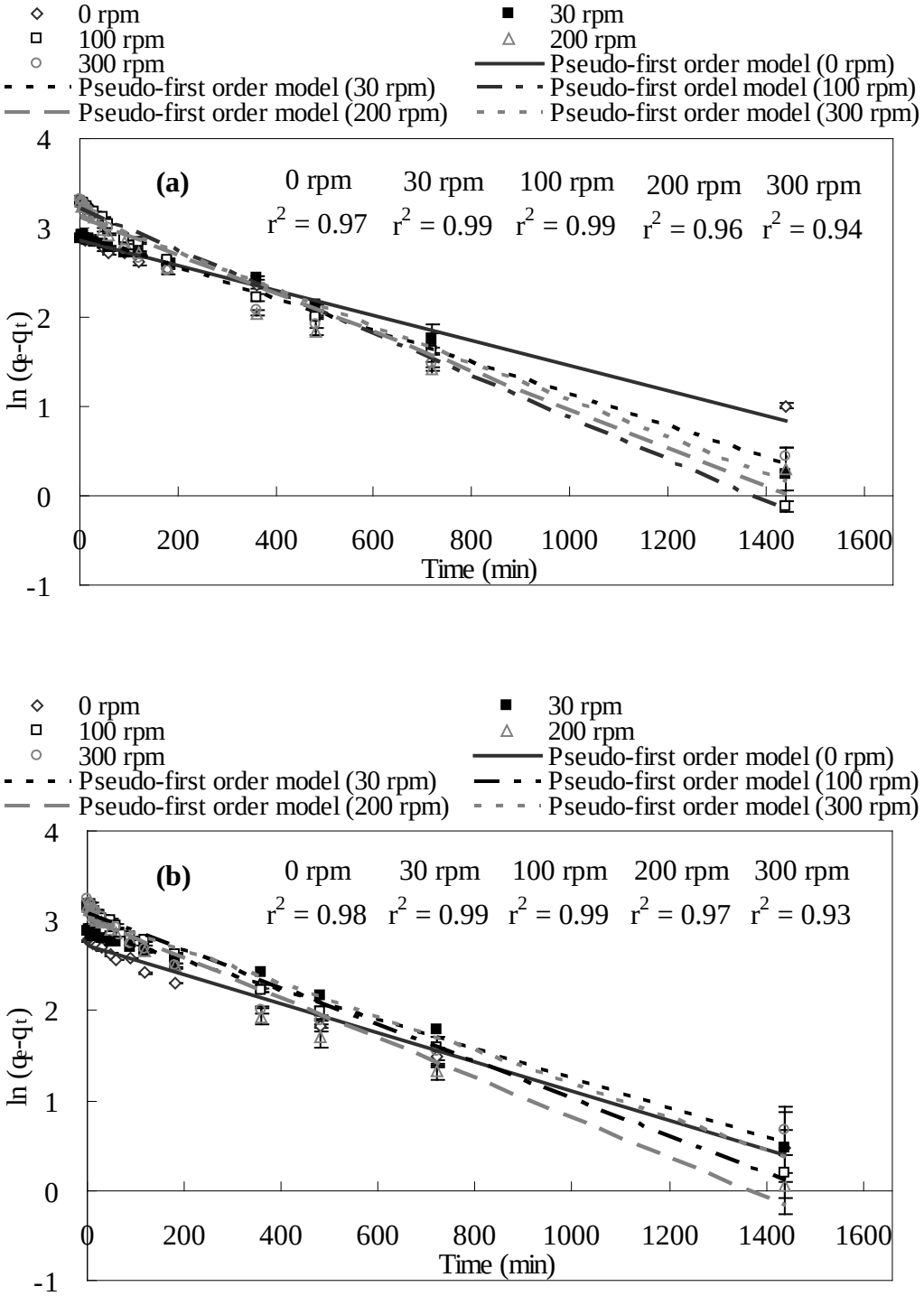

Figure 4.10. Effect of agitation speed on pseudo-first order kinetic model of copper(II) biosorption by (a) spherical biosorbent and (b) cylindrical biosorbent.

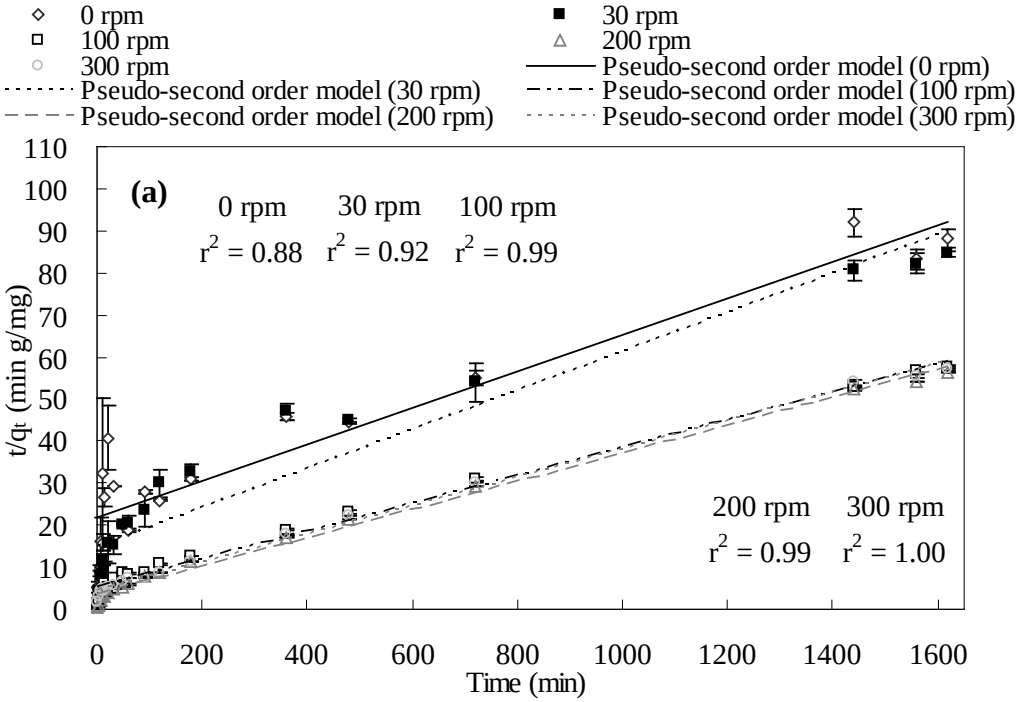

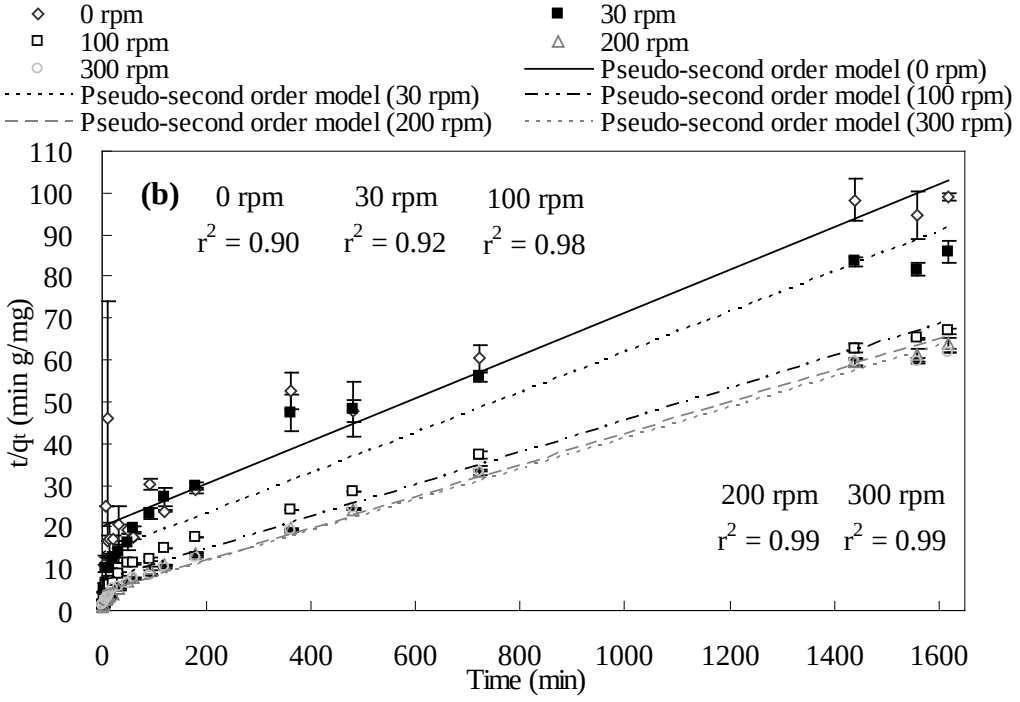

Figure 4.11. Effect of agitation speed on pseudo-second order kinetic model of copper(II) biosorption by (a) spherical biosorbent and (b) cylindrical biosorbent.

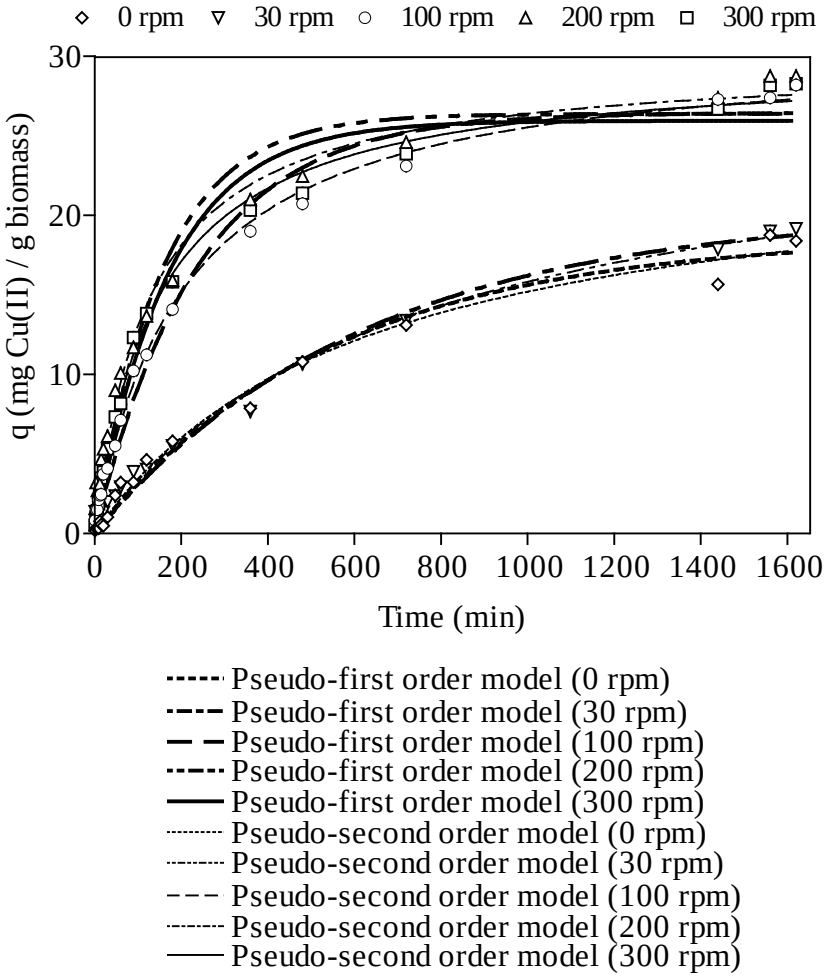

Figure 4.12. Non-linearized pseudo-first order and pseudo-second order kinetic models of copper(II) biosorption by spherical biosorbent under different agitation speeds.

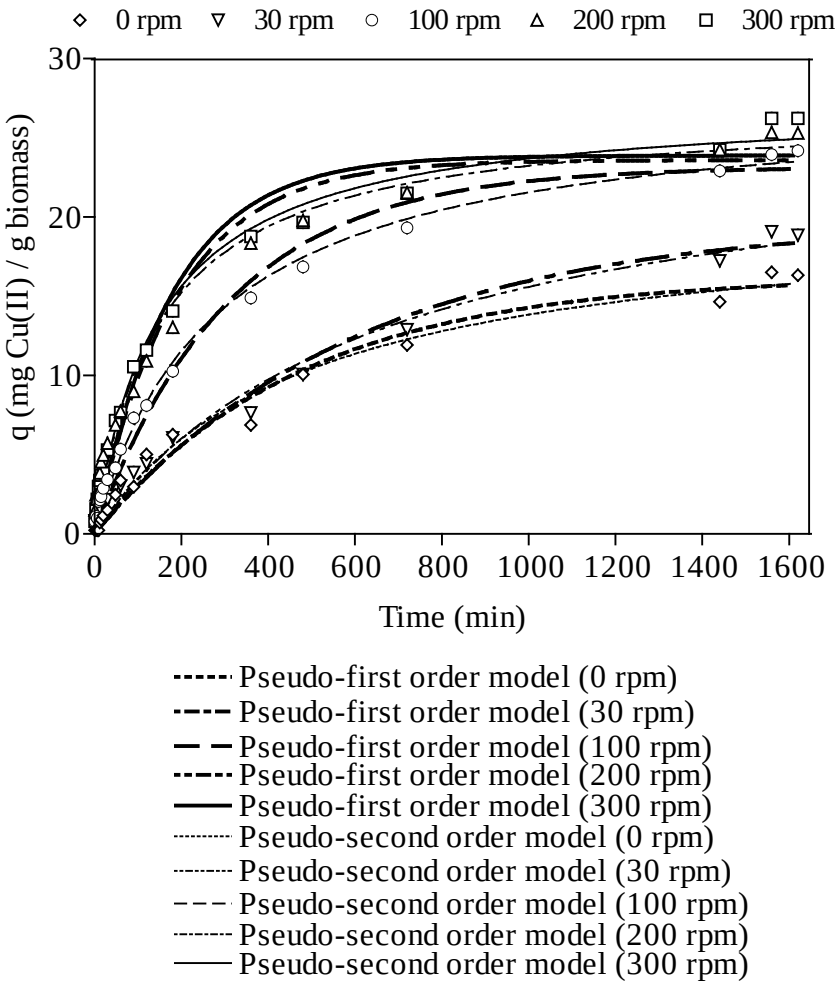

Figure 4.13. Non-linearized pseudo-first order and pseudo-second order kinetic models of copper(II) biosorption by cylindrical biosorbent under different agitation speeds.

Table 4.8. Parameters of pseudo-first order and pseudo-second order kinetic models for copper(II) biosorption by spherical biosorbent under different agitation speeds.

		Pseudo-first order			Pseudo-second order		
		k_1 (min^{-1})	q_e (mg/g-biomass)	r^2	k_2 (g/mg·min)	q_e (mg/g-biomass)	r^2
0 rpm	Linearized	0.0014 ± 0.0000	17.33 ± 0.62	0.97 ± 0.02	$0.88x10^{-4} \pm 0.07x10^{-4}$	22.98 ± 0.78	0.88 ± 0.00
	Non-linearized	0.0018 ± 0.0001	18.69 ± 0.79	0.99 ± 0.00	$0.66x10^{-4} \pm 0.10x10^{-4}$	24.66 ± 1.37	0.99 ± 0.00
30 rpm	Linearized	0.0018 ± 0.0002	18.64 ± 0.35	0.99 ± 0.00	$1.46x10^{-4} \pm 0.06x10^{-4}$	21.61 ± 0.66	0.92 ± 0.01
	Non-linearized	0.0016 ± 0.0001	20.28 ± 0.12	0.98 ± 0.00	$0.51x10^{-4} \pm 0.05x10^{-4}$	27.27 ± 0.23	0.99 ± 0.00
100 rpm	Linearized	0.0024 ± 0.0001	25.02 ± 0.02	0.99 ± 0.00	$2.11x10^{-4} \pm 0.09\ x10^{-4}$	30.08 ± 0.06	0.99 ± 0.00
	Non-linearized	0.0043 ± 0.0001	26.45 ± 0.20	0.98 ± 0.00	$1.58x10^{-4} \pm 0.02\ x10^{-4}$	30.78 ± 0.16	1.00 ± 0.00
200 rpm	Linearized	0.0022 ± 0.0001	22.78 ± 0.28	0.96 ± 0.02	$3.21x10^{-4} \pm 0.07x10^{-4}$	29.90 ± 0.06	0.99 ± 0.00
	Non-linearized	0.0063 ± 0.0001	26.38 ± 0.03	0.96 ± 0.00	$2.60x10^{-4} \pm 0.03x10^{-4}$	29.78 ± 0.04	0.99 ± 0.00
300 rpm	Linearized	0.0021 ± 0.0000	23.04 ± 0.29	0.94 ± 0.00	$2.51x10^{-4} \pm 0.09x10^{-4}$	29.85 ± 0.25	1.00 ± 0.00
	Non-linearized	0.0058 ± 0.0000	25.95 ± 0.14	0.98 ± 0.00	$2.30x10^{-4} \pm 0.04x10^{-4}$	29.67 ± 0.21	1.00 ± 0.00

Table 4.9. Parameters of pseudo-first order and pseudo-second order kinetic models for copper(II) biosorption by cylindrical biosorbent under different agitation speeds.

		Pseudo-first order			Pseudo-second order		
		k_1 (min^{-1})	q_e (mg/g-biomass)	r^2	k_2 (g/mg·min)	q_e (mg/g-biomass)	r^2
0 rpm	Linearized	0.0016 ± 0.0003	15.31 ± 0.37	0.98 ± 0.01	$1.30x10^{-4} \pm 0.12x10^{-4}$	19.53 ± 0.32	0.90 ± 0.08
	Non-linearized	0.0021 ± 0.0000	16.26 ± 0.66	0.98 ± 0.01	$0.99x10^{-4} \pm 0.04x10^{-4}$	20.57 ± 0.90	0.98 ± 0.01
30 rpm	Linearized	0.0017 ± 0.0001	17.90 ± 0.30	0.99 ± 0.01	$1.71x10^{-4} \pm 0.03x10^{-6}$	20.78 ± 0.52	0.92 ± 0.02
	Non-linearized	0.0017 ± 0.0002	19.77 ± 0.10	0.97 ± 0.01	$0.58x10^{-4} \pm 0.10x10^{-4}$	26.07 ± 0.60	0.98 ± 0.01
100 rpm	Linearized	0.0021 ± 0.0003	21.79 ± 0.23	0.99 ± 0.01	$2.09x10^{-4} \pm 0.01x10^{-4}$	26.04 ± 0.00	0.98 ± 0.00
	Non-linearized	0.0032 ± 0.0000	23.16 ± 0.06	0.98 ± 0.00	$1.31x10^{-4} \pm 0.00x10^{-4}$	27.54 ± 0.05	0.99 ± 0.00
200 rpm	Linearized	0.0023 ± 0.0001	20.54 ± 0.44	0.97 ± 0.00	$3.47x10^{-4} \pm 0.01x10^{-4}$	26.39 ± 0.10	0.99 ± 0.00
	Non-linearized	0.0053 ± 0.0001	23.60 ± 0.04	0.96 ± 0.00	$2.45x10^{-4} \pm 0.02x10^{-4}$	26.76 ± 0.01	0.98 ± 0.00
300 rpm	Linearized	0.0019 ± 0.0002	20.99 ± 0.07	0.93 ± 0.02	$3.15x10^{-4} \pm 0.03x10^{-4}$	27.14 ± 0.16	0.99 ± 0.00
	Non-linearized	0.0056 ± 0.0001	23.89 ± 0.23	0.97 ± 0.00	$2.48x10^{-4} \pm 0.02x10^{-4}$	27.22 ± 0.25	0.99 ± 0.00

4.2.4 Effect of pH

Solution pH plays an important role in the metal biosorption process since it greatly affects the ionization of metal binding sites on the cell surface and thus the surface charge on the biosorbent. The degree of ionization and speciation of the heavy metal ions in water can also be affected by the solution pH. The dominant species of copper in the pH range of 3.0 to 5.0 are Cu^{2+} and $CuOH^{+}$ while copper at pH above 6.0 precipitates as insoluble $Cu(OH)_2$. Therefore, copper(II) biosorption study could not be performed at pH above 6.0. Fig. 4.14 clearly shows that the copper(II) uptake was strongly affected by the solution pH. The uptake capacities of the two types of immobilized biosorbents showed a similar trend. The lowest copper(II) uptake was found at pH 2.0. Copper(II) removal then increased with the solution pH and a maximum value was reached at pH 5.0. At a lower solution pH, because of the high proton concentration, positive surface charge was induced on the cells, which retarded the biosorption of metal cations, thus a smaller value was obtained. As the solution pH increased, the cell surface became less positive and the electrostatic repulsion between the metal ions and the cell surface would decrease. Precipitation of $Cu(OH)_2$ was observed with further increase in solution pH to 6.0, which greatly reduced the biosorption capacity as illustrated in Fig. 4.14. Consequently, the optimum pH for copper(II) uptake was

found to about 5.0.

4.2.5 Effect of biomass dosage

The metal biosorption capacity and biosorption efficiency are equally important in the biosorption experiment as both usually take part in deciding the biosorption performance of a given biosorbent. The effect of biomass dosage is an important parameter affecting the biosorption capacity and biosorption efficiency. Fig. 4.15 shows the effect of biomass dosage on copper(II) biosorption by both spherical and cylindrical biosorbents. The biosorption capacity of both spherical and cylindrical biosorbents decreased as the biomass dosage was increased. The results can be explained as a consequence of a particle aggregation, which occurs at high biomass dosage resulting in a decrease in the number of the active sites. The percentage of copper(II) adsorbed increased when the biomass dosage was increased. This could be due to an increase in surface area of the biosorbent, which in turn increased the binding sites for adsorbing the copper(II) ions.

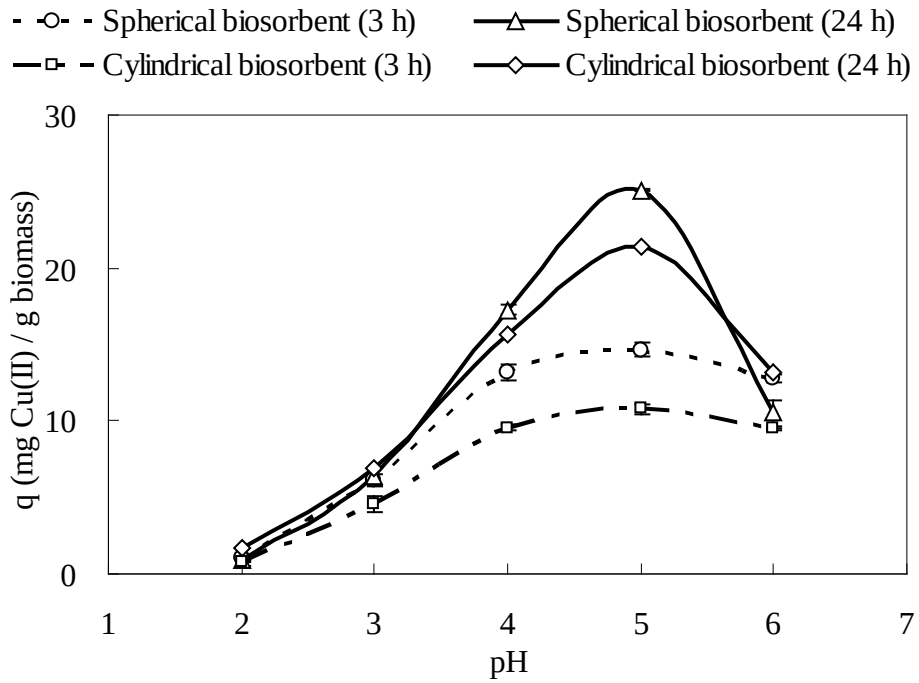

Figure 4.14. Effect of pH on copper(II) biosorption by spherical and cylindrical biosorbents.

[Experimental conditions: initial copper(II) concentration = 100 mg/L; biomass concentration = 1.5 g/L; agitation speed = 250 rpm]

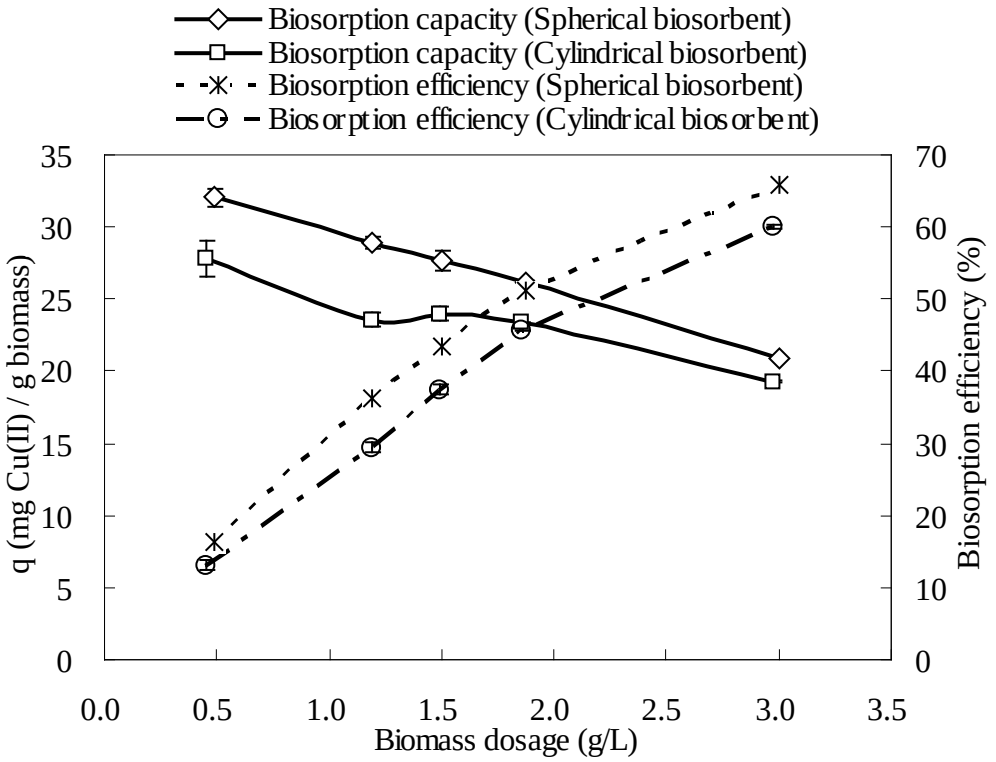

Figure 4.15. Effect of biomass dosage on copper(II) biosorption by spherical and cylindrical biosorbents.

[Experimental conditions: initial copper(II) concentration = 100 mg/L; agitation speed = 250 rpm; pH = 5]

4.2.6 Biosorption isotherms

Experimental equilibrium biosorption data are usually described, analyzed and modeled using the biosorption isotherm, which is related to the metal uptake per unit mass of the cells to the equilibrium metal concentration in the bulk phase. The copper(II) biosorption isotherms of the spherical and cylindrical biosorbents are shown in Fig. 4.16. The results demonstrate that the amount of the copper(II) uptake increased with an increase in the equilibrium metal concentration and reached the maximum at a higher metal concentration. It was found that the effect of metal concentration on copper(II) uptake by the spherical and cylindrical biosorbents was similar.

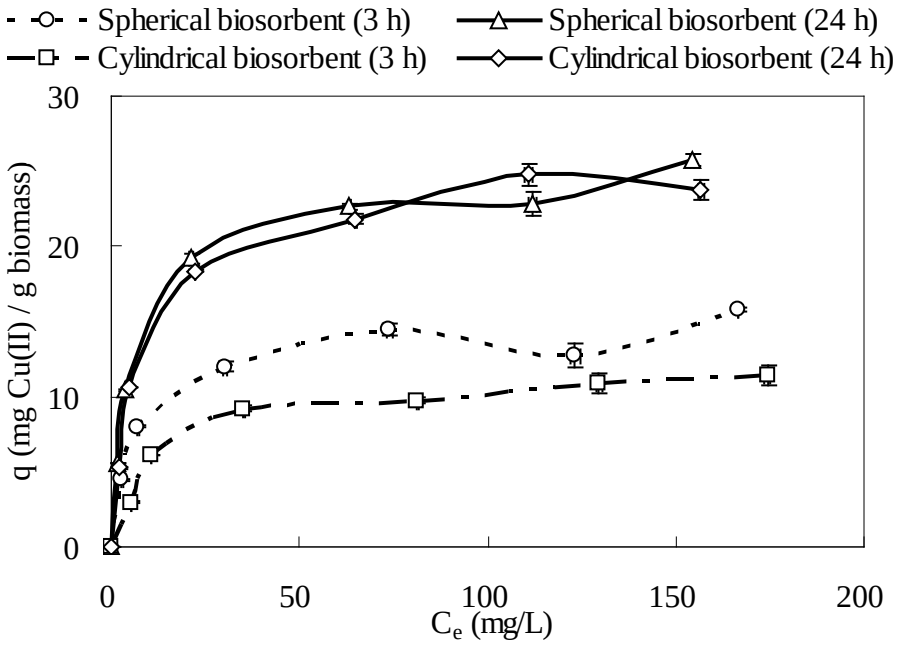

Figure 4.16. Copper(II) biosorption isotherms of spherical and cylindrical biosorbents.

[Experimental conditions: biomass concentration = 1.5 g/L; agitation speed = 250 rpm; pH = 5]

The Langmuir and Freundlich isotherm models were applied to evaluate the biosorption behavior of the sol-gel/PVA immobilized *Micrococcus* sp. with both spherical and cylindrical shapes. These two models have been widely used since they are simple and they can give a good description of the experimental behaviour. Both linear and non-linear regression analyses were used to fit the experimental biosorption data to the Langmuir and Freundlich isotherm models. The linear plots of C_e/q_e versus C_e for the Langmuir isotherm model as well as *ln q* versus *ln* C_e for the Freundlich isotherm model are shown in Figs. 4.17 and 4.18, respectively. The results of the non-linearized Langmuir and Freundlich isotherm models for both the spherical and cylindrical biosorbents are presented in Fig. 4.19. The non-linear regression analysis clearly indicates that the Langmuir model could better simulate the experimental data. The parameters and correlation coefficients (r^2) of the Langmuir and Freundlich isotherm models for copper(II) biosorption by the spherical and cylindrical biosorbents are calculated and summarized in Tables 4.10 and 4.11, respectively. The data show that the Langmuir isotherm can better model the copper(II) biosorption by both spherical and cylindrical biosorbents than the Freundlich isotherm. The r^2 of the Langmuir model for the linear and non-linear plots were higher than those of the Freundlich model. The isotherm parameters and r^2 calculated from the

non-linearized Langmuir model were similar to those obtained using linearized Langmuir model. The maximum biosorption capacities (q_{max}) of the spherical and cylindrical biosorbents estimated from the Langmuir model were similar (25 mg/g-biomass). A large value of affinity constant (b) indicates a high binding affinity between the biosorbate and the biosorbent, which is desirable in a good biosorbent. The affinity constants of the spherical and cylindrical biosorbents were nearly the same.

Fig. 4.20 presents the simulated copper(II) biosorption isotherms of the immobilized biosorbents using the isotherm parameters estimated from the linearized Langmuir and Freundlich models. The results further indicate that the Langmuir model could better simulate the experimental data.

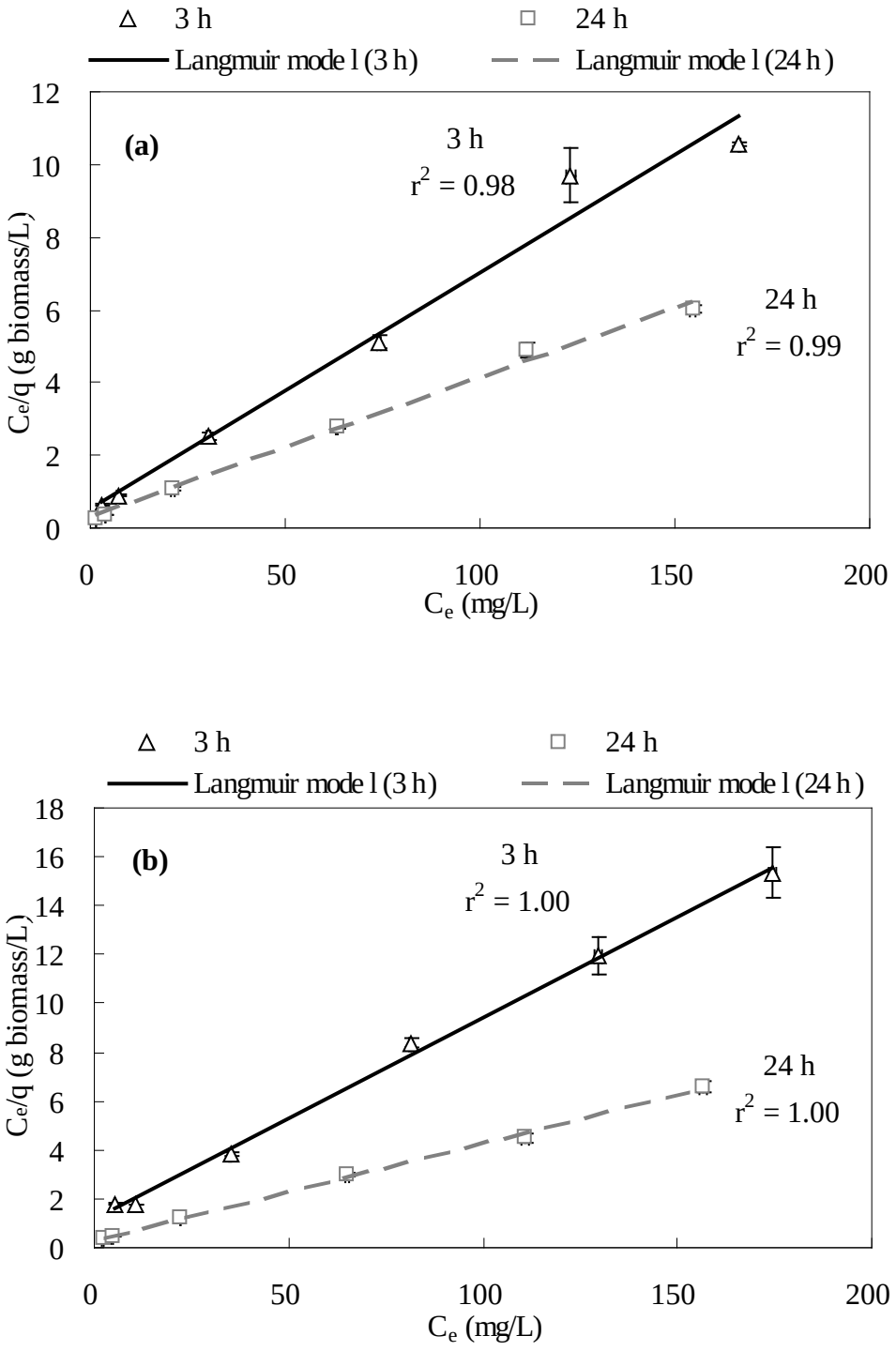

Figure 4.17. Langmuir model of copper(II) biosorption isotherms by (a) spherical biosorbent and (b) cylindrical biosorbent.

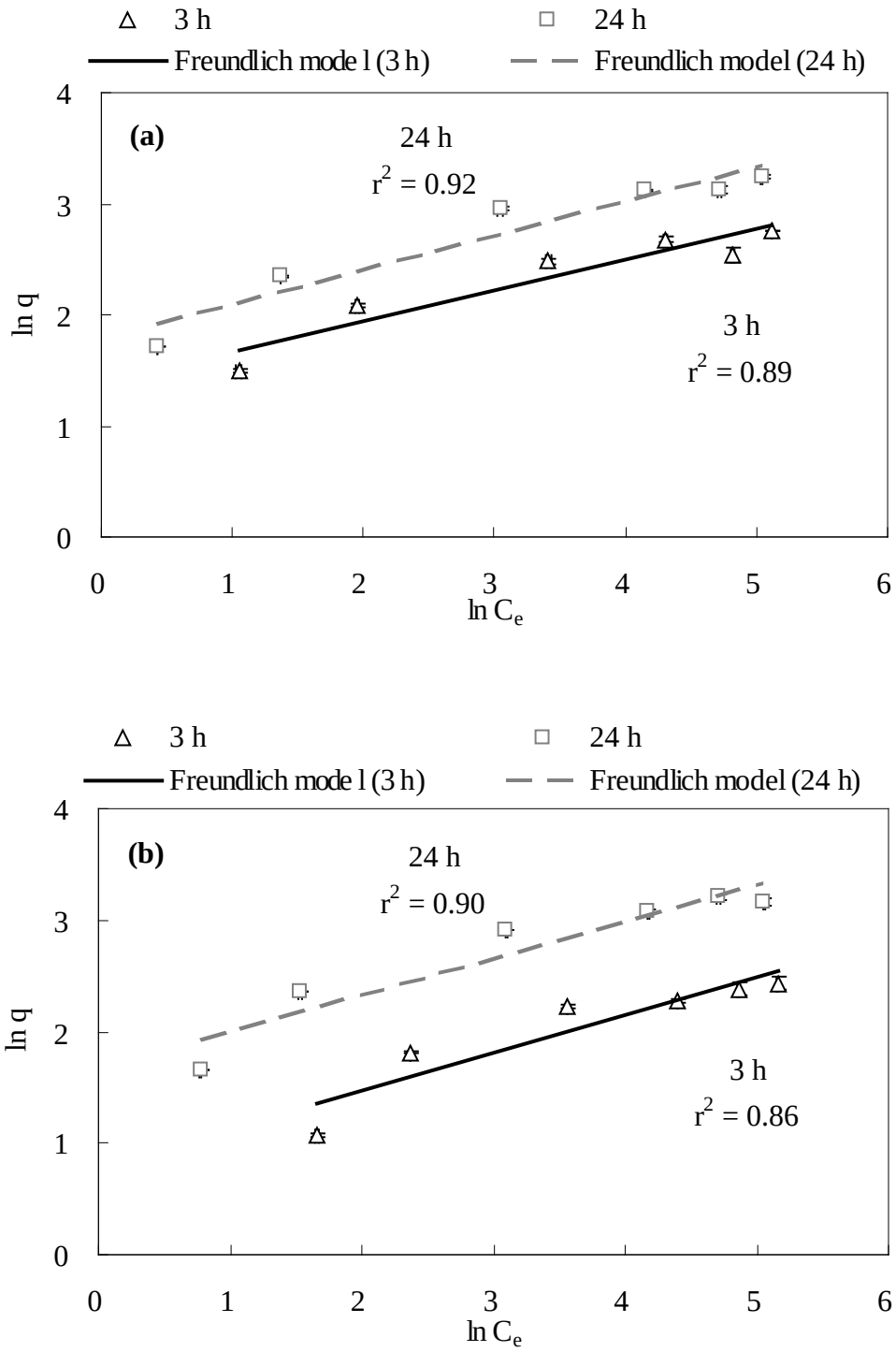

Figure 4.18. Freundlich model of copper(II) biosorption isotherms by (a) spherical biosorbent and (b) cylindrical biosorbent.

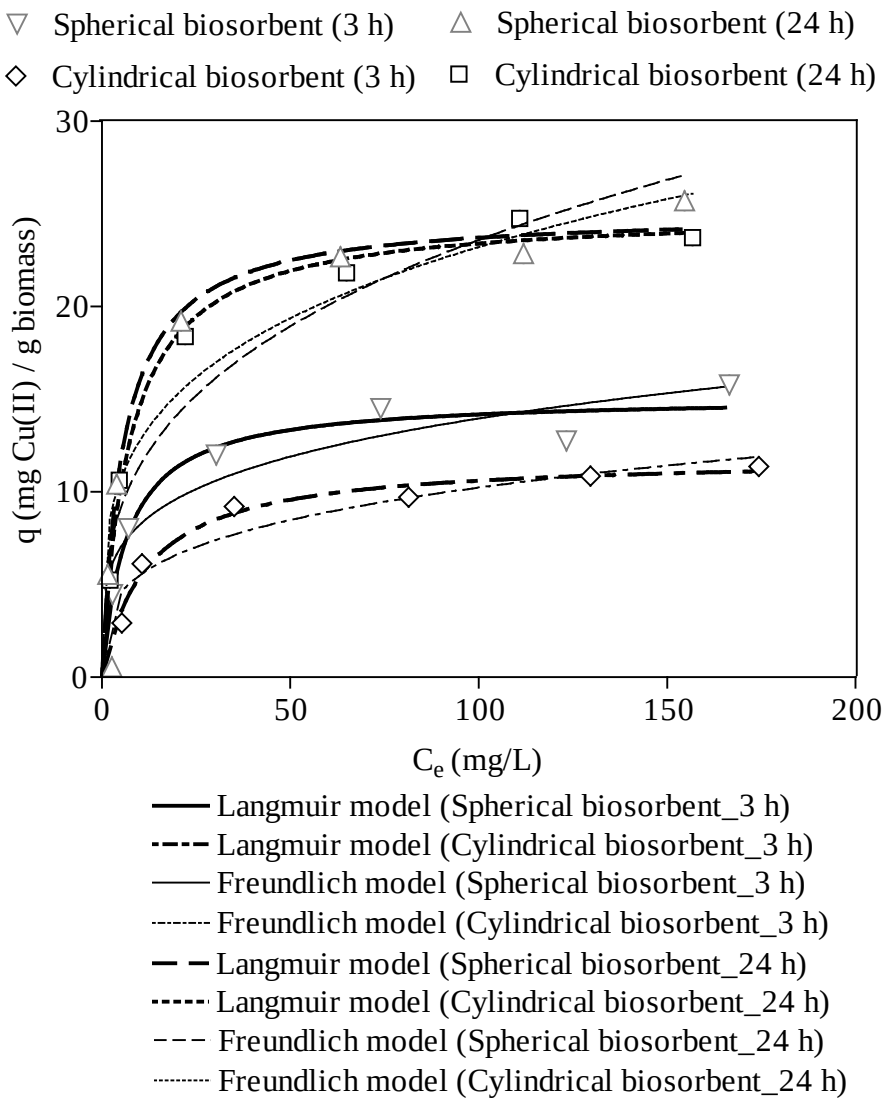

Figure 4.19. Non-linearized Langmuir and Freundlich isotherm models of copper(II) biosorption by spherical and cylindrical biosorbents.

Table 4.10. Parameters of Langmuir and Freundlich isotherm models for copper(II) biosorption by spherical biosorbent.

		Langmuir			Freundlich		
		q_{max} (mg/g-biomass)	b (L/mg)	r^2	K	n	r^2
Linearized	3 h	15.44 ± 0.51	0.12 ± 0.02	0.98 ± 0.01	4.04 ± 0.07	3.65 ± 0.08	0.89 ± 0.04
	24 h	25.87 ± 0.05	0.14 ± 0.00	0.99 ± 0.00	6.00 ± 0.05	3.25 ± 0.02	0.92 ± 0.01
Non-linearized	3 h	15.13 ± 0.18	0.15 ± 0.01	0.94 ± 0.03	4.84 ± 0.21	4.35 ± 0.22	0.88 ± 0.07
	24 h	25.08 ± 0.05	0.17 ± 0.01	0.99 ± 0.01	6.52 ± 1.58	3.60 ± 0.67	0.89 ± 0.04

Table 4.11. Parameters of Langmuir and Freundlich isotherm models for copper(II) biosorption by cylindrical biosorbent.

		Langmuir			Freundlich		
		q_{max} (mg/g-biomass)	b (L/mg)	r^2	K	n	r^2
Linearized	3 h	12.12 ± 0.83	0.07 ± 0.02	1.00 ± 0.00	2.19 ± 0.13	2.94 ± 0.17	0.86 ± 0.01
	24 h	25.27 ± 0.81	0.13 ± 0.02	1.00 ± 0.00	5.30 ± 0.04	3.03 ± 0.05	0.90 ± 0.01
Non-linearized	3 h	11.89 ± 0.57	0.09 ± 0.01	0.97 ± 0.01	2.95 ± 0.18	3.71 ± 0.29	0.89 ± 0.02
	24 h	25.11 ± 0.47	0.14 ± 0.01	0.99 ± 0.01	6.05 ± 1.43	3.46 ± 0.64	0.88 ± 0.03

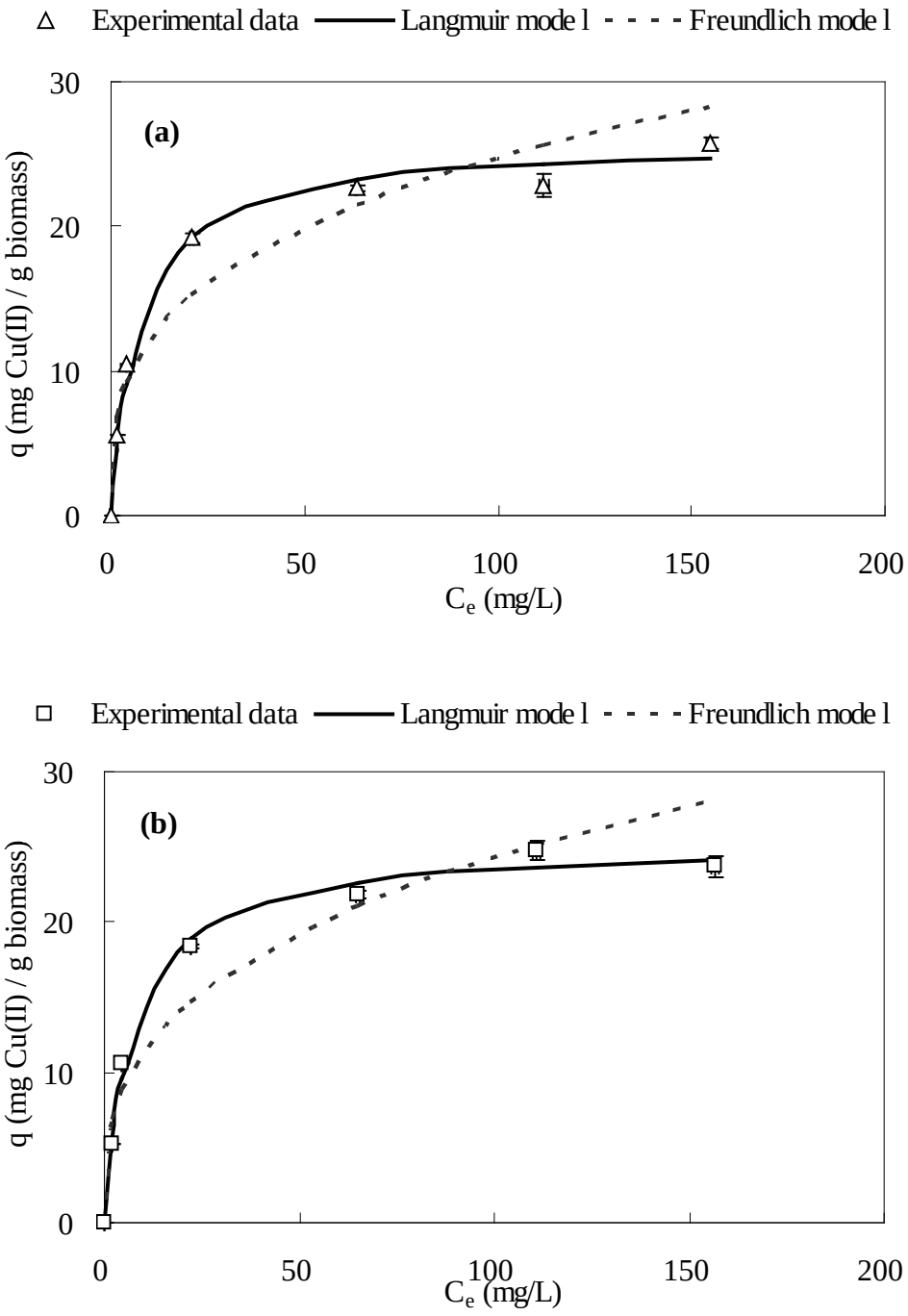

Figure 4.20. Simulation of copper(II) biosorption isotherms of (a) spherical biosorbent and (b) cylindrical biosorbent by linearized Langmuir and Freundlich isotherm models.

4.2.7 Effect of sodium ions

Industrial wastewater often contains other ions that may influence the uptake of heavy metals. The presence of sodium ions in the wastewater may affect the biosorption process. Therefore, experiment was conducted to evaluate the effect of sodium on copper(II) uptake by the spherical biosorbent. Fig. 4.21 illustrates the copper(II) biosorption efficiency in the presence of different sodium concentrations. The removal percentage of copper(II) ions decreased with an increase of sodium concentration. The presence of sodium ions with an initial concentration of 500 mg/L caused a 35% decrease in the copper(II) biosorption efficiency. This could be due to the competition of sodium ions with copper(II) ions for the available binding sites on the biomass. Dahiya *et al*. (2008) reported a similar result that a 32% decrease in copper(II) biosorption efficiency of the arca shell biomass was observed in the presence of 500 mg/L sodium ions.

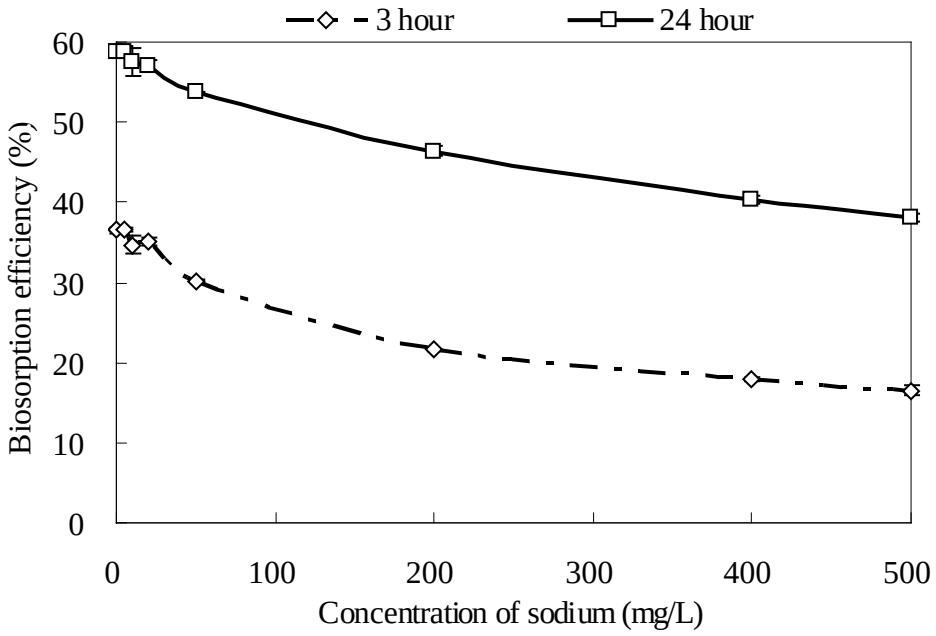

Figure 4.21. Effect of sodium concentration on the biosorption efficiency of copper(II) by spherical biosorbent.

[Experimental conditions: initial copper(II) concentration = 50 mg/L; biomass concentration = 1.5 g/L; agitation speed = 250 rpm; pH = 5]

4.3 Changes in surface morphology

Sol-gel/PVA matrix with and without the encapsulated biomass in both spherical and cylindrical shapes were examined using SEM to investigate the surface morphology of the biosorbents. The surfaces of both the spherical and cylindrical biosorbents before and after copper(II) biosorption were also compared using SEM. Fig. 4.22 shows that a uniform surface was observed on the biomass-free spherical biosorbent. The surface of the spherical biosorbent became rugged once *Micrococcus* sp. was encapsulated as shown in Fig. 4.23. After copper(II) biosorption, the surface of the spherical biosorbent was changed as indicated in Fig. 4.24. Sheng *et al*. (2008) reported a similar result that the surface of PVA-*Sargassum* beads was changed after copper(II) uptake. A rough surface with gel network was observed on the biomass-free cylindrical biosorbent as shown in Fig. 4.25. A comparison of Figs. 4.22 and 4.25 shows that the surface morphology of the cylindrical biosorbent was more uneven and irregular than that of the spherical biosorbent. The difference between the surfaces of the spherical biosorbent and the cylindrical biosorbent may be due to differences of the immobilization process. The biosorbent with spherical shape was prepared by dropping the sol-gel/PVA matrix into liquid nitrogen, which may change and smooth out its surface morphology. Ting and Sun (2000) also observed that the

surface of the biomass-free beads prepared by dropping the PVA into liquid nitrogen was uniform. Fig. 4.26 displays that the *Micrococcus* sp. was embedded within the silica matrix after the immobilization process. Similar to the spherical biosorbent, the surface of the cylindrical biosorbent was changed after copper(II) uptake as indicated in Fig. 4.27.

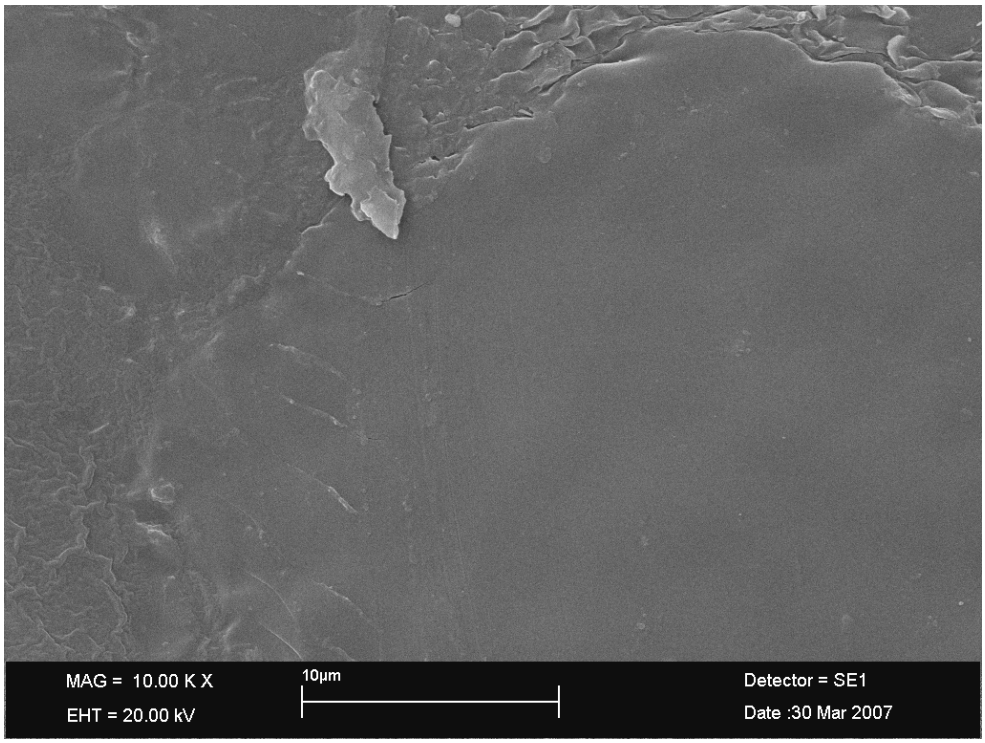

Figure 4.22. SEM micrograph of spherical biosorbent without *Micrococcus* sp.

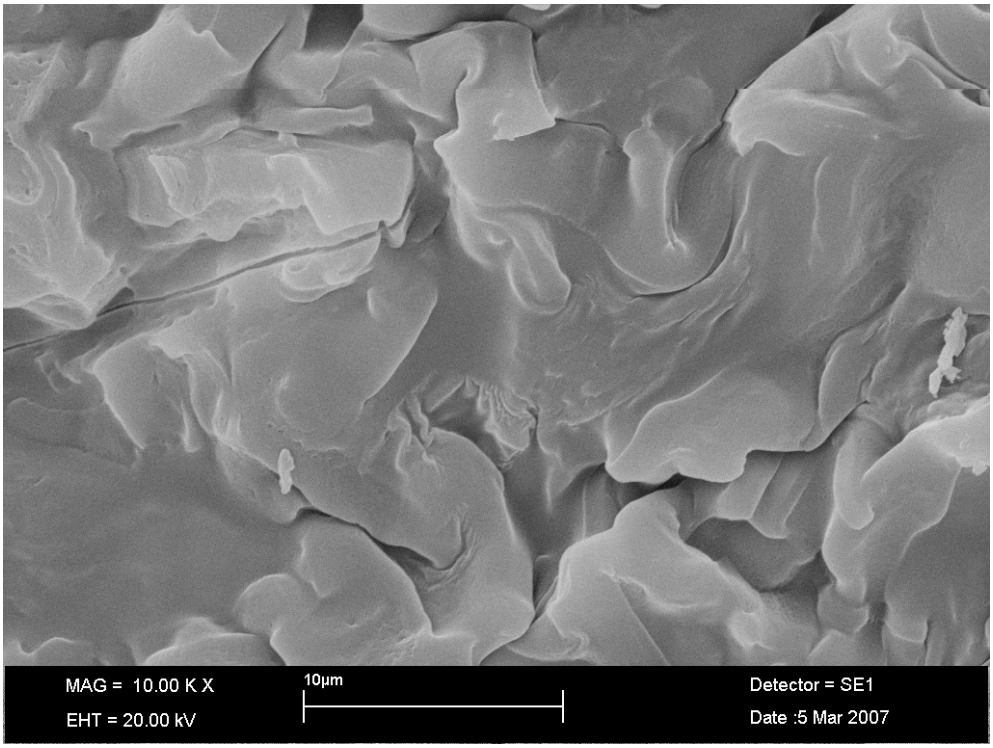

Figure 4.23. SEM micrograph of spherical biosorbent with *Micrococcus* sp. before copper(II) uptake.

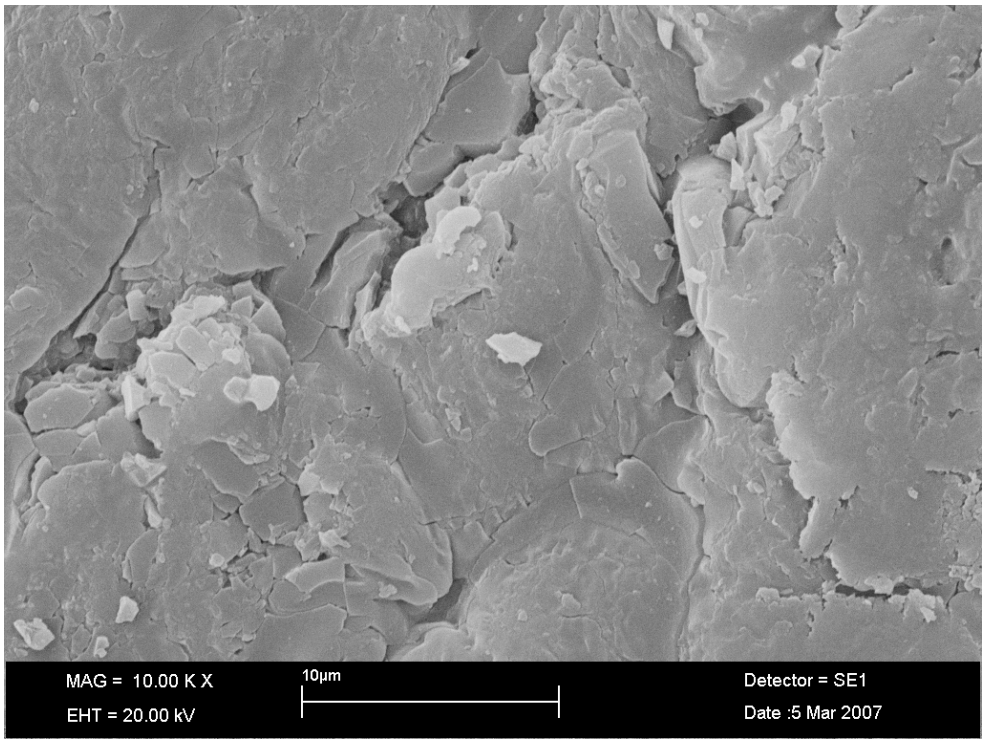

Figure 4.24. SEM micrograph of spherical biosorbent with *Micrococcus* sp. after copper(II) uptake.

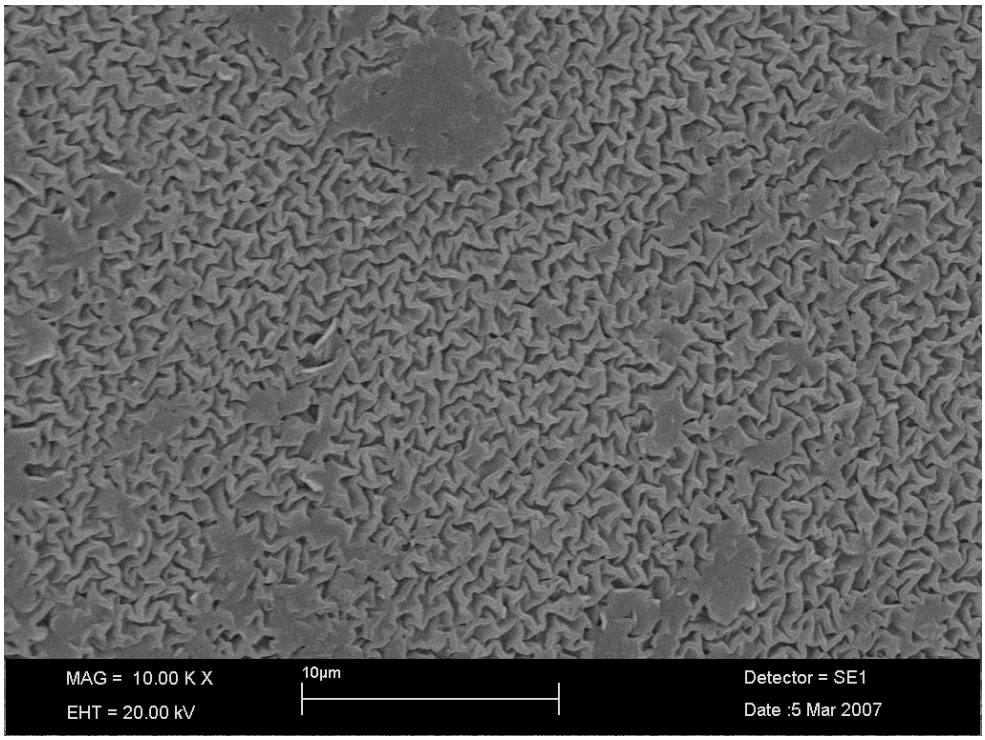

Figure 4.25. SEM micrograph of cylindrical biosorbent without *Micrococcus* sp.

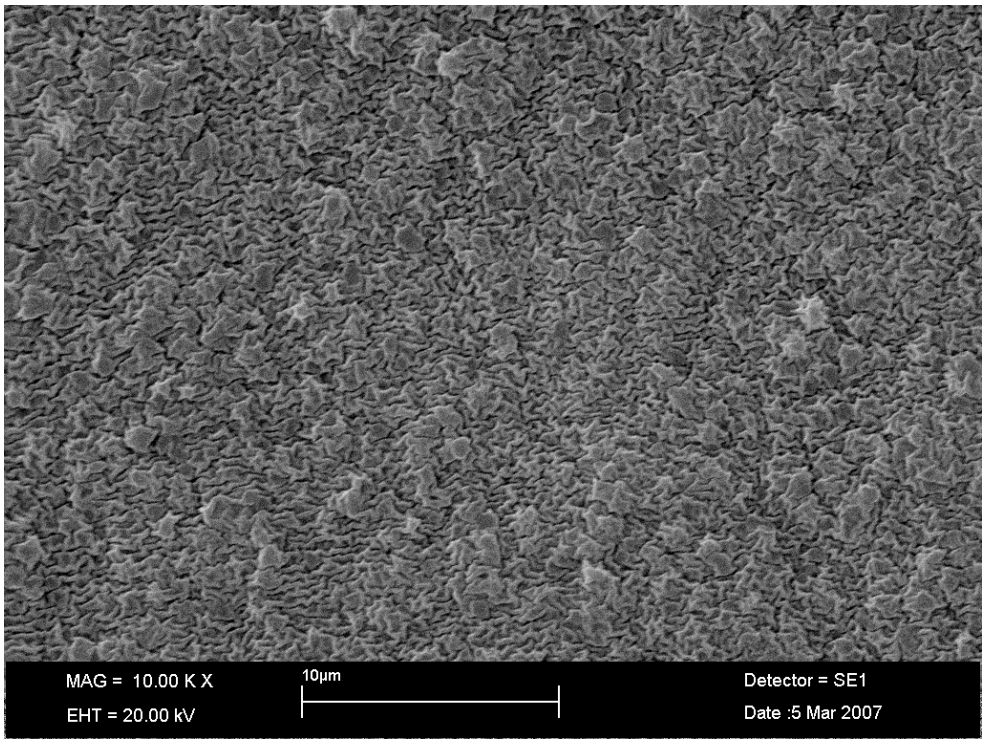

Figure 4.26. SEM micrograph of cylindrical biosorbent with *Micrococcus* sp. before copper(II) uptake.

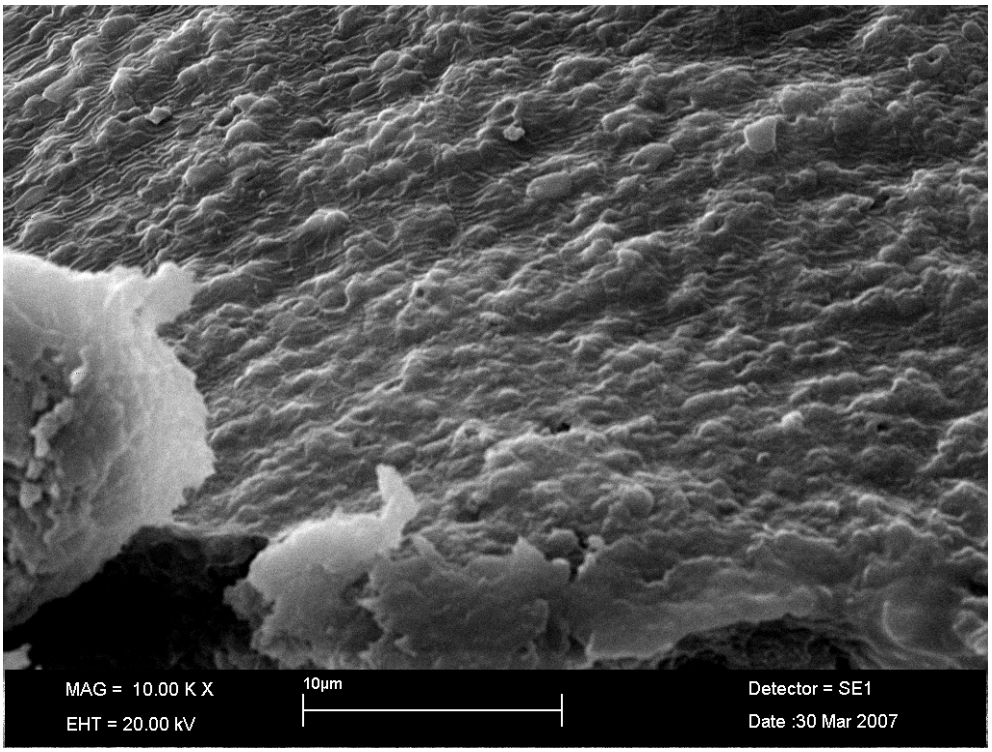

Figure 4.27. SEM micrograph of cylindrical biosorbent with *Micrococcus* sp. after copper(II) uptake.

4.4 Desorption of copper(II)-laden biosorbent

Biosorbent regeneration is an important issue for improving the process economics. The simplest and cheapest method for metal recovery is to desorb or elute the metal ions from the biosorbent using desorbing agents. Good desorbing agents should be effective, non-damaging to the biomass, non-polluting and cheap. Thus, desorption studies were conducted to find out an effective desorbing agent for biomass regeneration.

4.4.1 Screening of desorbing agents

Nine desorbing agents including mineral acids (HCl, HNO_3 and H_2SO_4); complexing agents (CA, EDTA and NTA); salts ($Na_5P_5O_{10}$ and $CaCl_2$) and DDI water were selected to desorb copper(II) ions from the metal-laden biosorbent. Previous studies reported that all these desorbing agents, with the exception of DDI water, gained a high desorption efficiency for copper(II) removal in the metal-laden *Micrococcus* sp. suspended cells (Wong, 2000). The amounts of copper(II) adsorbed and desorbed per gram of biomass from both the spherical and cylindrical biosorbents together with the recovery percentages are shown in Fig. 4.28. Copper(II) desorption from the spherical and cylindrical immobilized biosorbents generally gave a similar result when the same desorbing agent was

used. The results clearly indicate that the mineral acids (HCl, HNO_3 and H_2SO_4) can elute more than 90% of the adsorbed copper(II) ions. A high desorption efficiency suggests a high binding affinity between protons and binding sites in the biosorbent. The recovery percentages by chelating agents including CA, EDTA and NTA from the spherical biosorbent were 85.18%, 87.67% and 87.49%, respectively, whereas those from the cylindrical biosorbent were 79.52%, 84.75% and 84.12%, respectively. Only half of the adsorbed copper(II) ions were desorbed from the spherical or cylindrical biosorbents using $CaCl_2$ and $Na_5P_5O_{10}$ as the desorbing agents. Desorption using DDI water was negligible (< 0.5%), which indicated a strong affinity between the biomass and the metal ions.

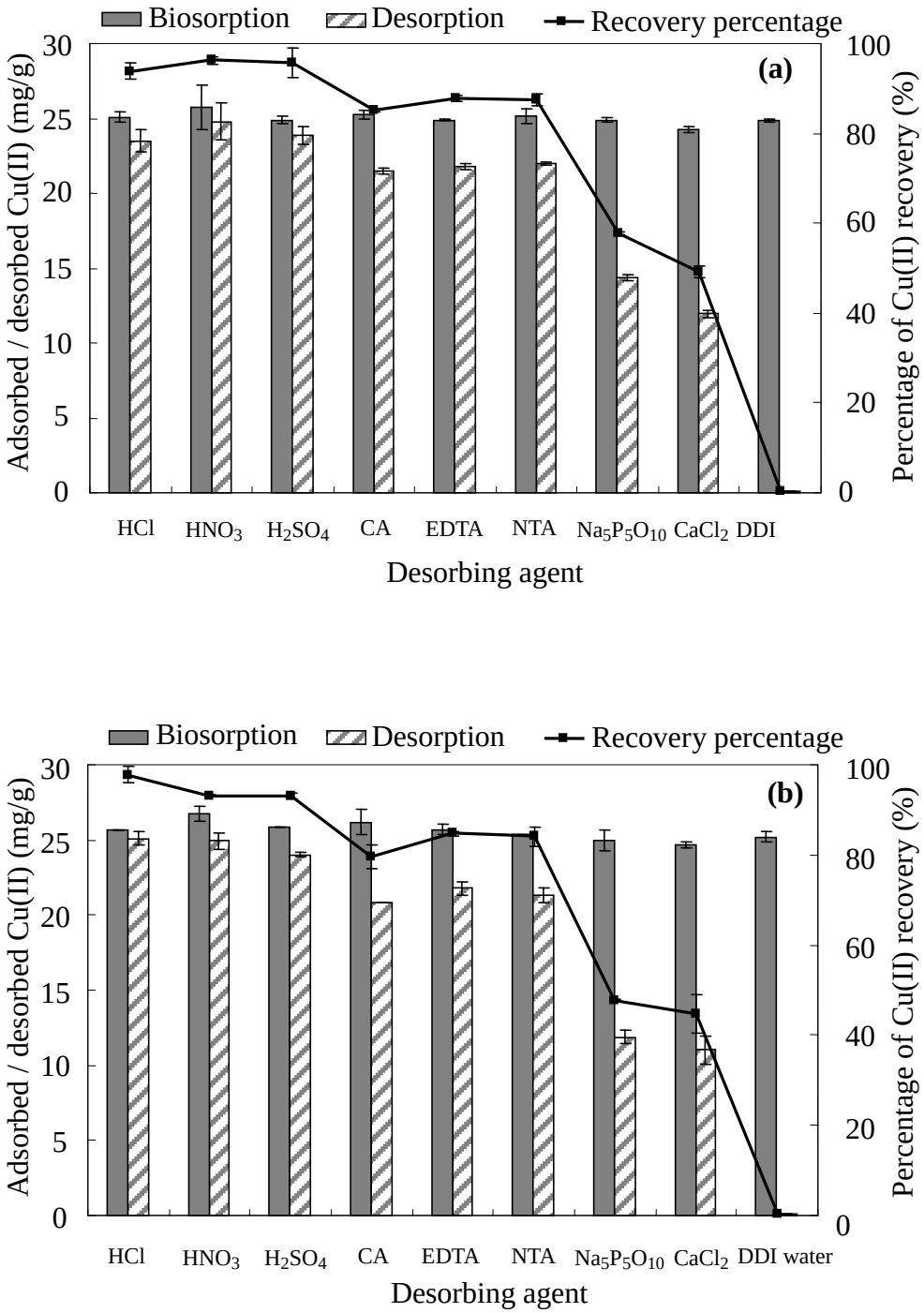

Figure 4.28. Desorption of copper(II) from (a) spherical biosorbent and (b) cylindrical biosorbent using different desorbing agents.

[Experimental conditions: initial copper(II) concentration = 100 mg/L; contact time = 24 h for biosorption & 6 h for desorption; pH = 5 for biosorption; agitation speed = 250 rpm; concentration of desorbing agent = 0.1 M (0.05 M for H_2SO_4)]

Repeated biosorption and desorption operations were performed to study the reusability and metal recovery efficiency of the biosorbent using different desorbing agents. The results of three biosorption/desorption cycles of the immobilized biosorbents are shown in Fig. 4.29. The copper(II) recovery and the biosorbent reusability using NTA as the desorbing agent were better. The copper(II) biosorption capacity decreased significantly in cycle 2 when HCl, HNO_3, H_2SO_4, CA, EDTA, and $CaCl_2$ were used as the desorbing agents. This could be due to the incomplete copper(II) desorption by CA, EDTA and $CaCl_2$ as well as changes of the biomass surface characteristics caused by HCl, HNO_3, H_2SO_4 and CA.

Among all the desorbing agents, HNO_3 and NTA were proved to be the best agents for copper(II) recovery in the first cycle. Thus, further studies on copper(II) desorption (i.e., desorption kinetics and concentrations of desorbing agents) were conducted in more details using these two desorbing agents to determine if there is any improvement in the reusability of the biosorbent.

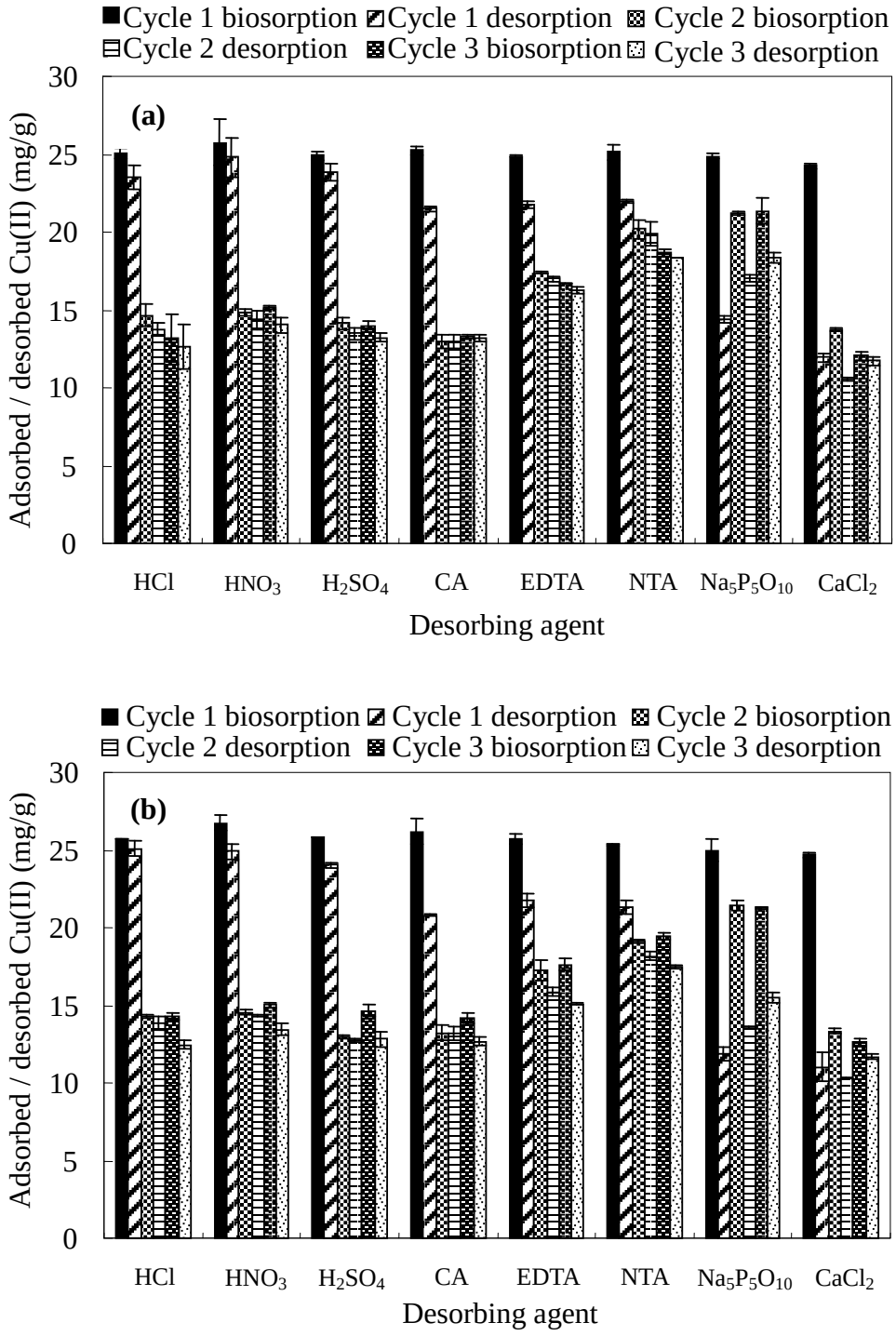

Figure 4.29. Copper(II) biosorption/desorption cycles of (a) spherical biosorbent and (b) cylindrical biosorbent using different desorbing agents.

[Experimental conditions: initial copper(II) concentration = 100 mg/L; contact time = 24 h for biosorption & 6 h for desorption; pH = 5 for biosorption; agitation speed = 250 rpm; concentration of desorbing agent = 0.1 M (0.05 M for H_2SO_4)]

4.4.2 Desorption kinetics

Desorption of copper(II) using mineral acids or NTA may cause substantial damage to the biosorbent. In order to minimize such damage, the effect of contact time on copper(II) desorption using 0.1 M HNO_3 and 0.1 M NTA was investigated in order to examine the minimum time required for copper(II) recovery from the immobilized biosorbents.

Fig. 4.30 compares the copper(II) desorption kinetics of the spherical biosorbent and the cylindrical biosorbent using 0.1 M HNO_3 and 0.1 M NTA as the desorbing agents. Desorption of copper(II) was faster and it promptly reached the equilibrium when using HNO_3 as the eluting agent. This could be due to the fast exchange of proton with the adsorbed metal ions. The desorption time required to elute more than 90% of copper(II) ions from the spherical biosorbent was 3 h by HNO_3 and 4 h by NTA. Many researchers reported that the use of mineral acid could recover almost all of the metals from the biosorbents (Akthar *et al.*, 1995; Aldor *et al.*, 1995; Tam *et al.*, 1998). Sar *et al.* (1999) demonstrated that mineral acid was an effective desorbing agent for copper(II) and nickel(II) recovery from *Pseudomonas aeruginosa*. Metal recovery from the spherical biosorbent was faster than the cylindrical biosorbent when the same

desorbing agent was used. This may be due to the smaller size of the spherical biosorbent, which reduced the diffusion time required for the desorbing agent to reach the biomass surface. The results reveal that more than 95% of copper(II) ions were eluted from the spherical biosorbent within 4 h using either HNO_3 or NTA. However, only 91% and 76% of copper(II) ions were eluted from the cylindrical biosorbent within 7 h using HNO_3 and NTA, respectively. Therefore, the spherical biosorbent seems to be better for copper(II) removal than the cylindrical biosorbent because of its faster copper(II) recovery.

To ensure high metal recovery and biosorbent reusability, further studies were conducted to determine and compare the effect of desorption time on the performance of three copper(II) biosorption/desorption cycles by both the spherical and cylindrical biosorbents.

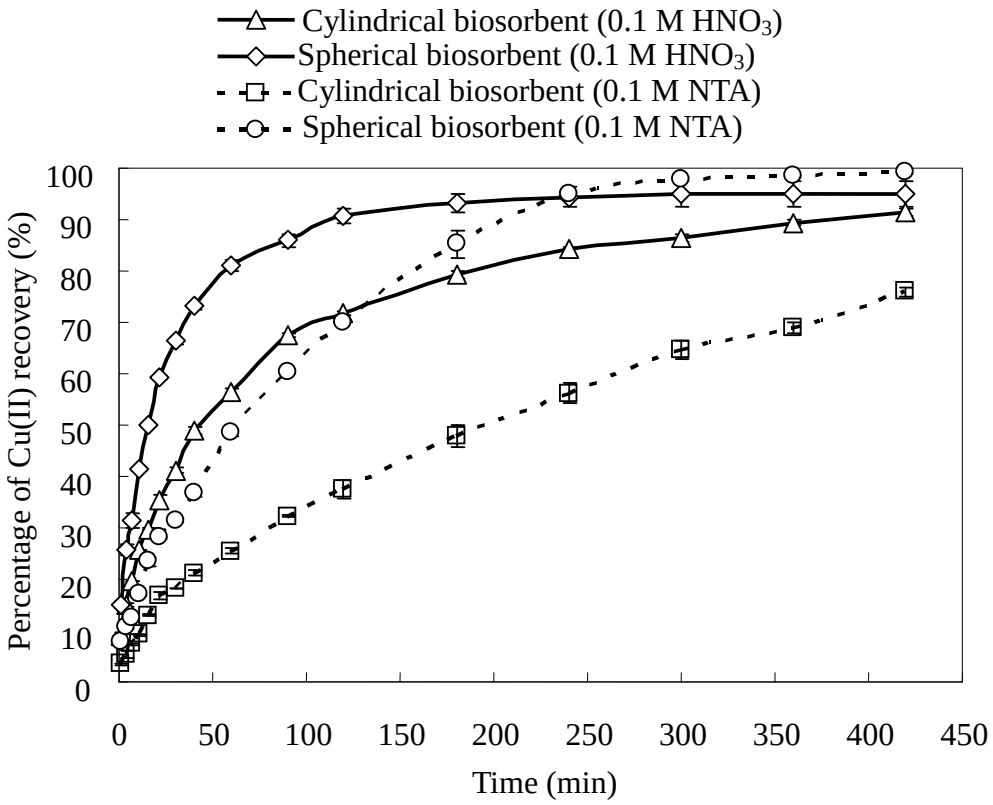

Figure 4.30. Effect of contact time on copper(II) desorption from spherical and cylindrical biosorbents using 0.1 M HNO_3 and 0.1 M NTA.

[Experimental conditions: agitation speed = 250 rpm]

4.5 Copper(II) biosorption/desorption cycles

An effective recovery of metal ions with good biosorbent reusability is an important criterion for metal removal in repeated biosorption/desorption cycles. In order to test the reusability of the biosorbent, repeated biosorption/desorption cycles were performed.

4.5.1 Effect of desorption time

Results in Section 4.4.2 indicated that almost all of the copper(II) ions were recovered from the biosorbents after contact with 0.1 M HNO_3 or 0.1 M NTA for 6 h. However, a long desorption time may damage the biosorbent and result in low metal uptake in the subsequent cycles. Therefore, experiments were performed to investigate the effect of desorption time on copper(II) biosorption/desorption cycles by both the spherical and cylindrical biosorbents.

Fig. 4.30 indicates that the minimum desorption time for copper(II) recovery from the spherical biosorbent and the cylindrical biosorbent by 0.1 M HNO_3 were 3 h and 6 h, respectively. Three consecutive biosorption/desorption cycles were then performed to investigate the reusability of both the spherical and cylindrical biosorbents using 0.1 M HNO_3 with 3 h and 6 h desorption time (Fig. 4.31). The

results demonstrate that HNO_3 could elute almost all of the adsorbed copper(II) ions from both the spherical and cylindrical biosorbents with 3 h and 6 h desorption time. However, the biosorbents could only retain half of its original biosorption capacity in cycle 2. This problem was also observed even when the desorption time was reduced to 3 h. This could be due to changes of the surface characteristics of the biomass by the strong acid.

According to Fig. 4.30, the minimum desorption time for copper(II) recovery from the spherical and cylindrical biosorbents by 0.1 M NTA were 4 h and 6 h, respectively. The results of three consecutive copper(II) biosorption/desorption cycles of the spherical biosorbent using 0.1 M NTA as the desorbing agent are shown in Fig. 4.32. More than 95% of copper(II) ions were recovered from the spherical biosorbent in cycles 1 to 3 after 6 h desorption by 0.1 M NTA (Table 4.12) and about 78% of the biosorption capacity was retained in cycle 2. However, the copper(II) recovery from the spherical biosorbent in the first cycle was incomplete (88%) if the desorption time was reduced to 4 h.

Fig. 4.32 also indicates that the performance of copper(II) biosorption/desorption cycle operation by the cylindrical biosorbent using 0.1 M

NTA as the desorbing agent was not as good as that by the spherical biosorbent because of incomplete copper(II) recovery from the cylindrical biosorbent. As a result of incomplete desorption, copper(II) uptake by the cylindrical biosorbent decreased continuously in the later cycles. A similar result was obtained in the cylindrical biosorbent which was desorbed for 4 h and 6 h.

In general, mineral acid is not a good desorbing agent for the removal and recovery of copper(II) from the sol-gel/PVA immobilized biosorbent. The biosorbent reusability was generally better when using NTA as the desorbing agent. The effect of NTA pretreatment on the performance of the spherical biosorbent was further studied. Fig. 4.33 shows that NTA pretreatment could reduce the amount of copper(II) ions adsorbed on the spherical biosorbent in the first cycle (*t*-test, $p < 0.05$). Biosorbent contacted with NTA could reduce the copper(II) biosorption capacity in cycle 2. However, the biosorption capacity of the biosorbent could still be completely retained after cycle 2. Therefore, NTA was used as the desorbing agent for further studies. Spherical biosorbent is a more promising material for the removal and recovery of copper(II) ions and it was selected for further studies. The optimum desorption time for copper(II) recovery from the spherical biosorbent is 6 h using NTA as the desorbing agent.

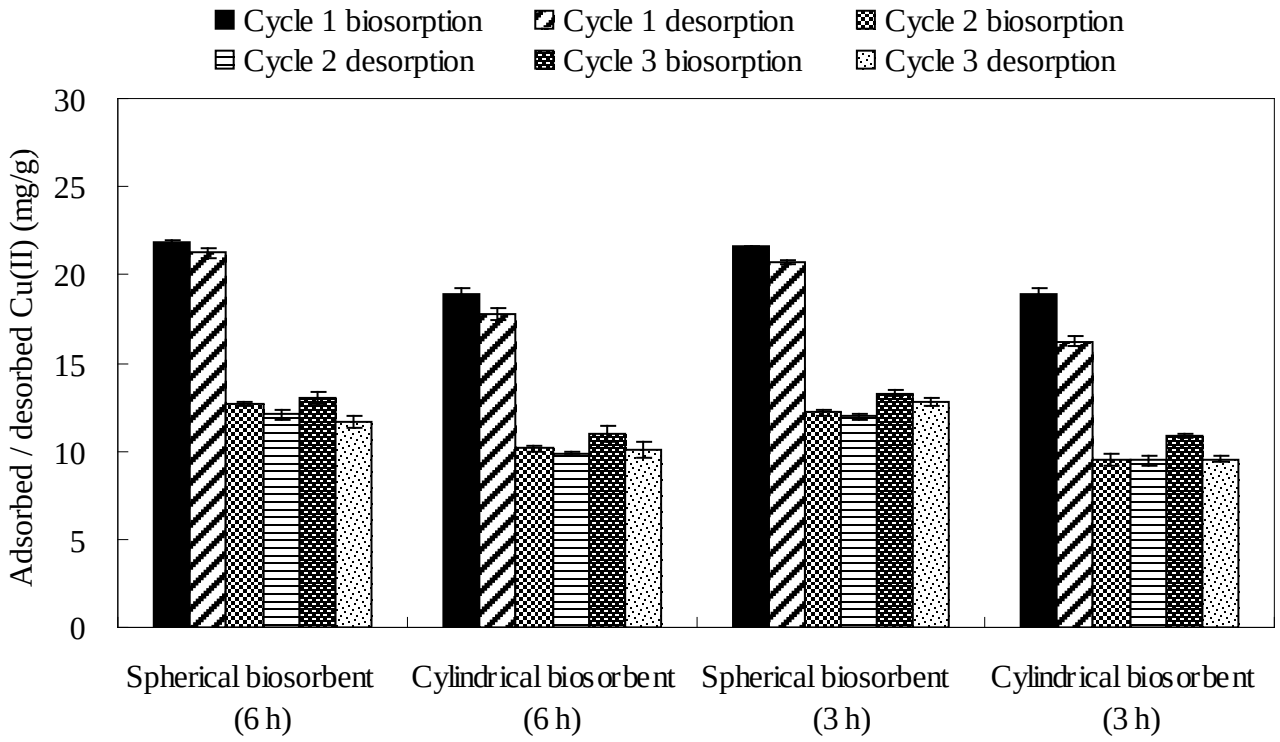

Figure 4.31. Effect of desorption time on copper(II) biosorption/desorption cycles using 0.1 M HNO_3.

[Experimental conditions: initial copper(II) concentration = 100 mg/L; contact time = 24 h for biosorption; pH = 5 for biosorption; agitation speed = 250 rpm]

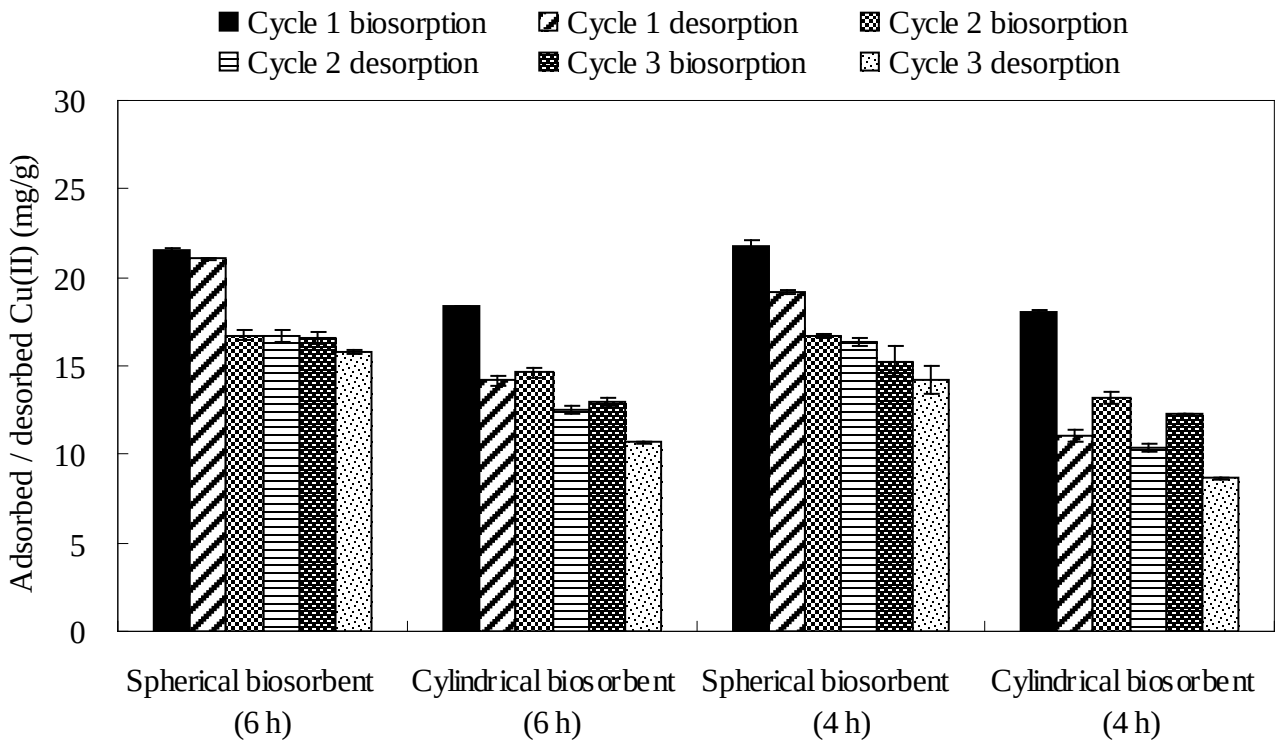

Figure 4.32. Effect of desorption time on copper(II) biosorption/desorption cycles using 0.1 M NTA.

[Experimental conditions: initial copper(II) concentration = 100 mg/L; contact time = 24 h for biosorption; pH = 5 for biosorption; agitation speed = 250 rpm]

Table 4.12. Percentage of copper(II) recovery from spherical and cylindrical biosorbents using 0.1 M HNO_3 and 0.1 M NTA at different desorption time.

Biosorbent	Desorbing agent	Desorption time (h)	Percentage of copper(II) recovery (%)		
			Cycle 1	Cycle 2	Cycle 3
Spherical	HNO_3	6	97.33 ± 0.79	95.13 ± 1.23	90.02 ± 0.47
Cylindrical	HNO_3	6	94.18 ± 0.11	97.61 ± 1.08	91.79 ± 0.33
Spherical	HNO_3	3	95.93 ± 0.07	98.40 ± 0.25	95.96 ± 0.34
Cylindrical	HNO_3	3	85.91 ± 0.18	99.88 ± 0.17	88.14 ± 0.86
Spherical	NTA	6	97.85 ± 0.08	99.72 ± 0.29	95.39 ± 0.95
Cylindrical	NTA	6	77.27 ± 1.64	85.35 ± 0.13	82.36 ± 0.74
Spherical	NTA	4	88.02 ± 1.50	98.03 ± 0.30	93.22 ± 0.01
Cylindrical	NTA	4	61.16 ± 2.13	78.81 ± 0.57	70.44 ± 0.52

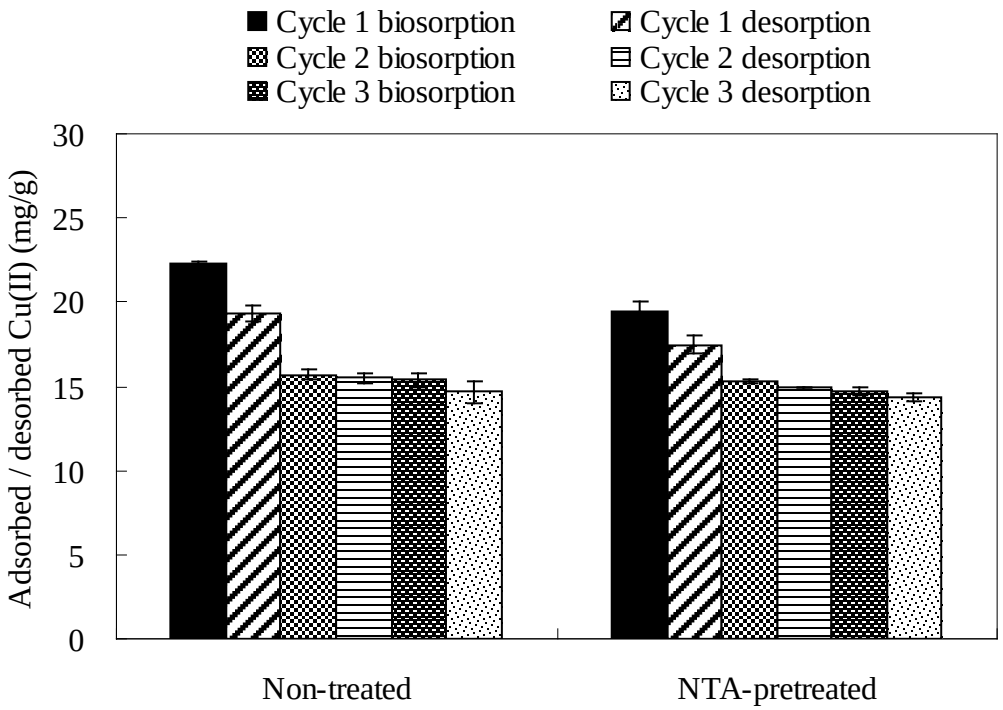

Figure 4.33. Effect of NTA pretreatment of the spherical biosorbent on copper(II) biosorption/desorption cycles.

[Experimental conditions: initial copper(II) concentration = 100 mg/L; contact time = 24 h for biosorption & 6 h for desorption; pH = 5 for biosorption; agitation speed = 250 rpm; desorbing agent = 0.1 M NTA]

4.5.2 Effect of NTA concentration

The most effective desorbing agent for copper(II) recovery from the sol-gel/PVA immobilized biosorbent is NTA. The recovery percentage of metal from the biosorbent should be affected by the concentration of the desorbing agent. Thus, the effect of NTA concentration on the biosorption/desorption cycle operation was examined by varying the NTA concentration from 0.010 M to 0.200 M. Fig. 4.34 and Table 4.13 reveal that the recovery percentage of copper(II) ions from the spherical biosorbent increased from 45% to 98% in cycle 1 when the concentration of NTA was increased from 0.010 M to 0.100 M. The incomplete copper(II) desorption in the first cycle by 0.010 M NTA caused a low copper(II) uptake (~10 mg/g-biomass) in the subsequent cycles. The performance of the biosorption/desorption cycle operation did not improve with 0.200 M NTA as the desorbing agent. Therefore, the optimal concentration of NTA as a desorbing agent was 0.100 M for the removal and recovery of copper(II) ions from sol-gel/PVA immobilized *Micrococcus* sp.

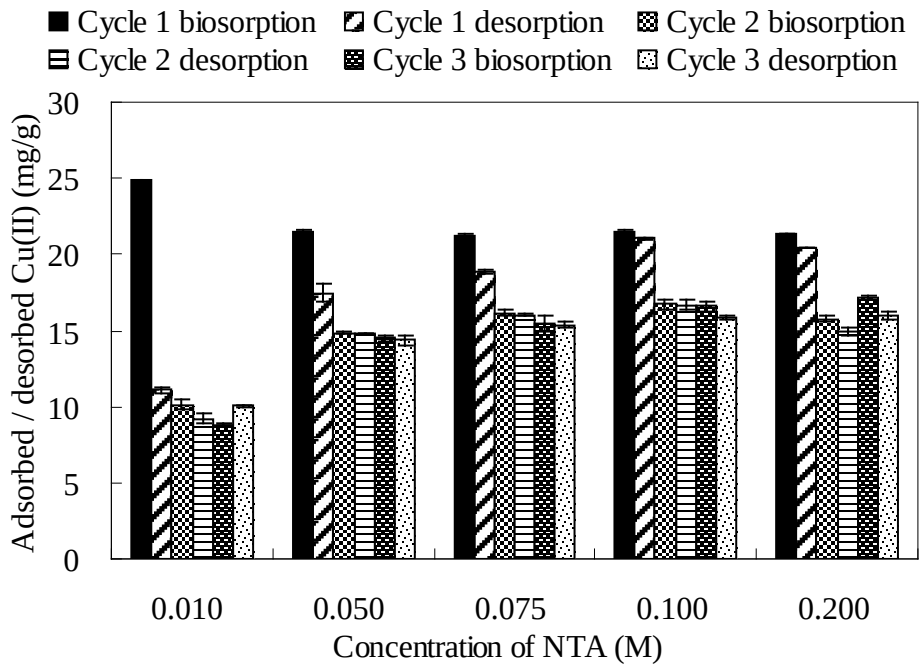

Figure 4.34. Effect of NTA concentration on copper(II) biosorption/desorption cycles by spherical biosorbent.

[Experimental conditions: initial copper(II) concentration = 100 mg/L; contact time = 24 h for biosorption & 6 h for desorption; pH = 5 for biosorption; agitation speed = 250 rpm]

Table 4.13. Percentage of copper(II) recovery from spherical biosorbent using different concentrations of NTA.

	Percentage of copper(II) recovery (%)		
	Cycle 1	Cycle 2	Cycle 3
0.010 M NTA	44.67 ± 0.93	91.08 ± 0.38	113.66 ± 1.25
0.050 M NTA	81.12 ± 2.82	99.42 ± 0.76	98.84 ± 0.80
0.075 M NTA	88.72 ± 1.11	99.09 ± 0.64	99.38 ± 1.94
0.100 M NTA	97.85 ± 0.08	99.72 ± 0.29	95.39 ± 0.95
0.200 M NTA	95.85 ± 0.21	95.03 ± 2.59	93.46 ± 1.03

4.5.3 Comparison of suspended cells and immobilized cells

The reusability of biosorbents is important for metal removal from wastewater. To demonstrate that the spherical immobilized biosorbent can be used repeatedly in the biosorption and desorption processes for metal removal, repeated biosorption/desorption cycles were performed to examine and compare the copper(II) recovery efficiency and the reusability of the suspended cells and the immobilized biosorbent. The copper(II)-laden biosorbent was desorbed using 0.1 M NTA for 6 h. Fig. 4.35 demonstrates that the copper(II) biosorption efficiency of the suspended cells decreased continuously from cycle 1 (46%) to cycle 6 (14%). However, the copper(II) biosorption efficiency of the immobilized biosorbent only decreased by 27% from cycles 1 to 2. The total decrease in the biosorption efficiency of the immobilized biosorbent was much smaller (37%) than that of the suspended cells (70%) after six cycles. About 50% loss in the concentration of the suspended cells was observed after six cycles (Table 4.14). The large decrease in the biosorption efficiency of the suspended cells could be due to a continuous loss of cells during the multiple biosorption/desorption cycle operations. Similarly, Chang *et al*. (1997) reported that about 30% to 45% of cell concentration was lost after four cycles because of the repeated centrifugation and rinse operations. Loss of suspended cells also

resulted in the reduction of desorption efficiency from cycle 1 (91%) to cycle 6 (27%) as shown in Fig. 4.36. In contrast, more than 90% of copper(II) ions were desorbed from the immobilized biosorbent in all cycles. The stable biosorption and desorption efficiencies of the immobilized biosorbent demonstrated that the biomass can be encapsulated within the sol-gel/PVA matrix without any loss of the cells during the biosorption/desorption processes.

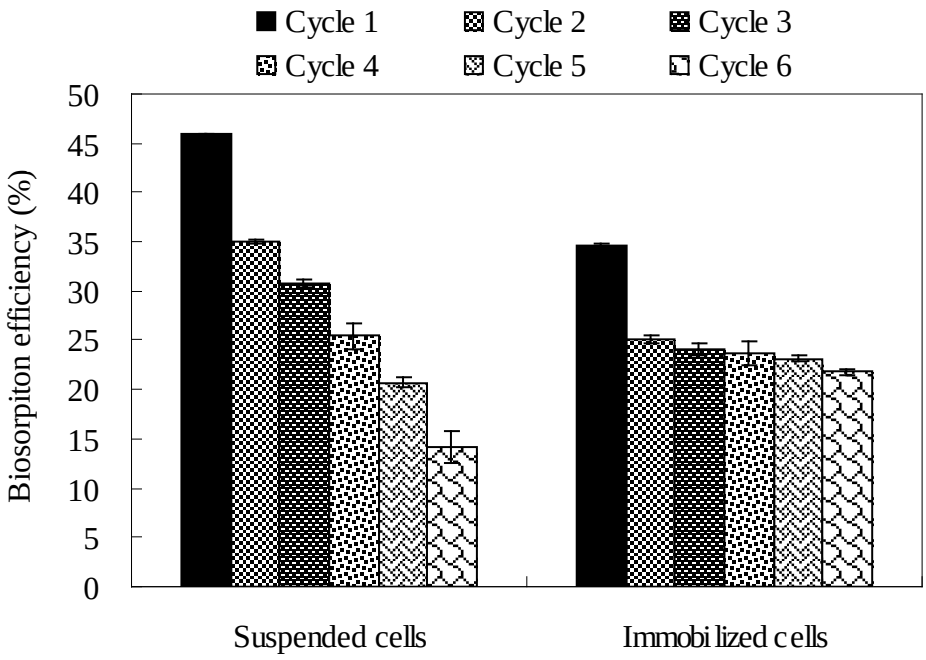

Figure 4.35. Biosorption efficiency of copper(II) by suspended and immobilized *Micrococcus* sp. cells in six cycles.

[Experimental conditions: initial copper(II) concentration = 100 mg/L; contact time = 24 h; agitation speed = 250 rpm; pH = 5]

Table 4.14. Biomass concentration in the reactor over six cycles.

	Concentration of cells in the reactor (g/L)	
	Suspended cells	**Immobilized cells**
Cycle 1	1.45	1.49
Cycle 2	1.42	1.49
Cycle 3	1.42	1.49
Cycle 4	1.22	1.49
Cycle 5	1.05	1.49
Cycle 6	0.70	1.49

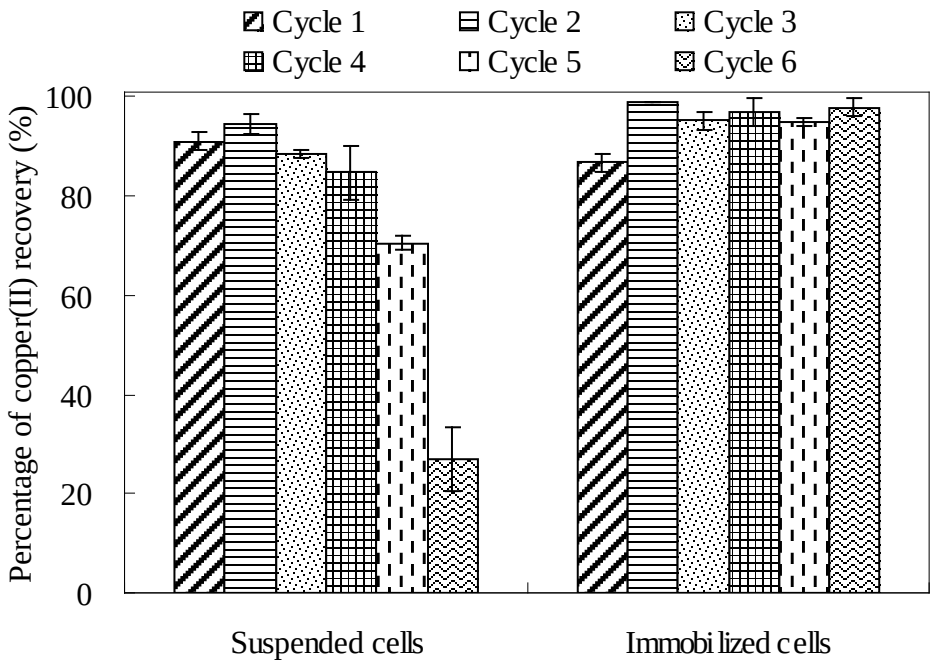

Figure 4.36. Percentage of copper(II) recovery from suspended and immobilized *Micrococcus* sp. cells in six cycles.

[Experimental conditions: contact time = 6 h; agitation speed = 250 rpm; desorbing agent = 0.1 M NTA]

4.6 Comparison of spherical and cylindrical biosorbents

Sections 4.1 to 4.5.1 present the biosorption and desorption performances of the spherical and cylindrical biosorbents. The results of the spherical and cylindrical biosorbents obtained from the immobilization, biosorption and desorption studies are summarized in Table 4.15. The same immobilization agents were used for the preparation of the spherical and cylindrical biosorbents. The surface area of the spherical biosorbent was smaller than that of the cylindrical biosorbent, which increased the surface area per mL of spherical biosorbent. Since the smaller size of the spherical biosorbent increased the drying rate of the biosorbent, the drying time of the spherical biosorbent was shorter than that of the cylindrical biosorbent. The biosorption performances of the spherical and cylindrical biosorbents were similar (Table 4.15). Spherical biosorbents gave a significantly higher biosorption capacity than that of cylindrical biosorbents (*t*-test, $p < 0.05$). Different desorption performances of the spherical and cylindrical biosorbents were observed. The optimum desorbing agent for copper(II) recovery from the spherical and cylindrical biosorbents was 0.1 M NTA. More copper(II) ions were recovered from the spherical biosorbent when compared with the cylindrical biosorbent. Incomplete copper(II) desorption from the cylindrical biosorbent reduced the copper(II) uptake in the

following cycles. As a result, a large decrease in copper(II) biosorption capacity was observed in the cylindrical biosorbent. The results from the desorption studies clearly indicate that the spherical biosorbent is a better biosorbent for copper(II) removal and recovery because of its higher desorption efficiency and better performance in biosorption/desorption cycle operations.

Table 4.15. Comparison of spherical and cylindrical biosorbents.

		Spherical biosorbent	**Cylindrical biosorbent**
Immobilization	Surface area per biosorbent (mm^2)	4.52 ± 0.80	69.98 ± 6.15
	Surface area per ml biosorbent (mm^2/ml)	2127.18 ± 22.35	1406.55 ± 27.48
	Drying time (days)	2	3
Biosorption	*q* (mg/g-biomass)	27.78 ± 0.28	23.30 ± 0.10
	Equilibrium biosorption time (min)	1400	1400
	Optimum agitation speed (rpm)	250	250
	Optimum pH	5.0	5.0
	Best-fit kinetic model	Pseudo-second order kinetic model ($r^2 \geq 0.99$)	Pseudo-second order kinetic model ($r^2 \geq 0.96$)
	Best-fit isotherm model	Langmuir model ($r^2 \geq 0.99$)	Langmuir model ($r^2 \geq 0.99$)
Desorption	Optimum desorbing agent	0.1 M NTA	0.1 M NTA
	% of copper(II) recovery after 6 h desorption	97.85 ± 0.08	77.27 ± 1.64
	% decrease in *q* after 3 cycles	22.92 ± 1.18	29.15 ± 0.90

4.7 Removal and recovery of copper(II) from industrial wastewater

To utilize the sol-gel encapsulated *Micrococcus* sp. for the removal of copper(II) from the copper(II)-laden wastewater, practical reactor system should be developed in order to treat the wastewater efficiently and effectively. In this study, a semi-continuous sol-gel/PVA-immobilized cell batch reactor system was used. Apart from synthetic wastewater, the treatment of industrial wastewater collected from a local electroplating company was also investigated in order to evaluate the applicability of the sol-gel encapsulated biomass for copper(II) removal and recovery. The metal removal performance of the biosorbent towards theses two types of wastewater may be different due to the presence of matrices in the industrial wastewater. In this section, the biosorption performance of a semi-continuous immobilized cell batch reactor system towards both synthetic and industrial wastewater will be compared.

4.7.1 Operating conditions in a semi-continuous batch reactor system

To implement a semi-continuous batch reactor system for copper(II) removal, it is necessary to formulate the operating conditions of the reactor system based on the results obtained in batch studies. Table 4.16 summarizes such operating

conditions in a semi-continuous batch reactor system. Since spherical biosorbent gave a better biosorption/desorption performance when compared with the cylindrical biosorbent (Section 4.5.1), it was selected for copper(II) removal in a semi-continuous batch reactor system. For preparing the spherical immobilized biosorbents, the composition ratio of TEOS:MTMS:HCl in the sol-gel stock solution was 2.10:1.00:1.40 and the ratio of sol-gel stock solution to PVA was 1:2 (Section 4.1.2). The biomass concentration in the sol-gel/PVA matrix was 40 g/L (Section 4.1.4). The biosorption time was 24 h, since equilibrium was generally reached as discussed in Section 4.2.1. An agitation speed of 250 rpm provided sufficient mixing for copper(II) removal in a batch system (Section 4.2.3). Study on the effect of pH indicates that the pH for copper(II) removal was 5.0 (Section 4.2.4). The desorbing agent used for copper(II) recovery was 0.1 M NTA (Section 4.5.2) with 6 h desorption time (Section 4.5.1).

A series of reactors were applied in a semi-continuous immobilized cell batch reactor system. The biosorption isotherm (Fig. 4.16) could be used to estimate the number of reactors required in the system. Four reactors were required to treat the wastewater containing 50 mg/L copper(II) ions. Therefore, a four-stage semi-continuous batch reactor system was applied in this study.

Table 4.16. Operating conditions in a batch reactor.

	Operating condition
Shape of biosorbent	Spherical
Volume of immobilized biosorbent (mL)	1.2
Biomass concentration in sol-gel/PVA matrix (g/L)	40
Biomass concentration in reactor (g/L)	1.5
Copper(II) concentration in wastewater (mg/L)	50
Biosorption time (h)	24
Agitation speed (rpm)	250
Solution pH	5.0
Volume of wastewater (mL)	200
Number of biosorption reactors	4
Desorbing agent	0.1 M NTA
Desorption time (h)	6
Volume of desorbing agent (mL)	50

4.7.2 Composition of industrial wastewater

Different components in the industrial wastewater may affect the copper(II) removal performance of the immobilized *Micrococcus* sp. Therefore, it is necessary to determine the detailed composition of the wastewater. Table 4.17(a) lists the concentrations of the cations and organic carbon in the industrial electroplating solution collected from a local company. The collected industrial sample is a stock solution for a plating bath, which is an electrolyte containing the dissolved copper(II) salt and other ions that permit the flow of electricity during the electroplating process. Table 4.17(a) indicates that a large amount of copper(II) ions (18446.04 mg/L) were present in the solution. After the electroplating process, the article (cathode) was removed from the plating bath and then rinsed in a series of water baths to dilute the excess electrolyte in the article. The rinsing water is thus a wastewater produced in a electroplating process typically containing about 1000 mg/L copper(II) ions. The wastewater was further diluted to the working concentration before biosorption. After dilution, the concentrations of other metal ions and organics present in the wastewater became very low (Table 4.17(b)), which could not significantly affect the copper(II) uptake from the wastewater. The concentrations of chromium(III), lead(II), nickel(II) zinc(II), and cadmium(II) were below the lowest detection

limits. The diluted wastewater was very acidic and thus NaOH was added to adjust the solution pH to 5.0, which increased the sodium concentration in the diluted wastewater.

Table 4.17(a). Composition of industrial electroplating solution.

Component	**Concentration (mg/L)**
Copper(II)	18446.04
Chromium(III)	16.00
Lead(II)	86.85
Nickel(II)	Below the lowest detection limit
Zinc(II)	1.18
Cadmium(II)	Below the lowest detection limit
Sodium	0.00
Total carbon	1307.29
Inorganic carbon	0.00
Total organic carbon	1307.29

Table 4.17(b). Composition of diluted and pH-adjusted industrial wastewater.

Component	**Concentration (mg/L)**
Copper(II)	50.20
Chromium(III)	0.04
Lead(II)	0.24
Nickel(II)	Below the lowest detection limit
Zinc(II)	Below the lowest detection limit
Cadmium(II)	Below the lowest detection limit
Sodium	447.84
Total carbon	3.55
Inorganic carbon	0.00
Total organic carbon	3.55

4.7.3 Application of semi-continuous batch reactor system for copper(II) removal

A series of four-stage semi-continuous batch reactor system was applied to evaluate the performance of the spherical biosorbent for copper(II) removal from synthetic wastewater and industrial wastewater. Table 4.16 summarizes the experimental conditions used in a semi-continuous batch reactor system. The reactor system was operated as described in Section 3.10 (Figs. 3.1(a) – 3.1(d)). The copper(II)-laden wastewater was fed counter-currently to the biosorbent in order to enhance the metal removal efficiency. In a counter-current scheme, the fresh or regenerated biosorbent is always fed to the reactor which is containing the lowest copper(II) concentration (R4) and it leaves the process after contacting with the most copper(II)-rich wastewater (R1). Therefore, the biosorbents left the process were saturated with the highest copper(II) concentration. A solid-liquid separation process was required to separate the copper(II)-laden biosorbents flowing in one direction from the wastewater which flows in the opposite direction.

The performance of a serial counter-current reactor system for treating the synthetic and industrial wastewater was studied. Figs 4.37 and 4.38 illustrate the

concentrations of copper(II) adsorbed by spherical biosorbent from both synthetic and industrial wastewater after passing through each reactor throughout eight cycles, respectively. The results indicate that the amount of copper(II) removed in reactor 1 decreased continuously, whereas the amount of copper(II) removed in reactor 4 kept increasing. This might be due to the counter-current scheme which was applied in the reactor system. In cycle 1, fresh biosorbent was placed in reactor 1, so the largest amount of copper(II) could be removed. During cycle 2, the biosorbent (B2) was fed counter-currently from reactor 2 (R2) to reactor 1 (R1) (Fig. 3.1(b)). Thus, the concentration gradient between the aqueous copper(II) solution and the biosorbent in cycle 2 would be less than that in cycle 1. A similar condition can be noticed for reactor 1 in cycle 3 (Fig. 3.1(c)). In cycle 4, the biosorbent (B4) in reactor 1 were gradually saturated with copper(II) ions after biosorption in the previous cycles (cycles 1 to 3) (Fig. 3.1(d)). Therefore, the amount of copper(II) removed in reactor 1 dropped gradually from cycles 1 to 4. Cycles 5 to 8 can be regarded as a repeated circulation of cycles 1 to 4.

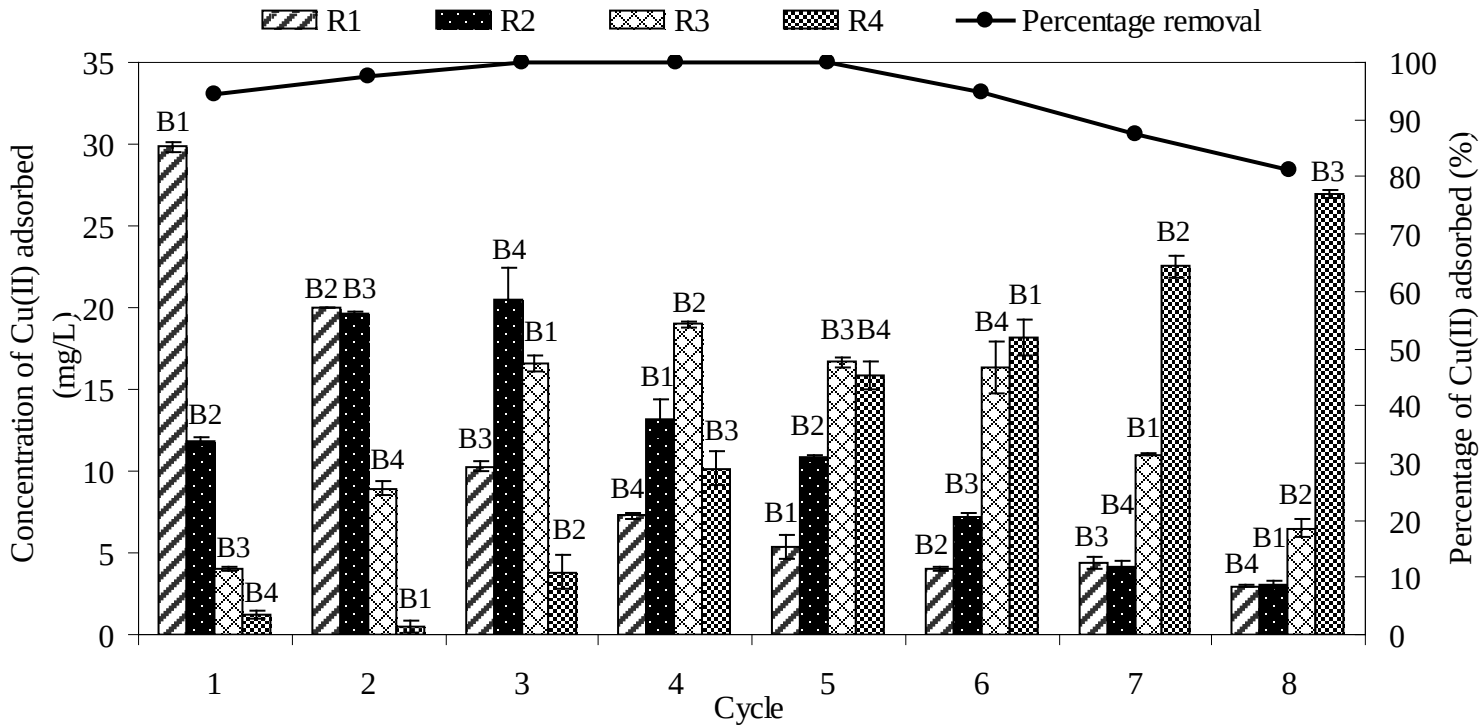

Figure. 4.37. Concentration of copper(II) adsorbed by spherical biosorbent from synthetic wastewater in a four-stage semi-continuous batch reactor system. [Experimental conditions: initial copper(II) concentration = 50 mg/L; biomass concentration = 1.5 g/L; contact time = 24 h; agitation speed = 250 rpm; pH = 5]

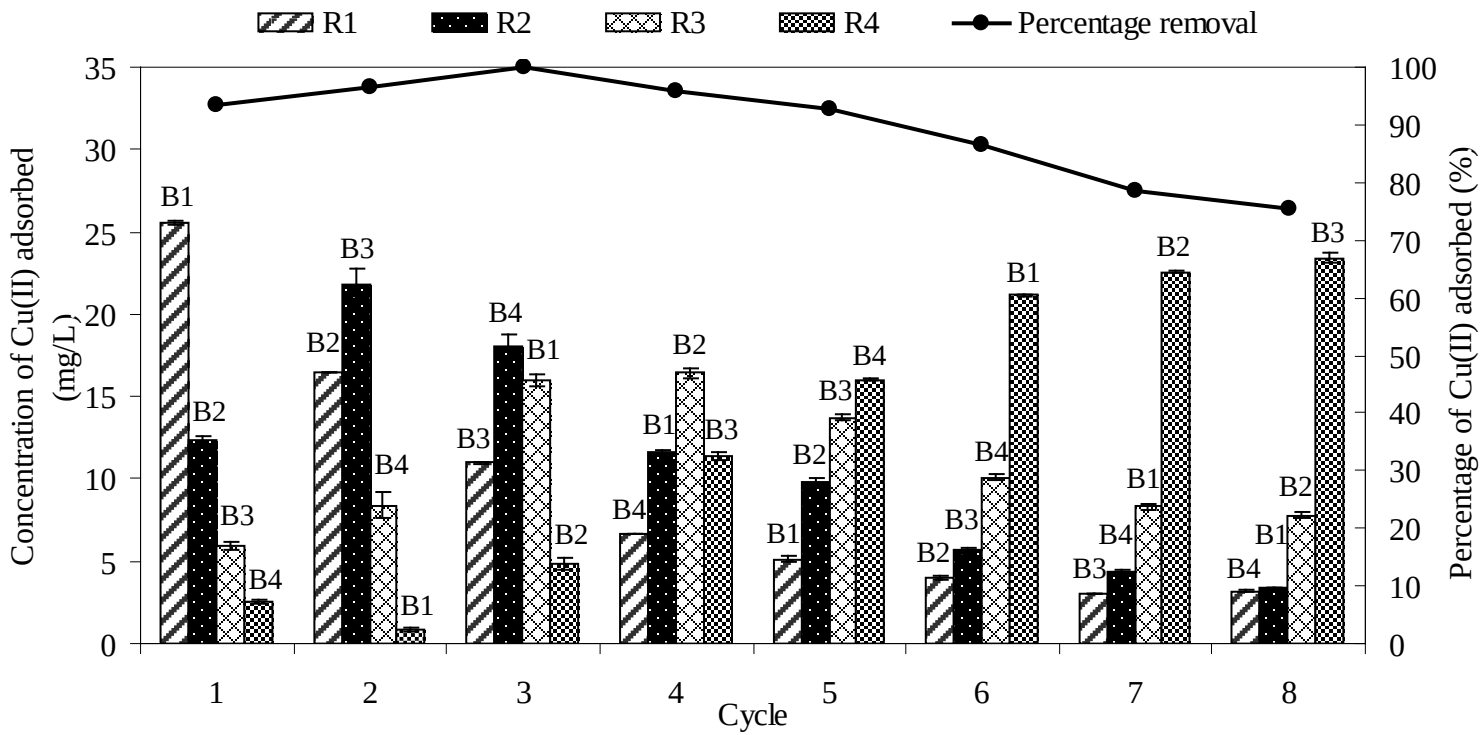

Figure. 4.38. Concentration of copper(II) adsorbed by spherical biosorbent from industrial wastewater in a four-stage semi-continuous batch reactor system. [Experimental conditions: initial copper(II) concentration = 50 mg/L; biomass concentration = 1.5 g/L; contact time = 24 h; agitation speed = 250 rpm; pH = 5]

Biosorbents in reactor 1 (R1) were contacted with the wastewater which contained the highest copper(II) concentration and they were then regenerated by 0.1 M NTA. The recovery percentage of copper(II) ions from the biosorbents over eight cycles is illustrated in Fig. 4.39. More than 85% of the adsorbed copper(II) ions could be recovered in all cycles. The un-desorbed copper(II) ions were accumulated in the biosorbent, which means that some binding sites were occupied by the copper(II) ions and unavailable for copper(II) biosorption until the copper(II) ions were desorbed. As discussed in Section 4.5.1, NTA has been shown to be an optimum desorbing agent for copper(II) recovery but it might also change the surface characteristics of the biomass and slightly decreased the biosorption capacity in the following cycles.

Tables 4.18 and 4.19 summarize the biosorption and desorption performances of the spherical biosorbent for treating the synthetic and industrial wastewater, respectively. The performance of the reactor system was slightly better in treating the synthetic wastewater than treating the industrial wastewater. This might be due to the presence of other components in the industrial wastewater, such as competitive cations, counter anions, organics or other unknown matrices, which could reduce the biosorption capacity of the biosorbent. In this study, the

industrial wastewater contained a large amount of sodium ions (447.84 mg/L), which could reduce the performance of the biosorbent for copper(II) removal.

The experimental data indicate that a four-stage semi-continuous immobilized cell batch reactor system can be used to remove copper(II) ions from both synthetic wastewater and industrial wastewater with a high percent removal and recovery in multiple biosorption/desorption cycle operations.

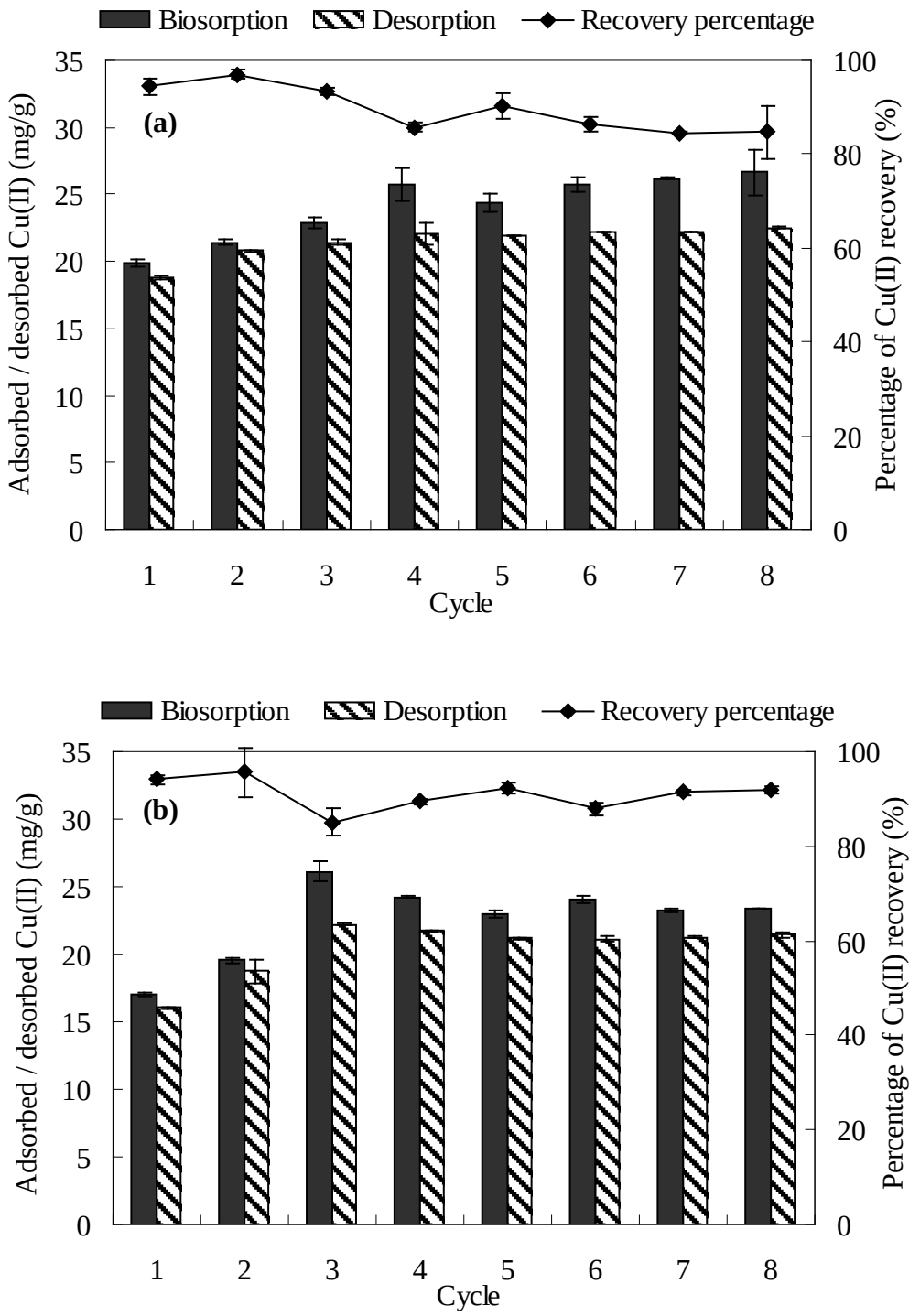

Figure 4.39. Desorption efficiency of copper(II) from biosorbent in (a) synthetic wastewater and (b) industrial wastewater using 0.1 M NTA.

[Experimental conditions: initial copper(II) concentration = 50 mg/L; contact time = 24 h for biosorption & 6 h for desorption; pH = 5 for biosorption; agitation speed = 250 rpm]

Table 4.18. Biosorption and desorption performances of the spherical biosorbent for treating the synthetic wastewater in a four-stage semi-continuous batch reactor system.

Cycle	Concentration of copper(II) adsorbed (mg/L)	Concentration of copper(II) in the effluent (mg/L)	Percentage of copper(II) adsorbed (%)	Percentage of copper(II) recovery (%)
1	46.89 ± 0.23	1.94 ± 0.23	94.42 ± 0.46	94.50 ± 1.78
2	49.10 ± 0.02	0.11 ± 0.02	97.58 ± 0.04	96.93 ± 0.96
3	51.23 ± 0.01	0.13 ± 0.01	100.00 ± 0.01	93.44 ± 0.79
4	49.65 ± 0.09	0.43 ± 0.09	100.00 ± 0.01	85.76 ± 0.88
5	48.72 ± 0.06	1.48 ± 0.06	99.84 ± 0.12	90.23 ± 2.59
6	45.64 ± 0.04	3.01 ± 0.04	94.95 ± 0.09	86.38 ± 1.65
7	42.01 ± 0.47	5.87 ± 0.47	87.56 ± 0.99	84.59 ± 0.32
8	39.44 ± 0.07	8.26 ± 0.07	81.30 ±0.15	84.63 ± 5.63

Table 4.19. Biosorption and desorption performances of the spherical biosorbent for treating the industrial wastewater in a four-stage semi-continuous batch reactor system.

Cycle	Concentration of copper(II) adsorbed (mg/L)	Concentration of copper(II) in the effluent (mg/L)	Percentage of copper(II) adsorbed (%)	Percentage of copper(II) recovery (%)
1	46.38 ± 0.03	3.85 ± 0.03	93.45 ± 0.06	94.08 ± 0.85
2	47.51 ± 0.01	0.17 ± 0.01	96.54 ± 0.01	95.61 ± 5.25
3	49.90 ± 0.01	0.38 ± 0.01	100.00 ± 0.01	85.08 ± 2.77
4	46.13 ± 0.00	1.52 ± 0.00	95.92 ± 0.00	89.48 ± 0.51
5	44.63 ± 0.03	3.60 ± 0.03	92.62 ± 0.06	92.37 ± 1.18
6	40.15 ± 0.35	6.75 ± 0.35	84.78 ± 0.75	87.90 ± 1.45
7	38.21 ± 0.21	9.49 ± 0.21	78.46 ± 0.44	91.35 ± 0.69
8	37.78 ± 0.23	11.95 ± 0.23	75.38 ± 0.45	91.92 ± 0.86

Chapter 5. Conclusions

Current technologies for heavy metal removal only provide a partially effective treatment. This study attempts to develop a novel and cost-effective process for copper(II) removal and recovery using *Micrococcus* sp. which was proved to be an effective biomass for copper(II) removal. However, the use of freely-suspended biomass for biosorption is impractical. Thus, this study develops a novel immobilization technique to improve the biosorption process. Sol-gel encapsulated biosorbents with spherical and cylindrical shapes were prepared and their biosorption performances were compared. The optimum conditions for the preparation of immobilized biosorbent were determined. Biosorption and desorption of copper(II) were performed in batch studies to evaluate and to compare the biosorption characteristics of the immobilized biosorbents. The reusability of the suspended biomass and the immobilized biosorbent was compared by performing the repeated biosorption/desorption cycles. A four-stage semi-continuous immobilized cell batch reactor system was then applied to determine the copper(II) removal and recovery efficiencies of both synthetic and industrial wastewater.

The results from this study show that the sol-gel/PVA matrix is a very promising material for cell immobilization. The immobilization process could

improve the biomass rigidity with high mechanical strength and facilitate the biomass separation from metal-laden wastewater. Copper(II) uptake by sol-gel/PVA matrix without cells was negligible. However, copper(II) uptake increased significantly once the cells were immobilized in the sol-gel/PVA matrix. Biomass encapsulated in two different metal alkoxide precursors was used for copper(II) removal. Biosorbents prepared by TEOS showed a higher potential in copper(II) removal than that prepared by TMOS. The biosorption of copper(II) ions was affected by the composition of the sol-gel stock solution. The optimum ratio of TEOS:MTMS:HCl in the sol-gel stock solution was chosen as 2.10:1.00:1.40. Copper(II) uptake increased slightly with an increase in the proportion of PVA in the sol-gel/PVA matrix. The optimum ratio of the sol-gel stock solution to PVA was chosen as 1:2. The biosorption capacity was affected by the concentration of biomass in the sol-gel/PVA matrix. The optimum biomass concentration in the sol-gel/PVA matrix was 40 g/L. The copper(II) uptake capacity was dependent on the drying time of the immobilized biosorbent. The optimum drying time of the spherical and the cylindrical biosorbents was two days and three days, respectively.

Copper(II) biosorption was highly dependent on solution pH. The

maximum copper(II) biosorption capacity was observed at pH 5.0. The biosorption of copper(II) ions was strongly affected by the equilibrium metal concentration. The Langmuir isotherm model could fit the experimental data better ($r^2 \geq 0.99$) than the Freundlich isotherm model ($r^2 \geq 0.88$). The q_{max} values of both the spherical and cylindrical biosorbents calculated from the Langmuir model were approximately 25 mg/g-biomass. Kinetic studies showed that the rate of copper(II) uptake by the spherical biosorbent was faster than that by the cylindrical biosorbent. The biosorption kinetics followed the pseudo-second order kinetic model with $r^2 \geq 0.96$ and the equilibrium biosorption capacities of the immobilized biosorbents in two different shapes were similar.

The effect of agitation speed on the kinetic profiles indicated that the copper(II) uptake rate was relatively slow in the biosorption system without agitation. The copper(II) uptake rate increased when the agitation speed was increased to 100 rpm, and little enhancement in the rate of copper(II) uptake was observed with a further increase in the agitation speed. These results implied that external diffusion was a rate limiting step when the agitation speed was 0 rpm, whereas intraparticle diffusion controlled the biosorption process when the agitation speed was over 100 rpm.

The surface morphology of the spherical and cylindrical biosorbents before and after copper(II) uptake was observed using SEM. The surface morphology of the spherical biosorbent as well as the cylindrical biosorbent changed after copper(II) uptake.

Desorption kinetics showed that the rate of copper(II) recovery from the spherical biosorbent was faster than that from the cylindrical biosorbent. It could be because the smaller size of the spherical biosorbent allowed a faster rate of copper(II) elution from the biosorbent. The spherical biosorbent was a more promising material for metal removal and recovery. The optimum experimental conditions for copper(II) recovery was to contact the copper(II)-laden biosorbent with 0.1 M NTA for 6 h. The biosorbent could be regenerated and reused in multiple biosorption/desorption cycles with only a minimal drop in copper(II) removal efficiency.

A four-stage semi-continuous sol-gel/PVA-immobilized cell batch reactor system was designed to remove copper(II) ions from both synthetic wastewater and industrial wastewater. Over 90% of the copper(II) ions were removed from the synthetic wastewater in the first six cycles and from the industrial wastewater

in the first five cycles. Over 85% of the adsorbed copper(II) could be recovered from the biosorbents in all cycles.

Micrococcus sp. is an effective biosorbent for copper(II) removal and the sol-gel/PVA matrix is a very promising material for cell immobilization. This study has demonstrated that the spherical biosorbent gives a better result on copper(II) biosorption and desorption. A high efficiency in both copper(II) removal and recovery strongly suggests that the spherical biosorbent can be further developed for industrial application.

Chapter 6. Further Studies

Further studies need to be extended to verify the applicability of other types of reactors for copper(II) removal and recovery. The packed bed column is one of the most convenient reactors in a continuous-flow system. The size and mechanical strength of the spherical biosorbent prepared in this study are suitable for column application. Therefore, column application can be further developed for the treatment of industrial wastewater.

Sol-gel/PVA matrix is a potential material for cell immobilization. More studies are recommended to investigate the applicability of the sol-gel/PVA immobilized biosorbent in the wastewater treatment process for immobilizing other types of biosorbents in the sol-gel/PVA matrix for the removal of other heavy metals.

In this study, only a preliminary study on the surface morphology of the immobilized biosorbent was conducted. The surface of the immobilized biosorbent can be examined by methods such as solid-state nuclear magnetic resonance spectroscopy (solid-NMR) and transmission electron microscopy (TEM).

Appendix 1

Intraparticle diffusion

The intraparticle diffusion coefficients of copper(II) ions in the spherical and cylindrical biosorbents were determined. Do (1998) develop a mathematical relationship to calculate the intraparticle diffusion coefficient. The mass balance equation of adsorbates between fluid phase and adsorbent particles are as follows:

$$\varepsilon\frac{\partial C}{\partial t}+(1-\varepsilon)\frac{\partial C_r}{\partial t}=\varepsilon D_p\frac{1}{r^s}\frac{\partial}{\partial r}\left(r^s\frac{\partial C}{\partial r}\right)+(1-\varepsilon)D_s\frac{1}{r^s}\frac{\partial}{\partial r}\left(r^s\frac{\partial C_r}{\partial r}\right) \qquad (10)$$

where ε is the porosity of the adsorbent particle; D_p and D_s are the diffusion coefficient in the pore space and the surface adsorbed phase, respectively (m^2/s); C is the concentration of the adsorbates in fluid ($mg_{adsorbates}/L_{fluid}$); C_r is the concentration of the adsorbates in the adsorbent particle ($mg_{adsorbates}/L_{adsorbents}$); s is the particle shape factor; and, r is the radius of the spherical and cylindrical particles (m).

The boundary and initial conditions for the sorption process are defined as follows:

$$C_r\big|_{r=R}=C \qquad (r=R,\ t>0) \qquad (11)$$

$$\left.\frac{\partial C_r}{\partial r}\right|_{r=0}=0 \qquad (r=0,\ t>0) \qquad (12)$$

$$C=C_i \qquad (t=0) \qquad (13)$$

$$C_r = 0 \qquad (t = 0,\ 0 \le r < R) \qquad (14)$$

where R is the half length of diffusion path (m); and, C_i is the initial metal concentration in fluid ($mg_{adsorbates}/L_{fluid}$).

With assumption of linear adsorption isotherm, Eq. (10) can be modified and solved by Laplace transform and is written as:

$$\frac{C(x,\tau)-C_i}{C-C_i} = 1 - \sum_{m=1}^{\infty} a_m K_m(x) \cdot \exp\left(-\zeta_m^2 \tau\right) \qquad (15)$$

where $x = \frac{r}{R}$; $\tau = \frac{D_{app}\, t}{R^2}$

For spherical biosorbent: $a_m = \frac{2(\sin\zeta_m - \zeta_m \cos\zeta_m)}{\zeta_m^2\left(1+\frac{\cos^2\zeta_m}{B_i-1}\right)}$; $K_m(x) = \frac{\sin(\zeta_m x)}{x}$;

$\zeta_m \cos\zeta_m = (1-B_i)\cdot\sin\zeta_m$

For cylindrical biosorbent: $a_m = \frac{2}{\zeta_m J_1(\zeta_m)\left[1+\left(\frac{\zeta_m}{B_i}\right)^2\right]}$; $K_m(x) = J_o(\zeta_m x)$;

$\zeta_m J_1(\zeta_m) = B_i \cdot J_o(\zeta_m)$

$$B_i = \frac{k_f\, R}{\left[\varepsilon\, D_p + (1-\varepsilon) K\, D_s\right]} \qquad (16)$$

where m is the number of experimental points; ζ_m is the eigenvalue; B_i is Biot number; and, k_f is the mass transfer coefficient of the boundary film (m/s).

Eq. (15) can further be substituted into Eq. (17), resulting in Eq. (18).

$$F = \frac{q_t}{q_e} = \frac{C_o - C_t}{C_o - C_\infty} \qquad (17)$$

$$F = 1 - \sum_{m=0}^{\infty} b_m \cdot \exp\left(-\zeta_m^2 \tau\right) \qquad (18)$$

where F is the fractional uptake of the adsorbate molecules at the time t.

For spherical biosorbent: $b_m = \dfrac{6\left(\sin\zeta_m - \zeta_m \cos\zeta_m\right)^2}{\zeta_m^4\left(1 + \dfrac{\cos^2\zeta_m}{B_i - 1}\right)}$

For cylindrical biosorbent: $b_m = \dfrac{4}{\zeta_m^2\left[1 + \left(\dfrac{\zeta_m}{B_i}\right)^2\right]}$

When the film resistance become negligible compared to the internal diffusion resistance ($B_i \to \infty$), Eq. (18) can be simplified to Eqs. (19) and (20). For biosorption onto spherical biosorbent with a constant intraparticle diffusion coefficient, the solution for the fractional uptake (F) is given below:

$$F = 1 - \frac{6}{\pi^2}\sum_{m=0}^{\infty}\left(\frac{1}{m}\right)^2 \exp\left\{\frac{-D_i m^2 \pi^2 t}{r^2}\right\} \qquad (19)$$

For cylindrical biosorbent, the fractional uptake (F) is represented as:

$$F = 1 - 4\sum_{m=0}^{\infty}\left(\frac{1}{\xi_m^2}\right)\exp\left\{\frac{-D_i \xi_m^2 t}{r^2}\right\} \qquad (20)$$

where D_i is the intraparticle diffusion coefficient (m^2/min).

Aharoni and Suzin (1982) stated that in the early stage (0–50 min in this system) of the adsorption process (t is relatively small), Eq. (19) can be reduced to

Eq. (21) for spherical biosorbent and Eq. (20) can be reduced to Eq. (22) for cylindrical biosorbent. Then, the intraparticle diffusion coefficient can be determined simply from the slope of the plot of F versus $t^{1/2}$.

$$F = \frac{6}{\pi^{1/2}} \frac{D_i^{1/2}}{r} t^{1/2} \qquad (21)$$

$$F = \frac{4}{\pi^{1/2}} \frac{D_i^{1/2}}{r} t^{1/2} \qquad (22)$$

At large time (after 120 min), Eq. (19) can be reduced to Eq. (23) for spherical biosorbent and Eq. (20) can be reduced to Eq. (24) for cylindrical biosorbent. Then, the intraparticle diffusion coefficient can be determined simply from the slope of the plot of ln (1-F) versus t.

$$\ln(1-F) = \ln\left(\frac{6}{\pi^2}\right) - \frac{\pi^2 D_i}{r^2} t \qquad (23)$$

$$\ln(1-F) = \ln 0.692 - \frac{5.783 D_i}{r^2} t \qquad (24)$$

The solutions of Eqs. (19) and (20) are based on the assumption of a linear adsorption isotherm. In this study, Fig. 4.16 shows that the biosorption isotherms of the spherical and cylindrical biosorbents can be regarded as linear if the amount of copper(II) uptake is in the range of 0 mg-Cu/g-biomass to 8 mg-Cu/g-biomass. To satisfy the assumption of a linear adsorption isotherm, kinetic data were taken only within the initial time period of 50 min and applied

for plotting F versus $t^{1/2}$ to determine the intraparticle diffusion coefficient. During the first 50 min, the amount of copper(II) uptake was less than 8 mg/g-biomass.

Fig. 1 shows the F versus $t^{1/2}$ plots of copper(II) biosorption by spherical and cylindrical biosorbents. Fig. 2 shows the ln (1-F) versus t plots of copper(II) biosorption, at large time, by spherical and cylindrical biosorbents. The copper(II) diffusion coefficients were calculated using the Eqs. (21) – (24). Table 1 shows the calculated diffusion coefficients of spherical and cylindrical biosorbents. The copper(II) diffusion coefficients calculated from two approaches were similar. The diffusion coefficient of copper(II) in spherical biosorbent was slower than that in cylindrical biosorbent. According to the literature, the diffusion coefficients of metal ions in solution in the dense silica glasses are usually larger than 10^{-14} m^2/s (Cusslle, 1984; Lenza and Vasconcelos, 2000).

Table 1. Diffusion coefficients of copper(II) ions in spherical and cylindrical biosorbents.

Biosorbent	**Intraparticle diffusion model, $t \rightarrow t_0$**		**Intraparticle diffusion model, $t \rightarrow t_\infty$**	
	D_i (m^2/s)	r^2	D_i (m^2/s)	r^2
Spherical	$6.10 \times 10^{-13} \pm 0.15 \times 10^{-13}$	0.95 ± 0.02	$8.02 \times 10^{-13} \pm 0.00$	0.97 ± 0.00
Cylindrical	$1.31 \times 10^{-11} \pm 0.27 \times 10^{-11}$	0.96 ± 0.04	$3.05 \times 10^{-11} \pm 0.15 \times 10^{-11}$	0.99 ± 0.00

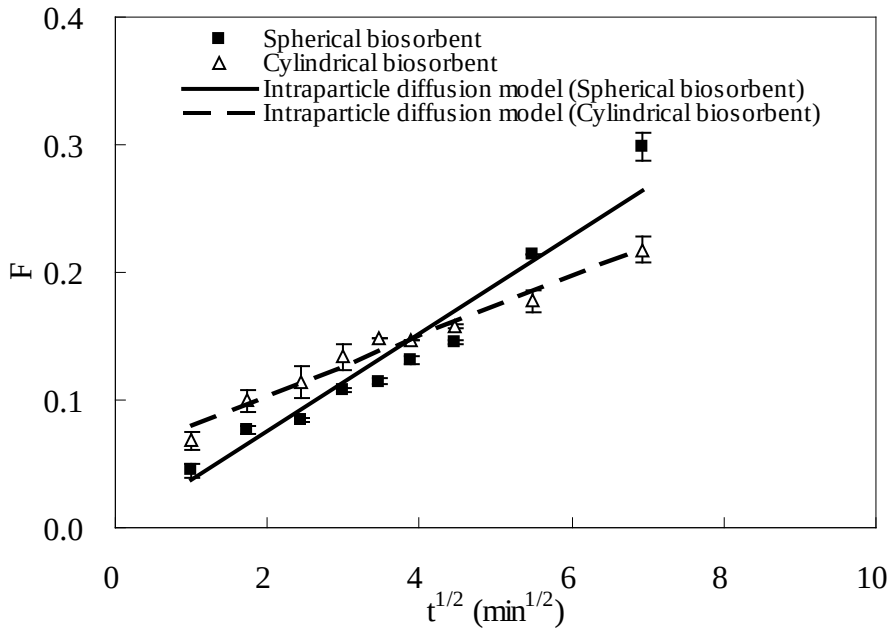

Figure 1. The F vs $t^{1/2}$ plot of copper(II) biosorption by spherical and cylindrical biosorbents ($t \rightarrow t_0$) (Agitation speed = 250 rpm).

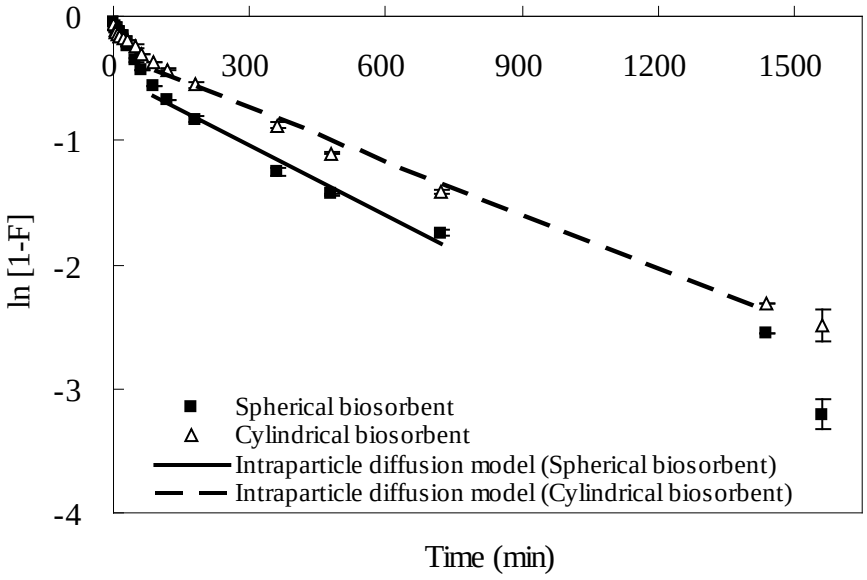

Figure 2. The ln (1-F) vs t plot of copper(II) biosorption by spherical and cylindrical biosorbents ($t \rightarrow t_\infty$) (Agitation speed = 250 rpm).

Appendix 2

External mass transfer

The external mass transfer coefficient (k_s) was calculated using there different methods. The first two methods are a correlation method and the third method is a dimensional analysis method. The results obtained from these three methods were described and compared below.

Furusawa and Smith (1973) developed a method to determine the external mass transfer coefficient using a single resistance model. This model assumes that the film diffusion is the only resistance to the mass transport and the intraparticle diffusion is negligible.

The Langmuir isotherm model effectively represented the experimental data throughout the concentration range. The Langmuir isotherm parameters (q_{max} *and b*) are therefore used to calculate the external mass transfer coefficient. The Langmuir isotherm model is represented as:

$$q = \frac{q_{\max} b C_e}{1 + b C_e} \qquad (25)$$

The change of the metal ions concentration in solution with respect to time is

related to the fluid-particle mass transfer coefficient (k_s) by the equation:

$$\frac{dC_t}{dt} = -k_s A_s (C_t - C_s) \qquad (26)$$

where A_s is the specific surface area of sorbent for mass transfer (m^2/m^3); k_s is the external mass transfer coefficient (m/s); C_s and C_t are the liquid phase metal concentrations at sorbent surface and at time t (mg/L), respectively.

Assuming smooth spherical particles, the specific surface area A_s for mass transfer is described as:

$$A_s = \frac{6m_b}{d\rho_p(1-\varepsilon_p)} \qquad (27)$$

where m_b is the concentration of biomass (g/m^3); d is the diameter of the sorbent (m); ρ_p is the density of the sorbent (g/m^3); and, ε_p is the particle porosity.

Adsorption at an interior site is assumed to be at equilibrium, q and C_r are thus related by the instantaneous equilibrium expression:

$$\frac{dq}{dt} = \frac{d}{dC_r}(q_{\max} bC_r)\frac{dC_r}{dt} \qquad (28)$$

where C_r is the liquid phase metal concentration at radius r (mg/L); at $t = 0$, $C_r = 0$ for $0 < r < R$.

Furusawa and Smith (1973) developed a method to calculate the external mass transfer coefficient by incorporating the Langmuir isotherm into Eq. (28).

By combining Eqs. (25), (26) and (28) gives

$$\ln\left(\frac{C_t}{C_0}-\frac{1}{1+m_b q_{\max} b}\right)=\ln\left(\frac{m_b q_{\max} b}{1+m_b q_{\max} b}\right)-\left(\frac{1+m_b q_{\max} b}{m_b q_{\max} b}k_s A_s\right)t \qquad (29)$$

In the early stage of the adsorption process (t is relatively small), external mass transfer will predominate and the assumptions of negligible intraparticle diffusion is valid. A plot of $\ln\left(\frac{C_t}{C_0}-\frac{1}{1+m_b q_{\max} b}\right)$ vs t will yield a straight line as t is relatively small. The external mass transfer coefficient can be calculated from the slope of the plot. Application of this method to determine the external mass transfer coefficient in a sorption system has been reported in the literature (Choy *et al.*, 2004; Leusch and Volesky, 1995). Kim *et al*. (2004) reported that the external mass transfer coefficient of copper(II) ions onto chitosan beads made by sol-gel method was 10^{-5} m/s. Choy *et al*. (2004) found that the external mass transfer coefficient of copper(II) ions onto bone char was 10^{-6} m/s. Leusch and Volesky (1995) studied the effect of agitation speed on external mass transfer coefficient of cadmium(II) ions by *Sargassum fluitans*. The results indicated that the external mass transfer coefficient of cadmium(II) ions was 10^{-5} m/s at different agitation speeds and the k_s value increased with the agitation speed.

The external mass transport of the copper(II) ions on spherical biosorbent under different agitation speeds was investigated. As discussed in Section 4.2.3, the external mass transfer of copper(II) ions is significantly affected by agitation speed. The external mass transfer resistance is proportional to the film thickness surrounding the particle. Increase in the agitation speed will decrease the film thickness and hence increase the external diffusion rate. Fig. 4.9 in Section 4.2.3 shows that the external diffusion rate increased significantly when the agitation speed was increased to 100 rpm and little enhancement was observed with a further increase in the agitation speed. A plot of $\ln\left(\frac{C_t}{C_0} - \frac{1}{1+m_b q_{\max} b}\right)$ vs t for external mass transfer of copper(II) ions on spherical biosorbent under different agitation speeds is shown in Fig. 3. The external mass transfer coefficient under different agitation speeds is summarized in Table 2. The lowest external mass transfer coefficient was observed at 0 rpm. The external mass transfer coefficient increased with an increase in the agitation speed. The highest external mass transfer coefficient (2.24×10^{-6} m/s) was reached at 300 rpm. The external mass transfer coefficient determined from this study was of the same order of magnitude as that reported in the literature (Choy *et al.*, 2004; Kim *et al.*, 2004; Leusch and Volesky, 1995).

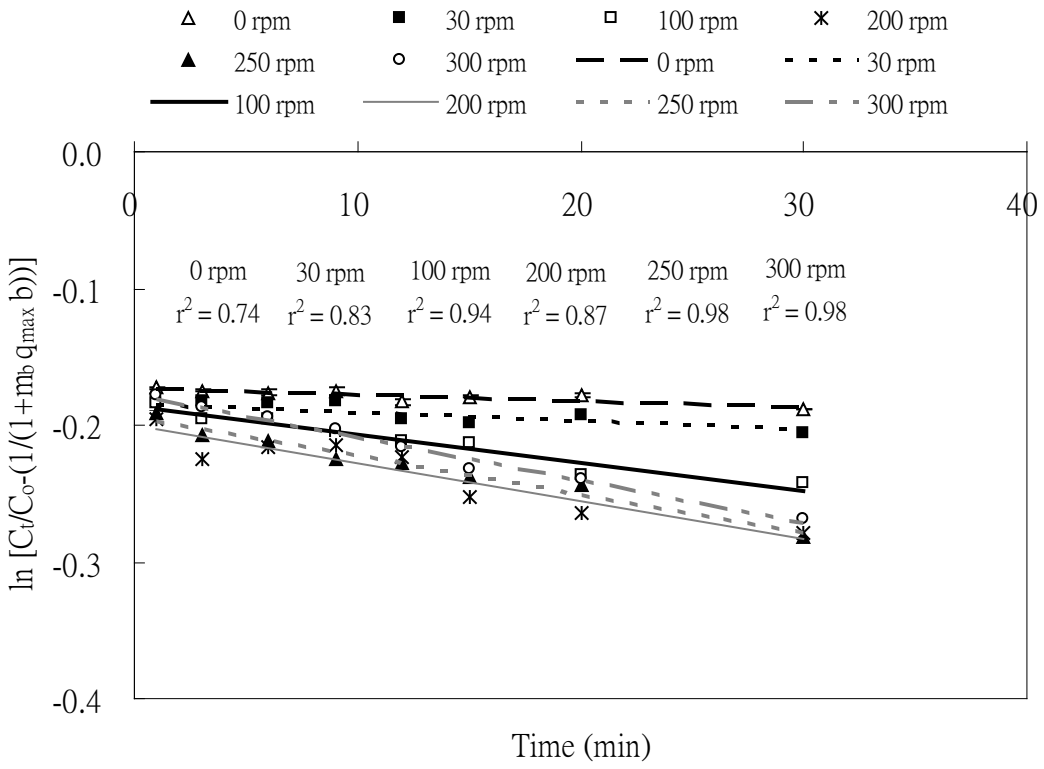

Figure 3. Plots for determination of external mass transfer coefficients of copper(II) ions on spherical biosorbent under different agitation speeds.

Table 2. Effect of agitation speed on external mass transfer coefficient (Furusawa and Smith).

	m_b (g/m^3)	$q_{max}b$ (L/g)	A_s (m^2/m^3)	k_s (m/s)	r^2
0 rpm	1500	3.622	19.48	$3.25 \times 10^{-7} \pm 0.51 \times 10^{-7}$	0.70 ± 0.06
30 rpm	1500	3.622	19.48	$4.70 \times 10^{-7} \pm 2.55 \times 10^{-7}$	0.83 ± 0.04
100 rpm	1500	3.622	19.48	$1.48 \times 10^{-6} \pm 0.05 \times 10^{-6}$	0.94 ± 0.04
200 rpm	1500	3.622	19.48	$1.99 \times 10^{-6} \pm 0.05 \times 10^{-6}$	0.87 ± 0.00
250 rpm	1500	3.622	19.48	$2.06 \times 10^{-6} \pm 0.05 \times 10^{-6}$	0.98 ± 0.00
300 rpm	1500	3.622	19.48	$2.24 \times 10^{-6} \pm 0.00$	0.98 ± 0.00

Apiratikul and Pavasant (2008) described another method to calculate the external mass transfer coefficient using the kinetic parameters obtained from the kinetic model. Kinetic study in Section 4.2.2 indicated that the pseudo-second order kinetic model could better simulate the experimental data of the spherical biosorbent. Hence, the pseudo-second order kinetic parameters were used to calculate the external mass transfer coefficient as described below:

$$\frac{dq}{dt} = -k_s A_s (C_t - C_s) \qquad (30)$$

$$k_s = \frac{\lim_{t \to 0} \frac{dq}{dt}}{A_s C_0} = \left(\frac{q_e{}^2 k_2}{A_s C_0} \right) / 60 \qquad (31)$$

$$A_s = \frac{6}{d \rho_p (1 - \varepsilon_p)} \qquad (32)$$

Table 3 summarizes the external mass transfer coefficient under different agitation speeds. Similar to the results obtained using a single resistance model (Table 2), the lowest external mass transfer coefficient was observed at 0 rpm. The external mass transfer coefficient increased with an increase in the agitation speed. The external mass transfer coefficient determined using this method was of the same order of magnitude as that using a single resistance model.

Table 3. Effect of agitation speed on external mass transfer coefficient (Apiratikul and Pavasant).

	A_s (m^2/g)	k_s (m/s)
0 rpm	0.0129	$6.09 \times 10^{-7} \pm 0.03 \times 10^{-7}$
30 rpm	0.0129	$9.00 \times 10^{-7} \pm 0.25 \times 10^{-7}$
100 rpm	0.0129	$2.42 \times 10^{-6} \pm 0.12 \times 10^{-6}$
200 rpm	0.0129	$3.56 \times 10^{-6} \pm 0.06 \times 10^{-6}$
250 rpm	0.0129	$3.59 \times 10^{-6} \pm 0.03 \times 10^{-6}$
300 rpm	0.0129	$2.87 \times 10^{-6} \pm 0.06 \times 10^{-6}$

The third method is a dimensional analysis method. In a batch agitated system, the external mass transfer increased with an increase in the agitation speed. The external mass transfer coefficient between the liquid phase and the biosorbent particles can be calculated by the relationship (Choy *et al.*, 2004; Tien, 1994):

$$\frac{k_s}{k_s^*} \cong 2 \qquad (33)$$

where k_s is the external mass transfer coefficient between the liquid phase and the biosorbent particles (cm/s); and, k^*_s is the mass transfer coefficient of the biosorbent particles moving at their terminal velocity (cm/s) in the same liquid phase.

k^*_s can be calculated using the following equation:

$$\frac{k_s^* d}{D_i} = 2.0 + 0.6\left[\frac{d_p u_T}{\mu}\right]^{0.5}\left[\frac{\upsilon}{D_i}\right]^{0.33} \qquad (34)$$

where d is the diameter of the spherical biosorbent (cm); D_i is the intraparticle

diffusion coefficient (cm^2/s); u_T is the terminal velocity; μ is the dynamic viscosity ($g/cm \cdot s$); and, υ is the kinematic viscosity (cm^2/s).

The correlation used to calculate the terminal velocity is expressed as:

$$u_T = \frac{0.153 g^{0.71} d_p^{1.14} \Delta\rho^{0.77}}{\rho^{0.29} \mu^{0.43}} \qquad (35)$$

where g is the gravitational acceleration (cm/s^2); ρ is the liquid density (g/cm^3); ρ_p is the particle density (g/cm^3); and, $\Delta\rho = \rho_p + \varepsilon\rho$ is the density difference between the wet particle and liquid (g/cm^3).

The external mass transfer coefficient (k_s) of the spherical biosorbent calculated using this method was 1.058×10^{-6} m/s. The k_s value was of the same order of magnitude as those obtained from using the single resistance model developed by Furusawa and Smith (1973) and the external mass transfer model described by Apiratikul and Pavasant (2008).

Appendix 3

Figures and Tables

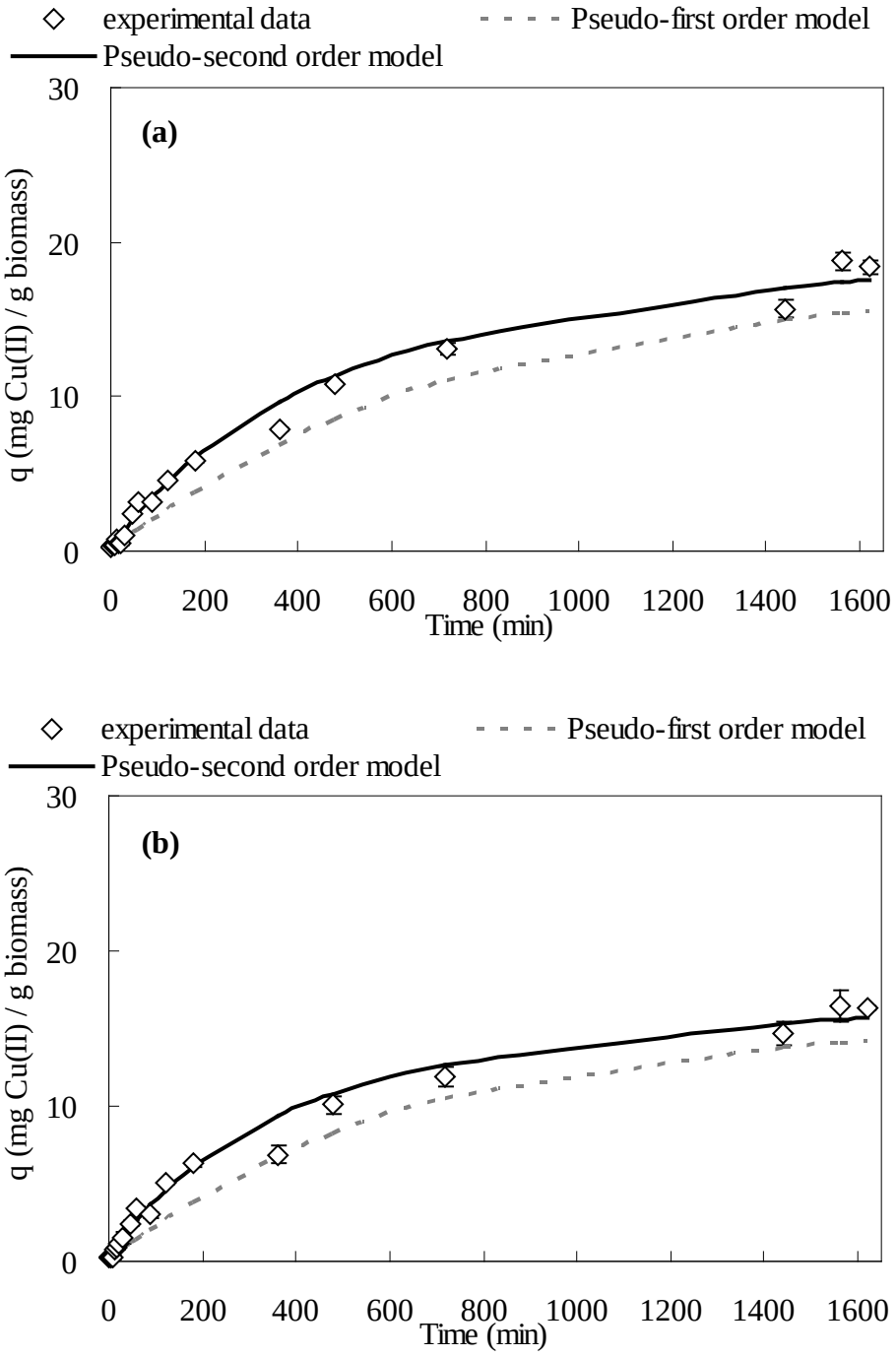

Figure 4. Simulation of copper(II) biosorption kinetics of (a) spherical biosorbent and (b) cylindrical biosorbent by linearized pseudo-first order and pseudo-second order kinetic models (Agitation speed = 0 rpm).

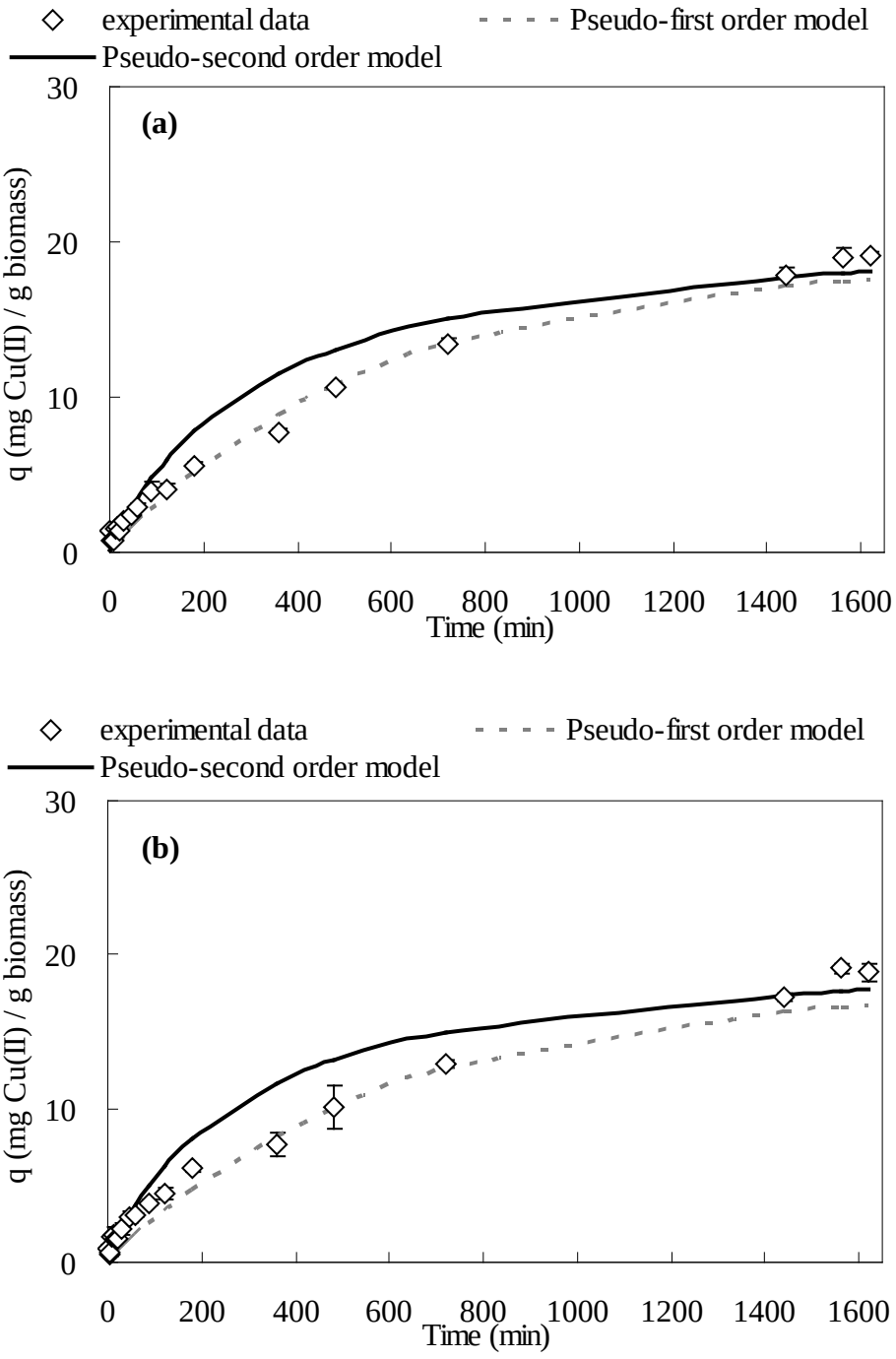

Figure 5. Simulation of copper(II) biosorption kinetics of (a) spherical biosorbent and (b) cylindrical biosorbent by linearized pseudo-first order and pseudo-second order kinetic models (Agitation speed = 30 rpm).

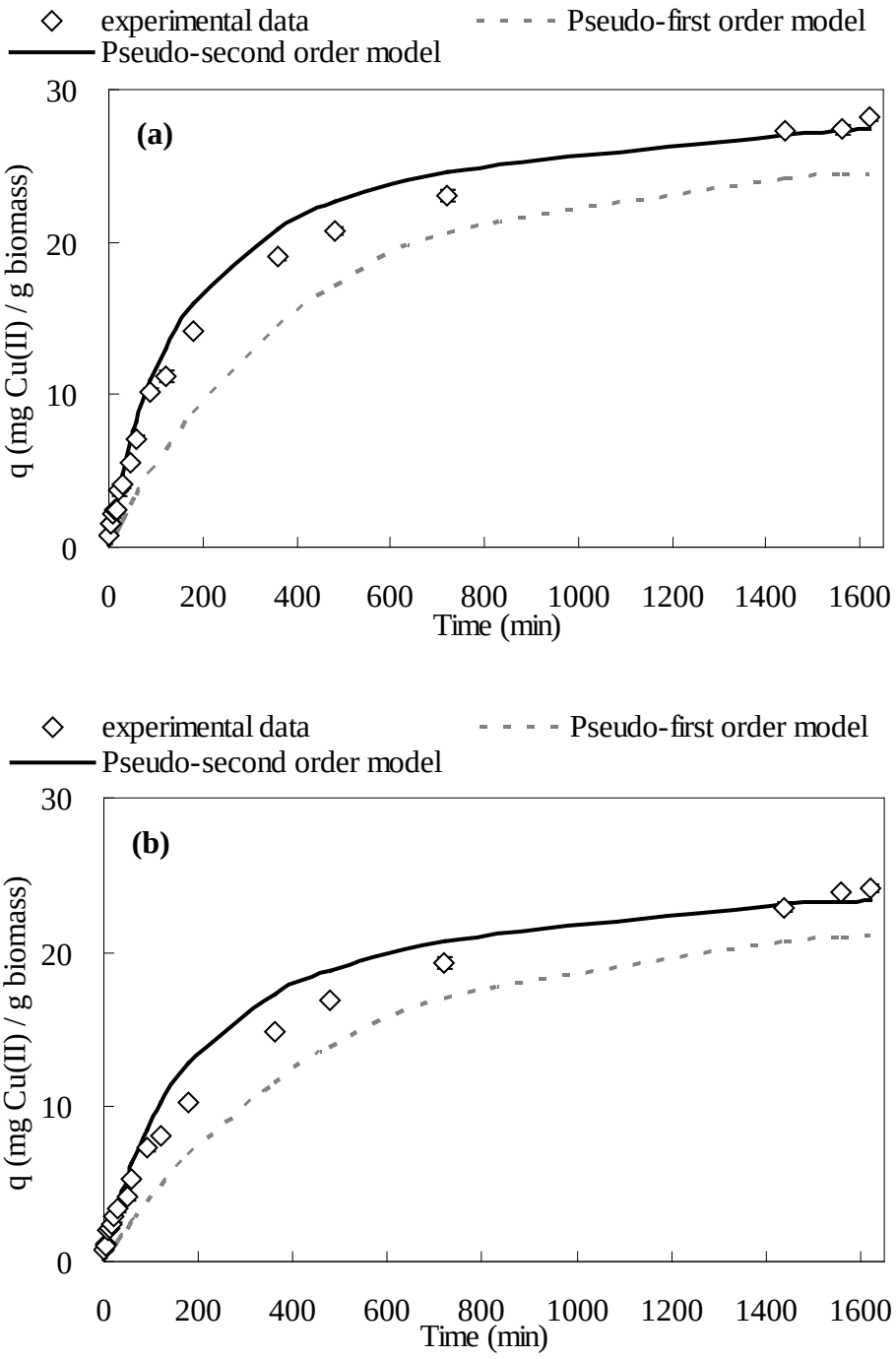

Figure 6. Simulation of copper(II) biosorption kinetics of (a) spherical biosorbent and (b) cylindrical biosorbent by linearized pseudo-first order and pseudo-second order kinetic models (Agitation speed = 100 rpm).

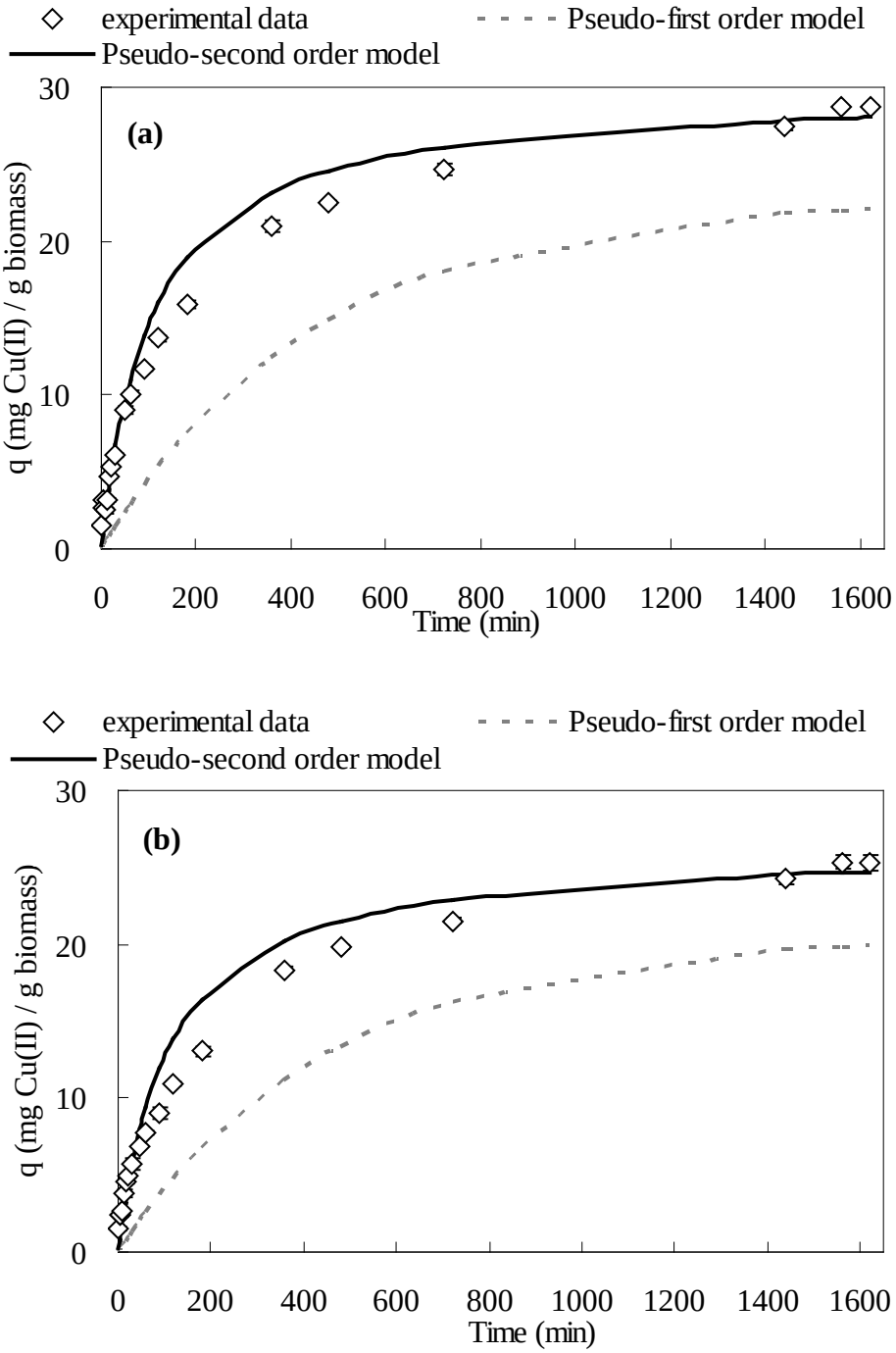

Figure 7. Simulation of copper(II) biosorption kinetics of (a) spherical biosorbent and (b) cylindrical biosorbent by linearized pseudo-first order and pseudo-second order kinetic models (Agitation speed = 200 rpm).

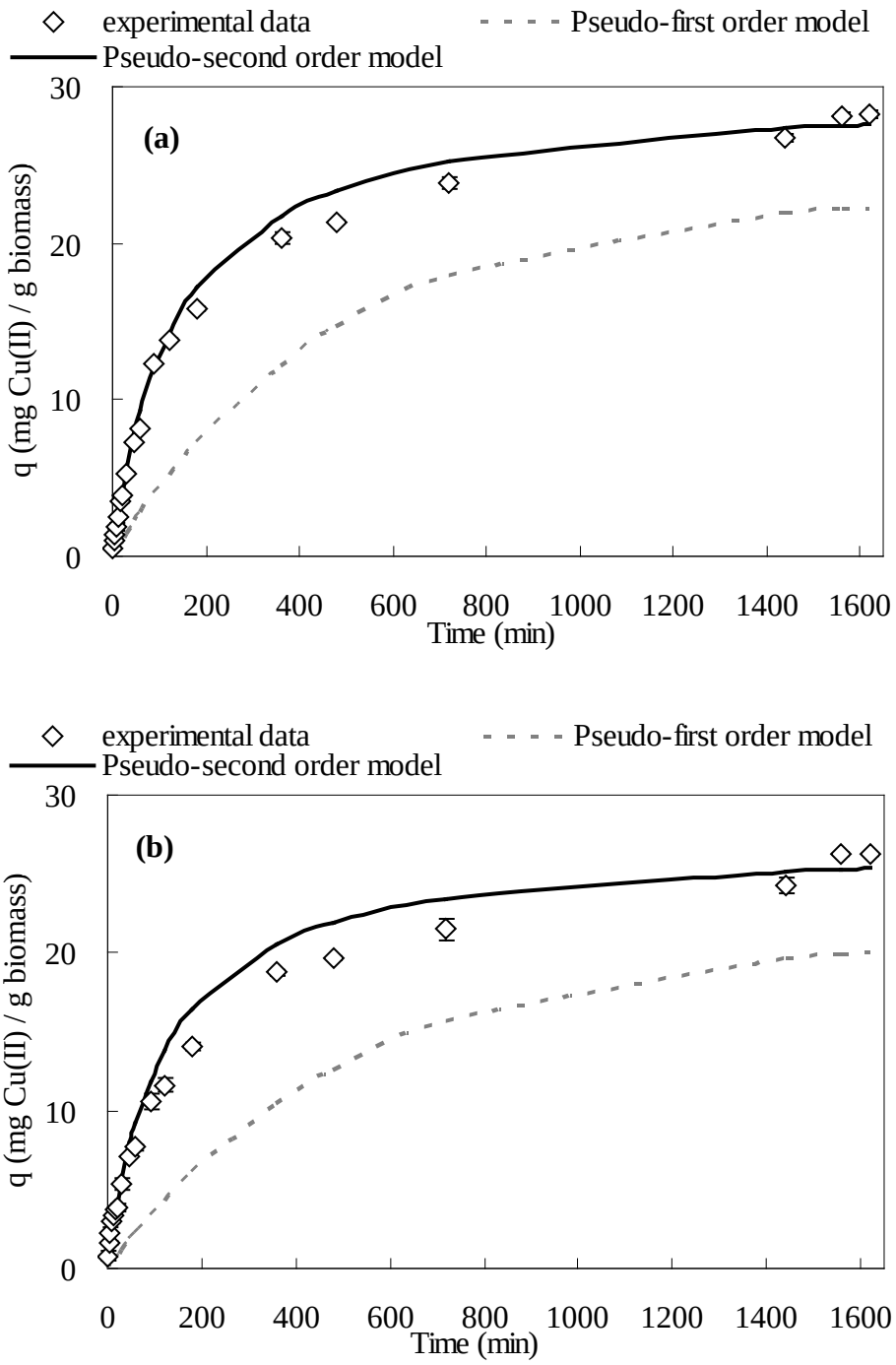

Figure 8. Simulation of copper(II) biosorption kinetics of (a) spherical biosorbent and (b) cylindrical biosorbent by linearized pseudo-first order and pseudo-second order kinetic models (Agitation speed = 300 rpm).

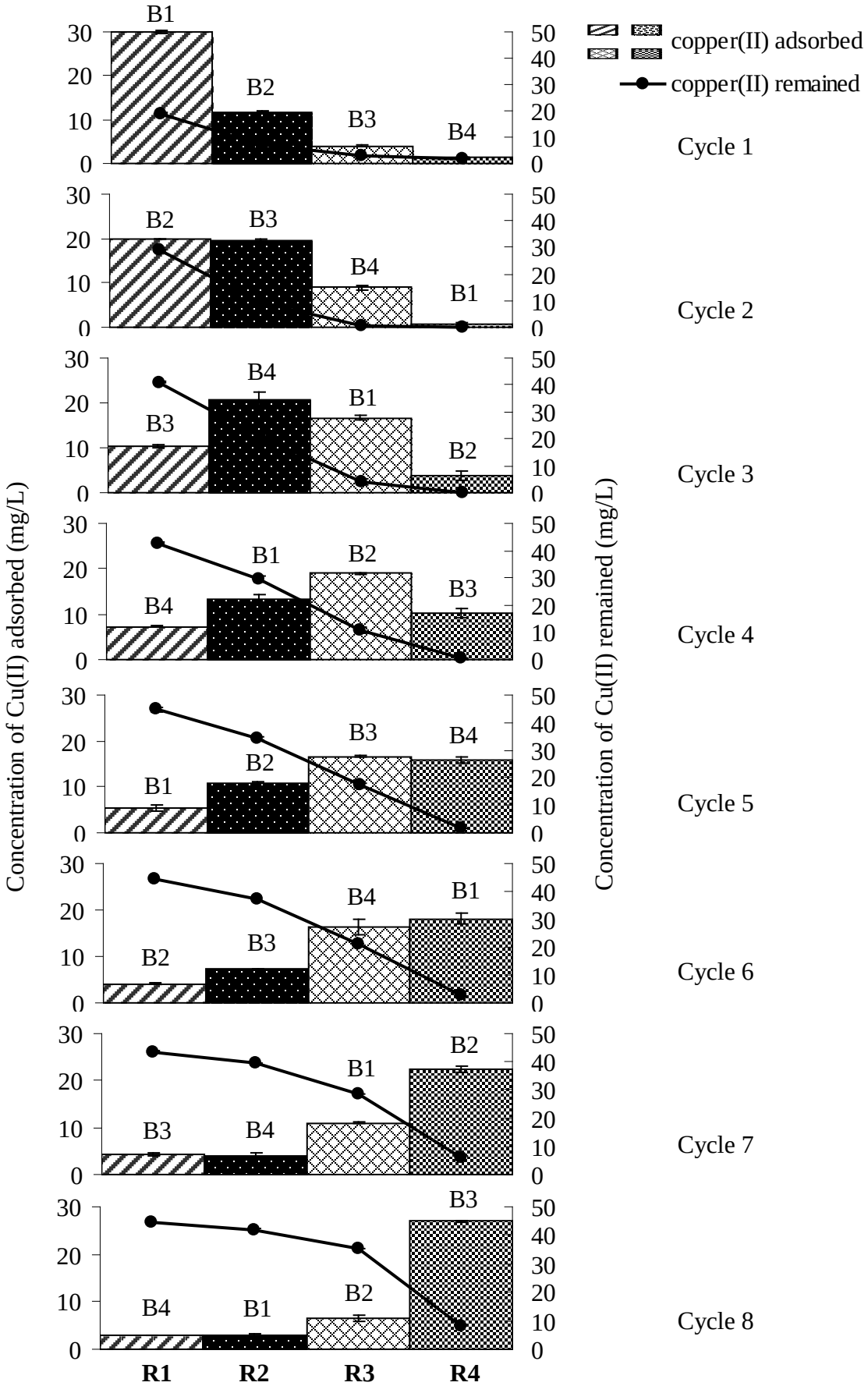

Figure 9. Concentration of copper(II) adsorbed and remained in synthetic wastewater.

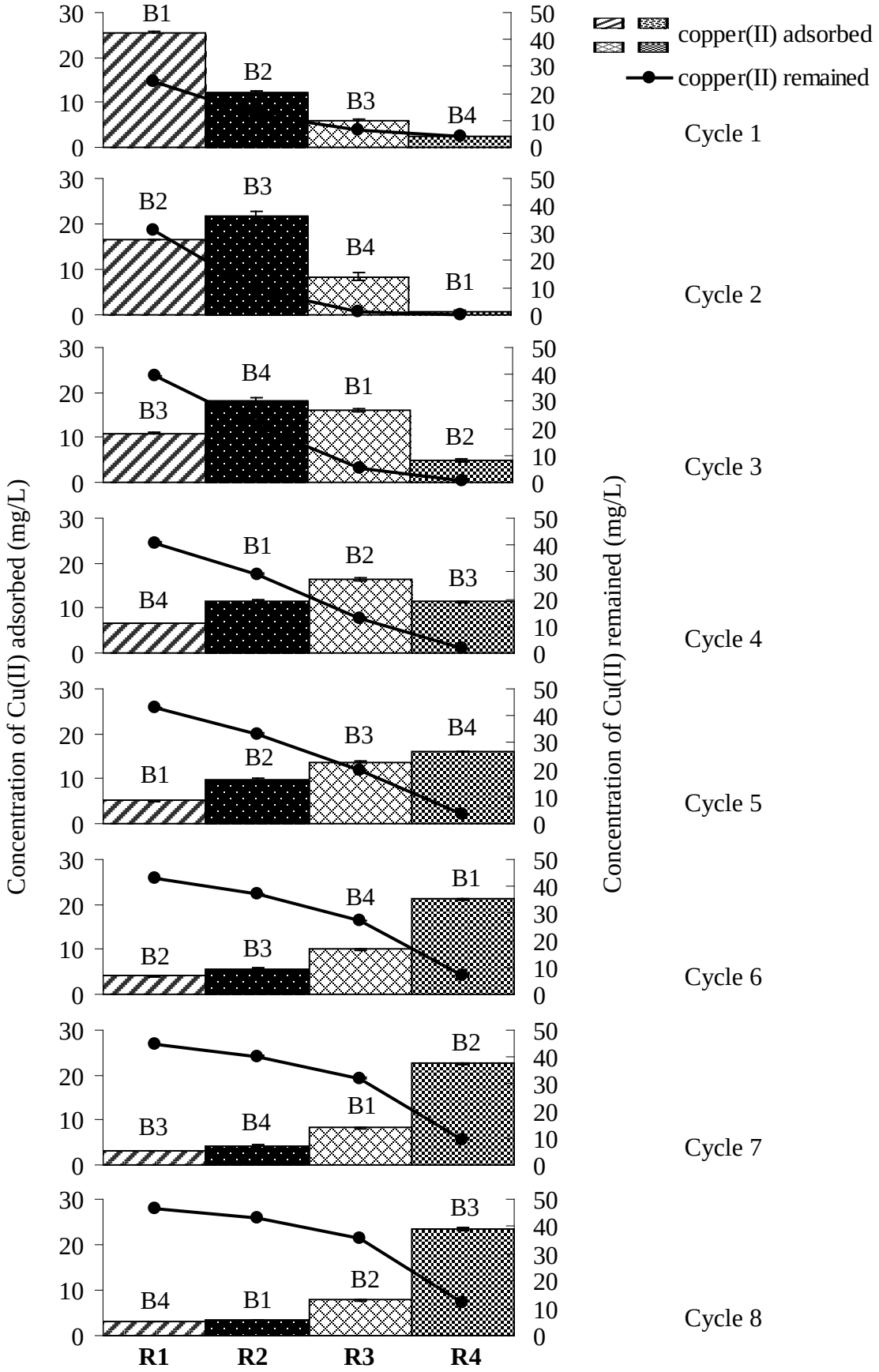

Figure 10. Concentration of copper(II) adsorbed and remained in industrial wastewater.

Table 4. Flow of the immobilized biosorbents (B1, B2, B3 and B4) from reactor 1 to reactor 4 over eight cycles.

	Cycle							
	1	**2**	**3**	**4**	**5**	**6**	**7**	**8**
Reactor 1	B1	B2	B3	B4	B1	B2	B3	B4
Reactor 2	B2	B3	B4	B1	B2	B3	B4	B1
Reactor 3	B3	B4	B1	B2	B3	B4	B1	B2
Reactor 4	B4	B1	B2	B3	B4	B1	B2	B3

Table 5. Critical values for t (*t*-test) (Michigan State University, n.d.).

Degree of freedom	Significance level
	0.05
1	12.71
2	4.30
3	3.18
4	2.78
5	2.57
6	2.45
7	2.36
8	2.31
9	2.26
10	2.23
11	2.20
12	2.18
13	2.16
14	2.14
15	2.13
16	2.12
17	2.11
18	2.10
19	2.09
20	2.09

Table 6. Critical values for F corresponding to significance level of 0.05 (ANOVA test) (Vassar College, n.d.).

		Degree of freedom (df_{among})									
		1	**2**	**3**	**4**	**5**	**6**	**7**	**8**	**9**	**10**
Degree of freedom (df_{within})	**2**	18.51	19.00	19.16	19.25	19.30	19.33	19.35	19.37	19.38	19.40
	3	10.13	9.55	9.28	9.12	9.01	8.94	8.89	8.85	8.81	8.79
	4	7.71	6.94	6.59	6.39	6.26	6.16	6.09	6.04	6.00	5.96
	5	6.61	5.79	5.41	5.19	5.05	4.95	4.88	4.82	4.77	4.74
	6	5.99	5.14	4.76	4.53	4.39	4.28	4.21	4.15	4.10	4.06
	7	5.59	4.74	4.35	4.12	3.97	3.87	3.79	3.73	3.68	3.64
	8	5.32	4.46	4.07	3.84	3.69	3.58	3.50	3.44	3.39	3.35
	9	5.12	4.26	3.86	3.63	3.48	3.37	3.29	3.23	3.18	3.14
	10	4.96	4.10	3.71	3.48	3.33	3.22	3.14	3.07	3.02	2.98

Table 7. Critical values for q corresponding to significance level of 0.05 (Tukey's HSD test) (University of Missouri-Rolla, n.d.).

		Number of treatments								
		2	**3**	**4**	**5**	**6**	**7**	**8**	**9**	**10**
Degree of freedom (df_{within})	**5**	3.64	4.60	5.22	5.67	6.03	6.33	6.58	6.80	6.99
	6	3.46	4.34	4.90	5.30	5.63	5.90	6.12	6.32	6.49
	7	3.34	4.16	4.68	5.06	5.36	5.61	5.82	6.00	6.16
	8	3.26	4.04	4.53	4.89	5.17	5.40	5.60	5.77	5.92
	9	3.20	3.95	4.41	4.76	5.02	5.24	5.43	5.59	5.74
	10	3.15	3.88	4.33	4.65	4.91	5.12	5.30	5.46	5.60
	11	3.11	3.82	4.26	4.57	4.82	5.03	5.20	5.35	5.49
	12	3.08	3.77	4.20	4.51	4.75	4.95	5.12	5.27	5.39
	13	3.06	3.73	4.15	4.45	4.69	4.88	5.05	5.19	5.32
	14	3.03	3.70	4.11	4.41	4.64	4.83	4.99	5.13	5.25
	15	3.01	3.67	4.08	4.37	4.59	4.78	4.94	5.08	5.20
	16	3.00	3.65	4.05	4.33	4.56	4.74	4.90	5.03	5.15
	17	2.98	3.63	4.02	4.30	4.52	4.70	4.86	4.99	5.11
	18	2.97	3.61	4.00	4.28	4.49	4.67	4.82	4.96	5.07
	19	2.96	3.59	3.98	4.25	4.47	4.65	4.79	4.92	5.04
	20	2.95	3.58	3.96	4.23	4.45	4.62	4.77	4.90	5.01

References

1. Abu Al-Rub, F.A., El-Naas, M.H., Benyahia, F. and Ashour, I., (2004). Biosorption of nickel on blank alginate beads, free and immobilized algal cells. *Process Biochemistry*, **39**, 1767-1773.

2. Agency for Toxic Substances and Disease Registry (ATSDR), (1990). *Toxicological profile for copper.* Syracuse Research Corporation for ATSDR, U.S. Public Health Service under Contract 88-0608-2. ATSDR/TP-90-08.

3. Aharoni, C. and Suzin, Y., (1982). Application of the Elovich equation to the kinetics of occlusion, Part 1. – Homogeneous microporosity. *Journal of the Chemical Society, Faraday Transaction 1: Physical Chemistry in Condensed Phases*, **78**, (8), 2313-2320.

4. Ahn, D.H., Chung, Y.C. and Pak, D., (1998). Biosorption of heavy metal ions by immobilized *Zoogloea* and *Zooglan*. *Applied Biochemistry and Biotechnology*, **73**, 43-50.

5. Akar, T. and Tunali, S., (2005). Biosorption performance of *Botrytis cinerea* fungal by-products for removal of Cd(II) and Cu(II) ions from aqueous solutions. *Minerals Engineering*, **18**, (11), 1099-1109.

6. Aksu, Z. and İşoğlu, I.A., (2005). Removal of copper(II) ions from aqueous solution by biosorption onto agricultural waste sugar beet pulp. *Process Biochemistry*, **40**, 3031-3044.

7. Aksu, Z. and Kutsal, T., (1998). Determination of kinetic parameters in the biosorption of copper(II) on *Cladophora sp.*, in a packed bed column reactor. *Process Biochemistry*, **33**, (1), 7-13.

8. Aksu, Z., Sag, Y. and Kutsal, T., (1992). The biosorption of Cu(II) by C. *vulgaris* and *Zramigera. Environmental Technology*, **13**, 579-586.

9. Akthar, N., Sastry, S.K. and Mohan, M.P., (1995). Biosorption of silver ions by processed *Aspergillus niger* biomass. *Biotechnology Letters*, **17**, (5), 551-556.

10. Aldor, I., Fourest, E. and Volesky, B., (1995). Desorption of cadmium from algal biosorbent. *Canadian Journal of Chemical Engineering*, **73**, 516-522.

11. Amuda, O.S., Giwa, A.A. and Bello, I.A., (2007). Removal of heavy metal from industrial wastewater using modified activated coconut shell carbon. *Biochemical Engineering Journal*, **36**, (2), 174-181.

12. Apiratikul, R. and Pavasant, P., (2008). Batch and column studies of biosorption of heavy metals by *Caulerpa lentillifera*. *Bioresource Technology*, **99**, 2766-2777.

13. Ashley, N.V. and Roach, D.J.W., (1989). Review of biotechnology applications to nuclear waste treatment. *Journal of Chemical Technology and Biotechnology*, **26**, 381-394.

14. Avnir, D., Coradin, T., Lev, O. and Livage, J., (2006). Recent bio-applications of sol-gel materials. *Journal of Materials Chemistry*, **16**, 1013-1030.

15. Bai, R.S. and Abraham, T.E., (2003). Studies on chromium(VI) adsorption–desorption using immobilized fungal biomass. *Bioresource Technology*, **87**, 17-26.

16. Beolchini, F., Pagnanelli, F., Toro, L. and Vegliò, F., (2003). Biosorption of copper by *Sphaerotilus natans* immobilised in polysulfone matrix: equilibrium and kinetic analysis. *Hydrometallurgy*, **70**, 101-112.

17. Bányik, T., Kuncová, G. and Páca, J., (2000). The use of silica gel prepared by sol-gel method and polyurethane foam as microbial carriers in the continuous degradation of phenol. *Applied Microbiology and Biotechnology*, **54**, 168-172.

18. Braun, S., Rappoport, S., Zusman, R., Avnir, D. and Ottolenghi, M., (1990). Biochemically active sol-gel glasses: the trapping of enzymes. *Material Letters*, **10**, 1-5.

19. Chang, J., Huang, J., Chang, C. and Tarn, T., (1998). Removal and recovery of lead fixed-bed biosorption with immobilized bacterial biomass. *Water*

Science and Technology, **38**, (4-5), 171-178.

20. Chang, J., Law, R. and Chang, C., (1997). Biosorption of lead, copper and cadmium by biomass of *Pseudomonas aeruginosa*. *Water Research*, **31**, (7), 1651-1658.

21. Chen, J. and Lin, Y., (2007). Sol-gel-immobilized recombinant E. coli for biosorption of Cd^{2+}. *Journal of the Chinese Institute of Chemical Engineers*, **38**, 235-243.

22. Chen, L., Zhong, Q., Cui, Y., Qian, G. and Wang, M., (2008). Preparation and nonlinear optical properties of hybrid sol-gel films doped with triphenylamino-substituted chromophores. *Dyes and Pigments*, **76**, (1), 195-201.

23. Cheung, Y.H., Neller, A., Chu, K.H., Tam, N.F.Y., Wong, C.K., Wong, Y.S. and Wong, M.H., (1997). Assessment of sediment toxicity using different trophic organisms. *Archives of Environmental Contamination and Toxicology*, **32**, 260-267.

24. Choy, K.K.H., Ko, D.C.K., Cheung, C.W., Porter, J.F. and McKay, G., (2004). Film and intraparticle mass transfer during the adsorption of metal ions onto bone char. *Journal of Colloid and Interface Science*, **271**, 284-295.

25. Chu, K.H. and Hashim, M.A., (2007). Copper biosorption on immobilized seaweed biomass: Column breakthrough characteristics. *Journal of Environmental Sciences*, **19**, (8), 928-932.

26. Cusslle, E.L., (1984). *Diffusion, mass transfer in fluid systems*. Cambridge University, Cambridge. Chapter 5.3.

27. Dahiya, S., Tripathi, R.M. and Hegde, A.G., (2008). Biosorption of lead and copper from aqueous solutions by pre-treated crab and arca shell biomass. *Bioresource Technology*, **99**, 179-187.

28. Davis, T.A., Volesky, B. and Mucci, A., (2003). A review of the biochemistry of heavy metal biosorption by brown algae. *Water Research*, **37**, 4311-4330.

29. Deng, S. and Ting, Y., (2005). Characterization of PEI-modified biomass and biosorption of Cu(II), Pb(II) and Ni(II). *Water Research*, **39,** (10), 2167-2177.

30. Do, D.D., (1998). *Adsorption Analysis: Equilibria and Kinetics*. Imperial College Press. Chapter 9.

31. Dunn, B., Miller, J.M., Dave, B.C., Valentine, J.S. and Zink, J.I., (1998). Strategies for encapsulating biomolecules in sol-gel matrices. *Acta Materialia*, **46**, (3), 737-741.

32. Environmental Protection Department (EPD), (2000). *Technical memorandum - standards for effluents discharged into drainage and sewerage systems, inland and coastal waters*. The Government of the Hong Kong Special Administrative Region, Hong Kong.

33. Environmental Protection Department (EPD), (2004). *Marine water quality in Hong Kong*. The Government of the Hong Kong Special Administrative Region, Hong Kong.

34. Fourest, E. and Roux, J.C., (1992). Heavy metal biosorption by fungal mycelial by-product: mechanism and influence of pH. *Applied Microbiology Biotechnology*, **37**, 399-403.

35. Furusawa, T. and Smith, J.M., (1973). Fluid-particle and intraparticle mass transport in slurries. *Industrial and Engineering Chemistry Fundamentals*, **12**, 197-203.

36. Göksungur, Y., Üren, S. and Güvenç, U., (2005). Biosorption of cadmium and lead ions by ethanol treated waste baker's yeast biomass. *Bioresource Technology*, **96**, 103-109.

37. Gong, R., Ding, Y., Liu, H., Chen, Q. and Liu, Z., (2005). Lead biosorption and desorption by intact and pretreated *Spirulina maxima* biomass. *Chemosphere*, **58**, 125-130.

38. Han, R., Zhang, J., Zou, W., Shi, J. and Liu, H., (2005). Equilibrium biosorption isotherm for lead ion on chaff. *Journal of Hazardous Materials*,

B125, 266-271.

39. Hashim, M.A. and Chu, K.H., (2004). Biosorption of cadmium by brown, green, and red seaweeds. *Chemical Enginering Journal*, **97**, 249-255.

40. Hence, L.L., (1998). *Sol-gel Silica: Properties, Processing, and Technology Transfer*. Noyes Publications. Chapter 2.

41. Ho, Y.S. and McKay, G., (1998). Sorption of dye from aqueous solution by peat. *Chemical Engineering Journal*, **70**, (2), 115-124.

42. Ho, Y.S. and McKay, G., (1999). The sorption of lead(II) ions on peat. *Water Research*, **33**, (2), 578-584.

43. Holan, Z.R., Volesky, B. and Prasetyo, I., (1993). Biosorption of cadmium by biomass of marine algae. *Biotechnology bioengineering*, **41**, 819-825.

44. Iqbal, M. and Edyvean, R.G.J., (2003). Biosorption of lead, copper and zinc ions on loofa sponge immobilized biomass of *Phanerochaete chrysosporium*. *Minerals Engineering*, **17**, 217-223.

45. Iqbal, M. and Edyvean, R.G.J., (2005). Loofa sponge immobilized fungal biosorbent: A robust system for cadmium and other dissolved metal removal from aqueous solution. *Chemosphere*, **61**, 510-518.

46. Jin, W. and Brennan, J.D., (2002). Properties and applications of proteins encapsulated within sol-gel derived materials. *Analytica Chimica Acta*, **461**, 1-36.

47. Karout, A., Chopard, C. and Pierre, A.C., (2007). Immobilization of a lipoxygenase in silica gels for application in aqueous media. *Journal of Molecular Catalysis B: Enzymatic*, **44**, 117-127.

48. Kato, M., Sakamoto, W. and Yogo, T., (2007). Synthesis of proton-conductive sol-gel membranes from trimethoxysilylmethylstyrene and phenylvinylphosphonic acid. *Journal of Membrane Science*, **303**, (1-2), 43-53.

49. Kim, T.Y., Kim, S.J., Yang, J.H. and Cho, S.Y. (2004). Environmentally friendly separation of heavy-metal ions onto porous chitosan beads. *Journal of Industrial and Engineering Chemistry*, **10**, (2), 201-207.

50. Kiran, I., Akar, T. and Tunali, S., (2005). Biosorption of Pb(II) and Cu(II) from aqueous solutions by pretreated biomass of *Neurospora crassa*. *Process Biochemistry*, **40**, 3550-3558.

51. Kurniawan, T.A., Chan, G.Y.S., Lo, W. and Babel, S., (2006). Comparisons of low-cost adsorbents for treating wastewaters laden with heavy metals. *Science of the Total Environment*, **366**, (2-3), 409-426.

52. Kurniawan, T.A., Chan, G.Y.S., Lo, W. and Babel, S., (2006). Physico-chemical treatment techniques for wastewater laden with heavy metals. *Chemical Engineering Journal*, **118**, 83-98.

53. Kursawe, M., Glaubitt, W. and Thierauf, A., (1998). Biodegradable silica fibers from sols. *Journal of Sol-Gel Science and Technology*, **13**, 267-272.

54. Kwok, N.Y., (2005). Development of high-throughput biosensors for multi-sample determination of biochemical oxygen demand (BOD) based on optical detection of oxygen. *Doctor of Philosophy Thesis*, Department of Applied biology and chemical technology, The Hong Kong Polytechnic University.

55. Kwok, N.Y., Dong, S.J., Lo, W.H. and Wong, K.Y., (2005). An optical biosensor for multi-sample determination of biochemical oxygen demand (BOD). *Sensors and Actuators B-Chemical*, **110**, (2), 289-298.

56. Lavela, P., Tirado, J.L. and Vidal-Abarca, C., (2007). Sol-gel preparation of cobalt manganese mixed oxides for their use as electrode materials in lithium cells. *Electrochimica Acta*, **52**, (28), 7986-7995.

57. Lenza, R.F.S. and Vasconcelos, W.L., (2000). Synthesis and properties of microporous sol-gel silica membranes. *Journal of Non-Crystalline Solids*, **273**, 164-169.

58. Leung, W.C., Chua, H. and Lo, W., (2001). Biosorption of heavy metals by bacteria isolated from activated sludge. *Applied Biochemistry and Biotechnology*, **91-93**, 171-184.

59. Leung, W.C., Wong, M.F., Chua, H., Lo, W., Yu, P.H.F. and Leung, C.K., (2000). Removal and recovery of heavy metals by bacteria isolated from activated sludge treating industrial effluents and municipal wastewater. *Water Science and Technology*, **14**, 233-240.

60. Leusch, A. and Volesky, B., (1995). The influence of film diffusion on cadmium biosorption by marine biomass. *Journal of Biotechnology*, **43**, 1-10.

61. Li, Z., Guo, S. and Li, L., (2006). Study on the process, thermodynamical isotherm and mechanism of Cr(III) uptake by *Spirulina platensis*. *Journal of Food Engineering*, **75**, (1), 129-136.

62. Lin, C. and Lin, H., (2005). Remediation of soil contaminated with the heavy metal (Cd^{2+}). *Journal of Hazardous Materials*, **A122**, 7-15.

63. Lin, L., Xiao, L.L., Huang, S., Zhao, L., Cui, J.S., Wang, X.H. and Chen, X., (2006). Novel BOD optical fiber biosensor based on co-immobilized microorganisms in ormosils matrix. *Biosensors and Bioelectronics*, **21**, 1703-1709.

64. Livage, J., (1997). Sol-gel processes. *Current Opinion in Solid State & Materials Scienc*e, **2**, 132-138.

65. Lovley, D.R., (2000). *Environmental Microbe-metal Interactions*. ASM Press. Chapter 14.

66. Maduraiveeran, G. and Ramaraj, R., (2007). Gold nanoparticles embedded in silica sol-gel matrix as an amperometric sensor for hydrogen peroxide. *Journal of Electroanalytical Chemistry*, **608**, (1), 52-58.

67. Malik, A., (2004). Metal bioremediation through growing cells. *Environment International*, **30**, (2), 261-278.

68. Marques, P.A.S.S., Rosa, M.F. and Pinheiro, H.M., (2000). pH effects on the removal of Cu^{2+}, Cd^{2+} and Pb^{2+} from aqueous solution by waste brewery waste. *Bioprocess Engineering*, **23**, 135-141.

69. Marseaut, S., Debourg, A., Dostálek, P., Votruba, J., Kuncova, G. and Tobin, J.M., (2004). A silica matrix biosorbent of cadmium. *International Biodeterioration & Biodegradation*, **54**, 209-214.

70. Martinez, M., Miralles, N., Hidalgo, S., Fiol, N., Villaescusa, I. and Poch, J., (2006). Removal of lead(II) and cadmium(II) from aqueous solutions using grape stalk waste. *Journal of Hazardous Materials*, **B133**, 203-211.

71. Melgar, M.J., Alonso, J. and García, M.A., (2007). Removal of toxic metals from aqueous solutions by fungal biomass of *Agaricus macrosporus*. *Science of the Total Environment*, **385**, (1-3), 12-19.

72. Michigan State University, (n.d.). Critical value for *t*. Retrieved October 26, 2007, from http://www.msu.edu/user/sw/tables/t-table.html.

73. Naja, G. and Volesky, B., (2006). Multi-metal biosorption in a fixed-bed flow-through column. *Colloids and Surfaces A: Physicochemical and Engineering Aspects*, **281**, 194-201.

74. Nakane, K., Yamashita, T., Iwakura, K. and Suzuki, F., (1999). Properties and structure of poly(vinyl alcohol)/silica composites. *Applied Polymer Science*, **74**, 133-138.

75. Nguyen-Ngoc, H. and Tran-Minh, C., (2006). Sol-gel process for vegetal cell encapsulation. *Materials Science and Engineering C*, **27**, (4), 607-611.

76. Olguin, E.J., Sanchez, G. and Hernandez, E., (2000). *Environmental Biotechnology and Cleaner Bioprocesses*. Taylor & Francis, Inc., U.S.A. Chapter 11.

77. Pagnanelli, F., Mainelli, S., Vegliò, F. and Toro, L., (2003). Heavy metal removal by olive pomace: biosorbent charaterisation and equilibrium modeling. *Chemical Engineering Science*, **58**, (20), 4709-4717.

78. Pan, X., Wang, J. and Zhang, D., (2005). Biosorption of Pb(II) by *Pleurotus ostreatus* immobilized in calcium alginate gel. *Process Biochemistry*, **40**, (8), 2799-2803.

79. Papageorgiou, S.K., Katsaros, F.K., Kouvelos, E.P., Nolan, J.W., Le Deit, H. and Kanellopoulos, N.K., (2006). Heavy metal sorption by calcium alginate beads from *Laminaria digitata*. *Journal of Hazardous Materials*, **137**, (3), 1765-1772.

80. Pavasant, P., Apiratikul, R., Sungkhum, V., Suthiparinyanont, P., Wattanachira, S. and Marhaba, T.F., (2006). Biosorption of Cu^{2+}, Cd^{2+}, Pb^{2+}, and Zn^{2+} using dried marine green macroalga *Caulerpa lentillifera*. *Bioresource Technology*, **97**, (18), 2321-2329.

81. Raize, O., Argaman, Y. and Yannai, S., (2004). Mechanisms of biosorption of different heavy metals by brown marine macroalgae. *Biotechnology Bioengineering*, **87**, (4), 451-458.

82. Rangsayatorn, N., Pokethitiyook, P., Upatham, E.S. and Lanza, G.R., (2004). Cadmium biosorption by cells of *Spirulina platensis* TISTR 8217 immobilized in alginate and silica gel. *Environment International*, **30**, 57-63.

83. Saeed, A., Akhter, W. and Iqbal, M., (2005). Removal and recovery of heavy metals from aqueous solution using papaya wood as a new biosorbent. *Separation and Purification Technology*, **45**, (1), 25-31.

84. Sağ, Y. and Kutsal, T., (1996). The selective biosorption of chromium(VI) and copper(II) ions from binary metal mixtures by *R. arrhizus*. *Process Biochemistry*, **31**, 561-572.

85. Sar, P., Kazy, S.K., Asthana, R.K. and Singh, S.P., (1999). Metal adsorption and desorption by lyophilized *Pseudomonas aeruginosa*. *International Biodeterioration & Biodegradation*, **44**, 101-110.

86. Sekhar, K.C., Kamala, C.T., Chary, N.S., Sastry, A.R.K., Rao, T.N. and Vairamani, M., (2004). Removal of lead from aqueous solutions using an immobilized biomaterial derived from a plant biomass. *Journal of Hazardous Materials*, **B108**, 111-117.

87. Sheng, P.X., Wee, K.H., Ting, Y.P. and Chen, J.P., (2008). Biosorption of copper by immobilized marine algal biomass. *Chemical Engineering Journal*, **136**, 156-163.

88. Stoll, A. and Duncan, J.R., (1997). Comparison of the heavy metal sorptive properties of three types of immobilized, non-viable *Saccharomyces cerevisiae* biomass. *Process Biochemistry*, **32**, (6), 467-472.

89. Szilva, J., Kuncova, G., Patzak, M. and Dostalek, P., (1998). The application of a sol-gel technique to preparation of a heavy metal biosorbent from yeast cells. *Journal of Sol-Gel Science and Technology*, **13**, 289-294.

90. Tam, N.F.Y., Wong, Y.S. and Simpson, C.G., (1998). Repeated removal of copper by alginate beads and the enhancement by microalgae. *Biotechnology techniques*, **12**, (3), 187-190.

91. Tien, C., (1994). *Adsorption Calculation and Modeling*. Butterworth-Heinemann, Newton.

92. Ting, Y.P. and Sun, G., (2000). Comparative study on polyvinyl alcohol and alginate for cell immobilization in biosorption. *Water Science Technology*, **42**, 85-90.

93. Tsezos, M. and Volesky, B., (1981). Biosorption of uranium and thorium. *Biotechnology Bioengineering*, **23**, 583-604.

94. Tunali, S. and Akar, T., (2006). Zn(II) biosorption properties of *Botrytis cinerea* biomass. *Journal of Hazardous Materials*, **B131**, 137-145.

95. United States Environmental Protection Agency (USEPA), (2002). *List of Drinking Water Contaminants & MCLs*. EPA 816-F-02-013.

96. University of Missouri-Rolla, (n.d.). Tukey's HSD post hoc test. Retrieved October 26, 2007, from http://web.umr.edu/~psyworld/virtualstat/tukeys/tukeyexamp.html.

97. Vassar College, (n.d.). Critical values of F. Retrieved October 26, 2007, from http://faculty.vassar.edu/lowry/apx_d.html.

98. Vegliò, F. and Beolchini, F., (1997). Removal of metals by biosorption: a review. *Hydrometallurgy*, **44**, 301-316.
99. Vijayaraghavan, K., Jegan, J., Palanivelu, K. and Velan, M., (2005). Biosorption of cobalt(II) and nickel(II) by seaweeds: batch and column studies. *Separation and Purification Technology*, **44**, 53-59.

100. Vijayaraghavan, K., Palanivelu, K. and Velan, M., (2006). Biosorption of copper(II) and cobalt(II) from aqueous solutions by crab shell particles. *Bioresource Technology*, **97**, 1411-1419.

101. Vilar, V.J.P., Botelho, C.M.S. and Boaventura, R.A.R., (2005). Influence of pH, ionic strength and temperature on lead biosorption by *Gelidium* and agar extraction algal waste. *Process Biochemistry*, **40**, (10), 3267-3275.

102. Volesky, B., (1987). Biosorbents for metal recovery. *Trends Biotechnology*, **5**, 96-101.

103. Volesky, B., (1990). *Biosorption of Heavy Metals*. CRC Press, Inc., U.S.A. Chapter 1.2.

104. Volesky, B., (2001). Detoxification of metal-bearing effluents: biosorption for the next century. *Hydrometallurgy*, **59**, 203-216.

105. Volesky, B., (2003). *Sorption and Biosorption*. St. Lambert, Québec: BV Sorbex. Chapter 6.

106. Volesky, B. and Naja, G., (2005). Biosorption: application strategies. *International Biohydrometallurgy Symposium*, Cape Town, South Africa (September 2005).

107. Wang, J., (2002). Biosorption of copper(II) by chemically modified biomass of *Saccharomyces cerevisiae*. *Process Biochemistry*, **37**, 847-850.

108. Wase, J. and Forster, C., (1997). *Biosorbents for Metal Ions*. Taylor & Francis, Inc., U.S.A. Chapter 2.

109. Wong, C.K.C., Cheung, R.Y.H. and Wong, M.H., (2000). Heavy metal concentrations in green-lipped mussels collected from Tolo Harbour and markets in Hong Kong and Shenzhen. *Environmental Pollution*, **109**, (1), 165-171.

110. Wong, M.F., (2000). Removal and recovery of copper(II) ions from industrial wastewater by bacteria isolated from activated sludge. *Master of Philosophy Thesis*, Department of Civil and Structural Engineering, The Hong Kong Polytechnic University.

111. Wong, M.F., Chua, H., Lo, W., Leung, C.K. and Yu, P.H.F., (2001). Removal and recovery of copper(II) ions by bacterial biosorption. *Applied Biochemistry and Biotechnology*, **91-93**, 447-457.

112. Wright, J.D. and Sommerdijk, N.A.J.M., (2001). *Sol-gel Materials Chemistry and Applications*. Gordon and Breach Science Publishers. Chapters 2 and 3.

113. Yang, J. and Volesky, B., (1999). Cadmium biosorption rate in protonated *Sargassum* biomass. *Environmental Science Technology*, **33**, 751-757.

114. Zhang, Y. and Banks, C., (2005). The interaction between Cu, Pb, Zn and Ni in their biosorption onto polyurethane-immobilised *Sphagnum* moss. *Journal of Chemical Technology and Biotechnology*, **80**, 1297-1305.

115. Zhou, D., Zhang, L. and Guo, S., (2005). Mechanisms of lead biosorption on cellulose/chitin beads. *Water Research*, **39**, (16), 3755-3762.

116. Zhou, J.L. and Kiff, R.J., (1991). The uptake of copper from aqueous solution by immobilized fungal biomass. *Journal of Chemical Technology and Biotechnology*, **52**, 317-330.

117. Ziagova, M., Dimitriadis, G., Aslanidou, D., Papaioannou, X., Litopoulou Tzannetaki, E. and Liakopoulou-Kyriakides, M., (2007). Comparative study of Cd(II) and Cr(VI) biosorption on *Staphylococcus xylosus* and *Pseudomonas* sp. in single and binary mixtures. *Bioresource Technology*, **98**, 2859-2865.

118. Zogorski, J.S., Faust, S.D. and Haas, J.H., (1975). The kinetics of adsorption of phenols by granular activated carbon. *Journal of Colloid and Interface Science*, **55**, (2), 329-341.

119. Zouboulis, A.I., Matis, K.A., Loukidou, M. and Šebesta, F., (2003). Metal biosorption by PAN-immobilized fungal biomass in simulated wastewaters. *Colloids and Surfaces A: Physicochemical and Engineering Aspects*, **212**, 185-195.